UNIVERSIDADE FEDERAL DO RIO GRANDE DO SUL
FACULDADE DE AGRONOMIA
PROGRAMA DE PÓS-GRADUAÇÃO EM ZOOTECNIA

DARILENE URSULA TYSKA

ABORDAGENS GENÔMICAS PARA CARACTERIZAÇÃO DA HOMOZIGOSIDADE NAS RAÇAS HEREFORD E BRAFORD

Porto Alegre

2022

UNIVERSIDADE FEDERAL DO RIO GRANDE DO SUL
FACULDADE DE AGRONOMIA
PROGRAMA DE PÓS-GRADUAÇÃO EM ZOOTECNIA

ABORDAGENS GENÔMICAS PARA CARACTERIZAÇÃO DA HOMOZIGOSIDADE NAS RAÇAS HEREFORD E BRAFORD

DARILENE URSULA TYSKA
Zootecnista/ UFPel
Mestre em Ciências/ UFPel

Tese apresentada como um dos requisitos à obtenção do grau de Doutor em Zootecnia

Área de concentração Melhoramento Genético Animal

Porto Alegre (RS), Brasil
Dezembro, 2022

CIP - Catalogação na Publicação

Tyska, Darilene Ursula
ABORDAGENS GENÔMICAS PARA CARACTERIZAÇÃO DA HOMOZIGOSIDADE NAS RAÇAS HEREFORD E BRAFORD / Darilene Ursula Tyska. -- 2022.
164 f.
Orientador: José Braccini Neto.

Tese (Doutorado) -- Universidade Federal do Rio Grande do Sul, Faculdade de Agronomia, Programa de Pós-Graduação em Zootecnia, Porto Alegre, BR-RS, 2022.

1. Assinaturas de seleção. 2. Corridas de Homozigose. 3. Gado de corte. 4. Ancestralidade. 5. Pintura cromossômica. I. Braccini Neto, José, orient. II. Título.

Elaborada pelo Sistema de Geração Automática de Ficha Catalográfica da UFRGS com os dados fornecidos pelo(a) autor(a).

Darilene Ursula Tyska
Mestre em Zootecnia

TESE

Submetida como parte dos requisitos
para obtenção do Grau de

DOUTORA EM ZOOTECNIA

Programa de Pós-Graduação em Zootecnia
Faculdade de Agronomia
Universidade Federal do Rio Grande do Sul
Porto Alegre (RS), Brasil

Aprovada em: 13.12.2022
Pela Banca Examinadora

Homologado em: 07/02/2023
Por

JOSÉ BRACCINI NETO
PPG Zootecnia/UFRGS
Orientador

SERGIO LUIZ VIEIRA
Coordenador do Programa de
Pós-Graduação em Zootecnia

Arione Augusti Boligon
UFPel

Pamela Itajara Otto
UFSM

Ricardo Vieira Ventura
USP

CARLOS ALBERTO BISSANI
Diretor da Faculdade de Agronomia

DEDICATÓRIA

Às minhas filhas, que me ensinaram a
perseverança e o amor incondicional.

Dedico.

AGRADECIMENTOS

Á minha filha Cecília, que veio junto com o doutorado, obrigada por tornar os meus dias mais felizes, meu raio de sol.

Á minha filha Mariana, que me motivou a conclusão desta tese.

Ao meu esposo Robson, pela paciência e companheirismo, por estar ao meu lado me motivando a seguir em frente e a não desistir. Obrigada por caminharmos juntos!

Aos meus pais, Flávio e Eliana, minha tia Tânia, meus sogros Dauria e Roberto por todo auxílio na reta final da conclusão da tese.

Ao meu orientador Professor Dr. José Braccini Neto, por me receber no seu grupo de pesquisa, e pela confiança em mim depositada na execução desse trabalho, e pela compreensão nos momentos difíceis.

Ao professor Dr. Nelson José Laurindo Dionello, pela amizade e carinho, que mesmo distante sempre esteve presente como um mestre.

À Empresa Brasileira de Pesquisa Agropecuária, em especial ao Dr. Fernando Flores Cardoso pelo fornecimento dos bancos de dados e disponibilidade.

Ao Dr. Gabriel Campos, sempre presente e disponível para auxiliar e escutar, me ajudando a resolver os problemas, tenho certeza de que fostes fundamental para execução desse trabalho.

Ao professor Dr. Jaime Araújo Cobuci e todos os docentes do PPGZ, pelos ensinamentos e esclarecimentos prestados.

Ao professor Dr. Tiago Paim e a Dr. Elisa Peripolli, pelo auxílio nas análises, scripts e apoio na pesquisa.

Ao grupo de pesquisa Megagen, em especial aos meus colegas, Karine, Giovani, Maíza, Renata e Fabiana, pelos ensinamentos e amizade.

Ao Programa de Pós-Graduação em Zootecnia da UFRGS pela compreensão e atenção dada as minhas solicitações de prorrogações.

À Coordenação de Aperfeiçoamento de Pessoal de Nível Superior (CAPES) pela bolsa de estudos concedida no doutorado.

OBRIGADA!

Nunca foi sorte, sempre foi Deus

ABORDAGENS GENÔMICAS PARA CARACTERIZAÇÃO DA HOMOZIGOSIDADE NAS RAÇAS HEREFORD E BRAFORD

Autor: Darilene Ursula Tyska
Orientador: Professor Dr. José Braccini Neto

RESUMO

A genotipagem dos animais domésticos possibilita a investigação e compreensão de como o genoma é moldado devido a seleção. O objetivo geral deste trabalho foi identificar e caracterizar segmentos homozigotos presentes no genoma dos bovinos das raças Hereford e Braford, associar regiões homozigotas mais frequentes nessa população a genes envolvidos na expressão de características econômicas, calcular e correlacionar os coeficientes de endogamia genômico oriundos das corridas de homozigose e da matriz genômica de parentesco e coeficiente endogâmico obtido através do pedigree. Identificar no Braford assinaturas de seleção e atribuir a ancestralidade dessas marcas. No capítulo II foram utilizados dados de 3.183 animais e 371.571 SNPs da raça Hereford e 3.854 animais e 494.481 SNPs da raça Braford, através do software PLINK foram identificadas um total de 531.992 ROHs (n=329.971 Hereford n=202.021 Braford). As ilhas de autozigosidade foram evidentes em regiões genômicas associadas a importantes características econômicas. Os genes dentro dos termos enriquecidos ($p<0,05$) para o gado Braford foram associados principalmente a características relacionadas à qualidade do leite, reprodução e metabolismo lipídico envolvido em características relacionadas à qualidade da carne. Para o gado Hereford, os genes estiveram envolvidos principalmente na expressão de características de pigmentação e pelagem da raça, produção/qualidade do leite, persistência da lactação e funções moleculares relacionadas à fertilidade de touros e novilhas. Os coeficientes de endogamia na população Hereford foram calculados usando o pedigree (F_{PED}: 0,003), matriz de relacionamento genômico (F_{GRM}: 0,263) e ROH ($F_{ROH\text{-}Mean}$: 0,132). Nos animais Braford, os valores médios foram 0,001 (F_{PED}), 0,215 (F_{GRM}) e 0,061 ($F_{ROH\text{-}Mean}$). A maior correlação entre os coeficientes de endogamia foi entre $F_{ROH>16Mb}$ e F_{PED} (0,33) para a população Hereford e F_{ROH_mean} e F_{GRM} (0,44) para a população Braford. A correlação entre $F_{ROH>16Mb}$ e F_{PED} evidenciou a superficialidade do pedigree, corroborando o conceito de que F_{ROH} pode captar níveis mais profundos de autozigosidade individual. No Capítulo III foram utilizados dados de SNPs de alta densidade de 7149 bovinos das raças Hereford-Embrapa, Braford, Braham, Nelore e Hereford USA, após controle de qualidade o banco de dados continha 310.816 SNPS comuns. Para determinar as regiões de baixa diversidade, o software PLINK v1.90 foi usado para calcular as ROHs, onde 1% dos SNPs mais frequentes foram usados para determinar as regiões de assinaturas de seleção. O software ADMIXTURE foi utilizado para calcular a probabilidade de ancestralidade das raças fundadoras de Braford. A ancestralidade do genoma do Braford, coberto por SNPs, manteve um percentual médio esperado por sua composição racial 3/8 Zebu. Dezenove ilhas de homozigose foram identificadas, essas regiões continham QTLs de características selecionadas nas raças. O uso de abordagens genômicas trouxe avanços, contribuindo com estimativas mais próximas da similaridade genética dos indivíduos da população. Coeficientes de endogamia estimados através de segmentos homozigotos no genoma (F_{ROH}) podem ser usados

---

[1]Tese de Doutorado em Zootecnia – Faculdade de Agronomia, Universidade Federal do Rio Grande do Sul, Porto Alegre, RS, Brasil. (164 p.), dezembro de 2022.

como estimadores mais precisos dos níveis de endogamia individual nos programas de melhoramento das raças, visando melhor direcionamento dos acasalamentos e cálculo de acuracia. A identificação das assinaturas de seleção no Braford, permitiu conhecer a estrutura de uma raça composta, e a contribuição no genoma dos fundadores do Braford, demonstra que a pressão de seleção na raça Braford mantem alelos favoráveis na complementariedade das raças, e as marcas no genoma estão relacionadas a importantes QTLs, na expressão de fenótipos de interesse da raça.

Palavras-chave: assinaturas de seleção, corridas de homozigose, gado de corte, ROH

[1]Tese de Doutorado em Zootecnia – Faculdade de Agronomia, Universidade Federal do Rio Grande do Sul, Porto Alegre, RS, Brasil. (164 p.), dezembro de 2022.

GENOMIC APPROACHES TO CHARACTERIZE HOMOZYGOSITY IN THE HEREFORD AND BRAFORD BREEDS

Author: Darilene Ursula Tyska
Adviser: Teacher José Braccini Neto

ABSTRACT:

The genotyping of domestic animals makes it possible to investigate and understand how the genome is shaped by selection. The general objective of this work was to identify and characterize homozygous segments present in the genome of Hereford and Braford cattle, to associate more frequent homozygous regions in this population to genes involved in the expression of economic characteristics, to calculate and correlate the genomic inbreeding coefficients derived from races of homozygosity and genomic matrix of kinship and inbreeding coefficient obtained through the pedigree. Identify selection signatures in Braford and assign the ancestry of these marks. In chapter II, data from 3,183 animals and 371,571 SNPs of the Hereford breed and 3,854 animals and 494,481 SNPs of the Braford breed were used. A total of 531,992 ROHs were identified through the PLINK software (n=329,971 Hereford n=202,021 Braford). Islands of autozygosity were evident in genomic regions associated with important economic traits. Genes within the enriched terms ($p<0.05$) for Braford cattle were mainly associated with traits related to milk quality, reproduction and lipid metabolism involved in traits related to meat quality. For Hereford cattle, genes were mainly involved in the expression of breed pigmentation and coat traits, milk production/quality, lactation persistence, and molecular functions related to fertility in bulls and heifers. Inbreeding coefficients in the Hereford population were calculated using pedigree (F_{PED}: 0.003), genomic relationship matrix (F_{GRM}: 0.263) and ROH ($F_{ROH\text{-}Mean}$: 0.132). In Braford animals, the mean values were 0.001 (F_{PED}), 0.215 (F_{GRM}) and 0.061 ($F_{ROH\text{-}Mean}$). The highest correlation between inbreeding coefficients was between $F_{ROH>16Mb}$ and F_{PED} (0.33) for the Hereford population and F_{ROH_mean} and F_{GRM} (0.44) for the Braford population. The correlation between $F_{ROH>16Mb}$ and F_{PED} evidenced the superficiality of the pedigree, corroborating the concept that F_{ROH} can capture deeper levels of individual autozygosity. In Chapter III, data from high-density SNPs of 7149 Hereford-Embrapa, Braford, Braham, Nellore and Hereford USA cattle were used. After quality control, the database contained 310,816 common SNPS. To determine the regions of low diversity, the PLINK v1.90 software was used to calculate the ROHs, where 1% of the most frequent SNPs were used to determine the selection signature regions. The ADMIXTURE software was used to calculate the probability of ancestry of the founding breeds of Braford. The ancestry of the Braford genome, covered by SNPs, maintained an average percentage expected for its 3/8 Zebu racial composition. Nineteen islands of homozygosity were identified, these regions contained QTLs of selected traits in the breeds. The use of genomic approaches brought advances, contributing with closer estimates of the genetic similarity of individuals in the population. Inbreeding coefficients estimated through homozygous segments in the genome (F_{ROH}) can be used as more accurate estimators of individual inbreeding levels in breed improvement programs, aiming at better targeting of mating and accuracy calculation. The identification of the selection signatures in the Braford, allowed to know the structure of a composite race, and the contribution in the genome of the founders of the Braford. The selection pressure in the Braford breed maintains

[1]Doctoral Thesis in Animal Science – Faculdade de Agronomia, Universidade Federal do Rio Grande do Sul, Porto Alegre, RS, Brazil. (164 p.), December, 2022.

favorable alleles in the complementarity of the breeds, and the marks in the genome are related to important QTLs, in the expression of phenotypes of interest to the breed.

Keywords: beef cattle, ROH, runs of homozygosity, selection signature

[1]Doctoral Thesis in Animal Science – Faculdade de Agronomia, Universidade Federal do Rio Grande do Sul, Porto Alegre, RS, Brazil. (164 p.), December, 2022.

SUMÁRIO

LISTA DE FIGURAS

CAPÍTULO I

LISTA DE TABELAS

CAPÍTULO II

LISTA DE FIGURAS

CAPÍTULO II

LISTA DE TABELAS

CAPÍTULO III

LISTA DE FIGURAS

CAPÍTULO III

LISTA DE ABREVIATURAS E SIGLAS

Bp = Par de base

cM = Centimorgan

DNA= Ácido Desoxirribonucleico

F_{GRM} = Inbreeding derived from a genomic relationship matrix

F_{PED} = Inbreeding coefficient based on pedigree

F_{ROH} = Inbreeding coefficient based on runs of homozygosity

GS = Genomic selection

HLD = High linkage disequilibrium

IBD = Identical by descent

IBS = Identical by state

kb= kilobase

LD = Linkage disequilibrium

MAF = Minor allele frequency

Mb = Mega pair of bases

Ne = Effective population size

QTL = Quantitative trait loci

ROH = Runs of homozygosity

ROHet= Corridas de heterozigosidade

SNP = Single nucleotide polymorphism

CAPÍTULO I

1. Introdução

O crescimento mundial e a demanda por proteína de alto valor biológico, faz da bovinocultura de corte um mercado em grande expansão no mundo. A pecuária brasileira e a produção agrícola têm um impacto proeminente sobre o comércio mundial de alimentos. Quando se pensa em qualidade de carne, as raças Hereford e Braford se destacam pela maciez e marmoreio da carne, sendo raças importantes para a produção de carne bovina no sul do Brasil.

A origem da raça Hereford teve início na Inglaterra passando por alguns cruzamentos para aprimorar qualidade de carcaça e eficiência produtiva, em 1788 já era considerada uma raça estabelecida, mas somente em 1906 os primeiros exemplares foram importados no Brasil, dando início aos registros de animais puros no país (ABHB, 2020). Na década de 60-70 os cruzamentos entre raças puras Europeias e Zebuínas começaram a ganhar espaço, surgindo oficialmente na Flórida (EUA) a raça sintética Braford, de composição 5/8 Hereford e 3/8 Zebuína, e no Brasil somente em 2003 foi reconhecida como raça pelo Ministério da Agricultura (ABHB, 2020).

O melhoramento genético, aliado a tecnologias reprodutivas, viabilizou as exigências do mercado, obtendo animais mais uniformes. Essa uniformidade é obtida através do aumento da frequência dos alelos favoráveis de uma determinada característica na população, o que possibilita ganhos a longo prazo. Contudo, isso causa uma diminuição da variabilidade genética dos rebanhos, uma vez que ao longo do tempo há o aumento de acasalamento entre animais aparentados mais do que a média da população, caracterizando endogamia (BOURDON, 1997).

A endogamia não é um processo de degeneração, mas uma consequência da segregação mendeliana (ALLARD, 1971), tendo como resultado direto a redução da heterozigozidade e, consequentemente, um aumento na homozigosidade. Esse aumento não é uniforme em todo genoma, onde regiões que estão relacionadas às características econômicas são mais homozigotas em detrimento a outras (MCQUILLAN *et al*., 2008). Através da genotipagem com marcadores tipo SNP, do o inglês, “Single Nucleotide Polymorphism” foi possível detectar esses segmentos contínuos homozigotos, denominados de corridas de homozigose, (ROH - do inglês “Runs of homozygosity”) (KIM *et al*., 2013).

Uma vantagem da utilização das ROH é a correta quantificação da autozigose (PERIPOLLI *et al*., 2017) que ocorre quando segmentos cromossômicos decorrentes de ancestrais são idênticos por descendência (IBD – do inglês "*identical by descent"*) herdados de ambos os pais no genoma da prole (BROMAN; WEBER, 1999), dando origem a segmentos contínuos caracterizados como ROH. Esses segmentos possibilitam a correta distinção entre os segmentos não autozigóticos que são idênticos por estado (IBS – do inglês "*Identity by state"*) daqueles autozigóticos IBD (HOWRIGAN; SIMONSON; KELLER, 2011).

A habilidade dos segmentos autozigóticos IBD em elucidar sobre eventos genéticos populacionais torna-os uma ferramenta capaz de prover informações valiosas a respeito da evolução demográfica de uma população ao longo do tempo (PERIPOLLI *et al*., 2018a). Os eventos de recombinação não são aleatórios ao longo do genoma, possibilitando a existência de regiões do genoma com uma alta frequência de ROH, chamadas de "ilhas de ROH", e sua ocorrência em um grande número de indivíduos da população pode ser um indicativo de pressão de seleção (ZAVAREZ *et al*., 2015).

O comprimento da ROH pode indicar se a presença da endogamia provém de tempos remotos ou recentes, onde os segmentos longos são quebrados em pedaços menores ao longo das gerações pelos eventos de recombinação (CURIK; FERENČAKOVIĆ; SÖLKNER, 2014). A ROH pode identificar os níveis de endogamia, além de fornecer suporte na estimativa do verdadeiro nível de autozigosidade nos níveis individual e populacional (FERENČAKOVIĆ; SÖLKNER; CURIK, 2013; LI; KIM, 2015; PERIPOLLI *et al*., 2018a; ZAVAREZ *et al*., 2015). Outro benefício da ROH, além de estimar os níveis de endogamia, é possibilitar conhecer a história dessas populações através das assinaturas de seleção (LAWSON *et al*., 2012) que revela a origem das marcas de seleção no genoma dessas populações.

2. Revisão Bibliográfica

2.1. Corridas de homozigose

As corridas de homozigose são segmentos homozigotos contínuos interruptos da sequência de DNA (ácido desoxirribonucleico) em genomas diploides (GIBSON; MORTON; COLLINS, 2006) que ocorrem quando pais com um ancestral comum passam segmentos cromossômicos compartilhados de origem IBD para progênie (WRIGHT, 1949). O processo de formação desse fenômeno pode ser visualizado na Figura 1, onde o indivíduo A representa o ancestral comum dos pais D e E do indivíduo F. O cromossomo homólogo que deu origem a essa ROH está representado em verde e as demais cores indicam fragmentos de cromossomos não homólogos (GOMEZ-RAYA *et al*., 2015).

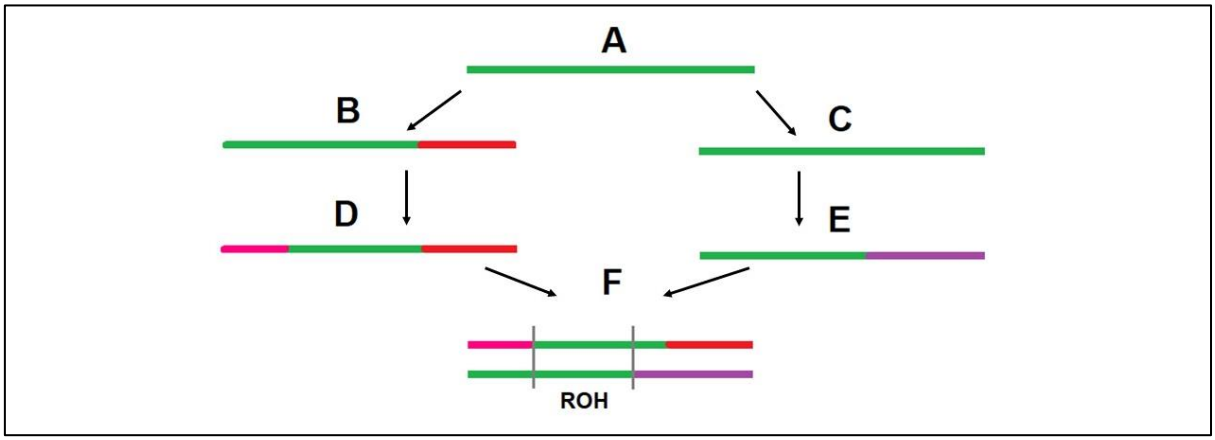

Figura 1. Representação da formação de uma ROH (segmento em verde) no indivíduo "F" originada no ancestral comum A, onde apenas um dos dois cromossomos homólogos (verde) do ancestral está representado. Adaptado de GOMEZ-RAYA *et al*., (2015).

A terminologia ROH foi utilizada primeiramente em seres humanos, para denominar trechos de 100 ou mais SNPs consecutivos, com ausência de heterozigotos em um único cromossomo, onde os painéis de densidades superiores a 50K já estavam disponíveis (LENCZ *et al*., 2007). Estudos em outras espécies de animais só foram realizados quando se popularizou esses painéis para os animais de produção (GIBSON; MORTON; COLLINS, 2006).

O potencial da caracterização das corridas de homozigose tem sido utilizado em diferentes populações, raças e linhagens de uma espécie, possibilitando obter

informações acerca da história evolutiva (METZGER *et al*., 2015; SORBOLINI *et al*., 2015; ZAVAREZ *et al*., 2015), demográficas (BOSSE *et al*., 2012) ou relacionadas à endogamia de uma população (MARRAS *et al*., 2015; REBELATO; CAETANO, 2018).

2.2. A utilização da ROH em populações de bovinos

O primeiro trabalho identificando ROH em bovinos foi publicado por Sölkner *et al*. (2010) seguido por outros autores que aprofundaram a metodologia em diversas raças bovinas (PERIPOLLI *et al*., 2016; FERENČAKOVIĆ; SÖLKNER; CURIK, 2013; FORUTAN *et al*., 2018; KIM *et al*., 2013; PERIPOLLI *et al*., 2018a, 2018c; PURFIELD *et al*., 2012; WILLIAMS *et al*., 2016), sempre buscando identificar e caracterizar os segmentos homozigotos em relação a história da população e a consanguinidade. Esses trabalhos contribuíram muito para elucidar os padrões de ROH em bovinos, além de permitir uma associação com regiões do genoma sob pressão de seleção, além de fornecer uma estimativa da endogamia.

No estudo pioneiro de Sölkner *et al*. (2010) foi utilizado um chip de densidade de 50K em 910 touros da raça Simental, onde concluíram que os valores de endogamia baseados em homozigosidade são substancialmente mais precisos na previsão do nível de autozigosidade e de depressão por endogamia do que a variação dos valores baseados em genótipos. Os autores Purfield *et al*. (2012), comparando os padrões de ROH de diversas raças bovinas, observaram que as raças estudadas diferiram acentuadamente, e que os animais da raça Holandesa apresentavam ROHs mais longas no genoma, contudo, para quase todas as raças a maior parte das ROHs identificadas eram curtas (1-5 Mb).

Observando a frequência e a distribuição de ROHs no genoma das raças Pardo Suíço, Simental, Norueguês Vermelho e Tyrol Grey, Ferenčaković *et al*. (2013) concluíram que não existe um padrão entre as raças, e que os níveis de autozigosidade derivados de ROH fornecem uma indicação dos níveis de endogamia individual mais precisas, quando comparadas a abordagens probabilísticas de linhagens. Além de que, os desvios padrão mais altos dos F_{ROHs}, sugerem superioridade para estimar a depressão por endogamia, além de permitir estimar a distância entre a população atual e a população fundadora.

Estudando o efeito da seleção artificial nas ROH em gado Holandês dos EUA, Kim *et al*. (2013) comparam a autozigosidade genômica entre os grupos selecionados ou não selecionados (desde 1964) para a produção de leite, e revelaram diferenças significativas em relação à frequência e distribuição geral de ROH. Os resultados deste estudo indicam que a distribuição de ROH foi mais variável entre os genomas de animais selecionados em comparação com a distribuição de ROH mais uniforme para animais não selecionados. Além disso uma análise mais profunda identificou assinaturas de seleção correspondentes as características quantitativas para produção de leite, quantidade de gordura e proteína.

Utilizando o mesmo princípio do cálculo para ROH, Williams *et al*. (2016) calcularam trechos consecutivos de genótipos heterozigotos ROHet, e identificaram regiões do genoma onde há alta heterozigozidade em raças de bovinos localmente adaptados, localizaram genes que estão sob seleção natural, e que contribuíram para características de aptidão e/ou sobrevivência.

Buscando avaliar o efeito da seleção genômica na distribuição de ROH pelo genoma do gado Holandês da América do Norte após a seleção genômica, Forutan *et al*. (2018) realizaram um estudo de simulação, onde compararam três softwares, sendo que o SNP1101 forneceu as estimativas mais próximas da verdadeira consanguinidade no estudo de simulação realizado. Os autores concluíram que o uso das ROHs também tornou possível avaliar o efeito da estrutura e seleção da população, evidenciando como diferentes estratégias de seleção afetam a distribuição de ROHs, e como a distribuição das ROH se comportou na população de gado leiteiro da América do Norte nos últimos 25 anos.

Avaliando seis linhagens de uma população de gado Nelore, Peripolli *et al*. (2018a) caracterizaram os padrões de ROH e as ilhas de autozigosidade no genoma e compararam as estimativas de endogamia calculadas a partir de ROH (F_{ROH}), matriz de relacionamento genômico (F_{GRM}) e coeficiente baseado em linhagem (F_{PED}). Os autores concluíram que o F_{ROH} deve ser utilizado quando o arquivo de pedigree não se estende por muitas gerações, e que as ilhas de ROH compartilhadas sugerem uma forte seleção para resposta imune nessa população e, que as ilhas não sobrepostas dentro das linhagens explicam a seleção para características funcionalmente importantes em bovinos Nelore. Utilizando as ROHs para calcular endogamia genômica numa população de 582 bovinos Gir, Peripolli *et al*. (2018b) sugerem que o

F_{ROH} pode ser usado como alternativa para estimar a endogamia na ausência do pedigree, e que a estimativa F_{PED} não é a mais adequada para capturar a consanguinidade antiga. Além disso, localizaram genes dentro das ilhas ROH que apontam uma forte seleção de características leiteiras e enriquecimento para adaptação ambiental.

Pesquisas mais recentes têm demonstrado o potencial das ROHs além de estimar a endogamia, associar as regiões genômicas a características de produção selecionadas para cada raça. Ao avaliarem os padrões de homozigose em todo o genoma e os níveis de endogamia em bovinos chineses da raça Wagyu, Zhao *et al*. (2020) identificaram várias regiões candidatas e genes sobrepostos a ROH para várias características importantes, como altura corporal, circunferência torácica, cobertura de gordura, espessura de toucinho, área do olho de lombo e comprimento da carcaça.

Os autores Biscarini *et al*. (2020) buscaram estimar a diversidade genética em gado Maremmana semi-selvagem, descreveram regiões de homozigosidade (ROH) e heterozigosidade (ROHet) no genoma, que ainda são mal caracterizadas na raça Maremmana. Além disso, os autores identificaram genes que apontam para características fenotípicas relacionadas à adaptação ambiental e robustez deste gado localmente adaptado.

Avaliando os efeitos da depressão endogâmica na fertilidade e produção de leite do gado de leiteiro Finlandês Ayrshire, os autores Martikainen *et al*. (2020) associaram picos ROHs a uma redução na produção, tanto para a produção de leite, quanto para proteína e gordura nessa população. Peripolli *et al*. (2020), avaliando diferentes tipos biológicos dentro da raça composta Montana Tropical® através das ROHs, identificaram genes associados com a resposta imune e inflamatória, homeostase, reprodução, absorção de minerais e metabolismo de lipídios, descritos dentro das ilhas de autozigosidade.

Os autores Dixit *et al*. (2020) utilizaram sete raças de bovinos nativos da Índia *(Bos taurus indicus)* e concluíram que as raças diferiram quanto aos padrões de ROH e que as ilhas abrigavam maior proporção de QTLs para características de produção, mas menor para características reprodutivas localizadas nas raças leiteiras. Já nas raças de tração foram identificados genes nas ilhas de ROH associados a resistência a doenças/imunidade e genes tolerantes ao estresse.

Os autores Toro Ospina *et al*. (2020) analisaram duas populações de gado Gir, uma selecionada para produção de leite, e outra para produção de carne, e concluíram que a seleção pode moldar a distribuição das ilhas ROH dentro da mesma raça, quando os animais são selecionados para diferentes fins, como produção de leite ou carne.

Utilizando as ROHs para identificar assinaturas de seleção na raça composta Brangus, Paim *et al*. (2020) identificaram assinaturas de seleção nas regiões de ilhas de ROH dos animais Brangus advindas das populações fundadoras, além de identificar a predominância da composição genética das raças fundadoras em regiões genômicas específicas do gado Brangus. Caivio-Nasner *et al*. (2021) utilizaram as ROHs em busca de assinaturas de seleção no gado Blanco Orejinegro adaptado ao trópico colombiano, e concluíram que a endogamia nesta população é significativamente recente, e que as ilhas de ROH detectadas correspondem a QTLs relacionados às características de produção, como leite, conformação, reprodução, saúde e carcaça.

Buscando identificar regiões homozigotas no genoma que afetam características produtivas no gado Chines Simental (ZHAO *et al*., 2021), localizaram 101 regiões de ROH associadas a características de produção, além de identificarem 17 genes candidatos relacionados ao tamanho do corpo, qualidade de carne e características reprodutivas.

Na raça Hereford linhagem 1 dos Estados Unidos, Pilon *et al*. (2021) avaliaram a endogamia nesta população fechada de bovinos de corte, concluindo que a endogamia deve ser avaliada em regiões individuais do genoma, e que os esquemas de acasalamento com a finalidade de evitar depressão por endogamia devem se concentrar mais em ROH específicos com efeitos negativos. Sumreddee *et al*. (2020) concluíram que apesar do alto nível de endogamia nessa população, seu impacto negativo no desempenho do crescimento não foi tão severo quanto o esperado, o que pode ser atribuído à eliminação dos alelos deletérios devido à seleção natural ou artificial ao longo do tempo.

2.3. Critérios e Softwares utilizados para calcular ROH

Os critérios para definir os segmentos de ROH é um dos desafios da análise, pois a falta de consenso entre os pesquisadores em estabelecer critérios para definir os padrões da ROH (KU *et al*., 2011), que são usados para identificar e diferenciar os segmentos autozigotos -IBD de segmentos IBS. Isso acaba tornando difícil a comparação entre os estudos, já que a falta de consenso permite que os pesquisadores utilizem diferentes limiares para definição das ROH, tanto entre espécies quanto dentro delas (HOWRIGAN; SIMONSON; KELLER, 2011; KU *et al*., 2011).

A revisão feita por Peripolli *et al*. (2017) apresenta dados de 22 trabalhos com os principais critérios utilizados para detecção das ROHs em várias espécies. Os autores referem que o número de SNPs consecutivos varia de 10 a 58 (SNP/ROH), com a densidade variando de 1/50 e 1/100 (SNPs/ kb), e a distância entre SNPs homozigotos consecutivos foi de 100 até 1.000 kb, e o comprimento mínimo estabelecido para uma ROH variou de 10 a 5.000 kb. Essa grande variação nos parâmetros utilizados e a falta de critérios bem específicos podem ser responsáveis pelas estimativas viesadas na determinação do coeficiente de endogamia calculado através dos segmentos homozigotos, pois esses critérios afetam o número e a duração da ROH (HOWRIGAN; SIMONSON; KELLER, 2011).

Os autores Ferenčaković *et al*. (2013) ressaltam que além dos critérios utilizados o poder de detectar um comprimento mínimo de ROH está relacionado com a densidade do chip, e apontou que a utilização do painel de 50k pode superestimar o número de pequenos segmentos (1-4 Mb), e ao utilizar o chip de alta densidade, subestimou-se segmentos com mais de 8 Mb.

Outro fator que dificulta a comparação é a diferença entre os algoritmos utilizados pelos softwares disponíveis para identificar as ROHs. Alguns pesquisadores buscaram elucidar a diferença entre os softwares, avaliando o desempenho e os resultados gerados. Os autores Howrigan *et al*. (2011) avaliaram os softwares, PLINK (PURCELL *et al*., 2007), GERMLINE (GUSEV *et al*., 2009) e o BEAGLE (BROWNING; BROWNING, 2010), e observaram que o software PLINK gerou a maior proporção de resultados significativos para detectar a autozigosidade de ancestrais comuns distantes e sugeriram que o software BEAGLE produziria a melhor precisão na

detecção da autozigosidade, porque incorporava o desequilíbrio de ligação ("*linkage disequilibrium*" - LD), mas isso não foi comprovado no estudo.

Em 2013, a pesquisadora Karimi (2013) realizou um estudo, no qual comparou resultados das frequências de ROH detectadas nos programas PLINK (PURCELL *et al*., 2007), SVS (Golden Helix SNP & Variation Suite v.7.6.8) e cgaTOH (ZHANG *et al*., 2013), e reportou que os resultados apontaram uma diferença significativa (P<0,001) entre eles. Contudo, os três programas localizaram ilhas em regiões semelhantes do genoma, com os resultados do SVS e PLINK se sobrepuseram mais, e o software cgaTOH detectou um número maior de indivíduos em ilhas de ROH.

O software PLINK é um dos mais utilizados para detectar segmentos de ROH, tanto em populações humanas quanto em animais (MEYERMANS *et al*., 2020). É um software gratuito de fácil manuseio, que utiliza o método de janelas deslizantes, ou seja, uma janela de um comprimento (pré-determinado) é movida pelos genomas de acordo com os parâmetros definidos pelo pesquisador (KARIMI, 2013), como o número máximo de heterozigotos permitidos em uma janela para ser considerada essa janela homozigota, assim como o número máximo de SNPs faltantes. Por fim, o programa verifica se o comprimento final dos segmentos homozigotos atende ao tamanho mínimo estabelecido para o número e comprimento dos SNPs, para ser considerado um segmento homozigoto (MEYERMANS *et al*., 2020).

2.4. Coeficiente de endogamia calculado utilizando ROH

O coeficiente de endogamia é um dos parâmetros centrais na teoria da genética de populações, intimamente ligado a ideia de parentesco, podendo ser definido como a probabilidade de que dois alelos escolhidos aleatoriamente em um lócus homólogo dentro de um indivíduo sejam IBD, considerando uma população base-referência, na qual todos os alelos são independentes (CURIK; FERENČAKOVIĆ; SÖLKNER, 2014). Como a endogamia muda as frequências genotípicas, aumentando a homozigosidade às custas da heterozigozidade, isso pode levar a redistribuição das variações genéticas dentro e entre populações, aumentando a incidência de defeitos recessivos homozigotos, e uma redução da produção principalmente para características relacionadas a aptidão (CURIK; FERENČAKOVIĆ; SÖLKNER, 2014).

A endogamia recente origina longos segmentos de ROH no genoma dos seus sucessores (KU *et al*., 2011), detectados por meio de segmentos autozigotos, através dos padrões de marcadores moleculares do tipo SNP (KIM *et al*., 2013). A fórmula para calcular o F_{ROH} com dados de chip de SNP é: $F_{ROHi} = \frac{\sum_{j=1}^{n} L_{ROHj}}{L_{total}}$, onde $\sum_{j=1}^{n} L_{ROHj}$é a nde a soma de todos os comprimentos de ROH no genoma para o i-ésimo animal e $Ltotal$ é o comprimento total do genoma autossômico coberto por marcadores (MCQUILLAN *et al*., 2008).

O coeficiente de endogamia F_{ROH}, quando comparado ao coeficiente de endogamia baseado na matriz de relacionamento genômico (F_{GRM}), tem a vantagem de distinguir os segmentos IBD dos IBS, e assim não superestimar o valor de F (BAES *et al*., 2019; HOWRIGAN; SIMONSON; KELLER, 2011). Outra vantagem, é que pode ser calculado independentemente da presença ou profundidade do pedigree. O coeficiente de endogamia (FPed) é uma medida do grau de parentesco entre os indivíduos de uma população e é usado para estimar a probabilidade de que duas cópias de um alelo herdado por um indivíduo sejam idênticas por descendência (IBD), levando em consideração as relações entre os ancestrais do indivíduo.

2.5. Assinaturas de seleção

A domesticação do gado (*Bos taurus taurus e Bos taurus indicus*) ocorreu há 8.000-10.000 anos (LOFTUS *et al*., 1994), onde espécies domésticas modernas são resultado de reprodução seletiva para muitas características de importância econômica e adaptativa desde a domesticação. O termo domesticar significa adaptar o comportamento de um animal para atender às necessidades das pessoas (MIRKENA *et al*., 2010).

As pegadas da criação seletiva no genoma dos animais podem agora ser caracterizadas com o desenvolvimento de plataformas de sequenciamento e genotipagem em larga escala explorando SNPs (OLEKSYK; SMITH; O'BRIEN, 2010). Dentro do genoma de populações sujeitas à seleção, padrões genéticos distintos, chamados de assinaturas de seleção, são regiões com variabilidade genética reduzida, formadas a partir da pressão seletiva sobre uma mutação (Figura 2) ao longo de gerações consecutivas (URBINATI *et al*., 2016).

Se um alelo confere vantagem de aptidão, seu portador tem maior probabilidade de prosperar e deixar mais descendentes. O haplótipo contendo esse alelo benéfico tende a se espalhar rapidamente e aumentar sua frequência na população (SABETI *et al*., 2002). Variantes vizinhas a essa mutação benéfica também tendem a aumentar em frequência (efeito carona), podendo ser observados padrões de desequilíbrio de ligação entre a mutação favorável e os SNPs vizinhos (SABETI *et al*., 2002).

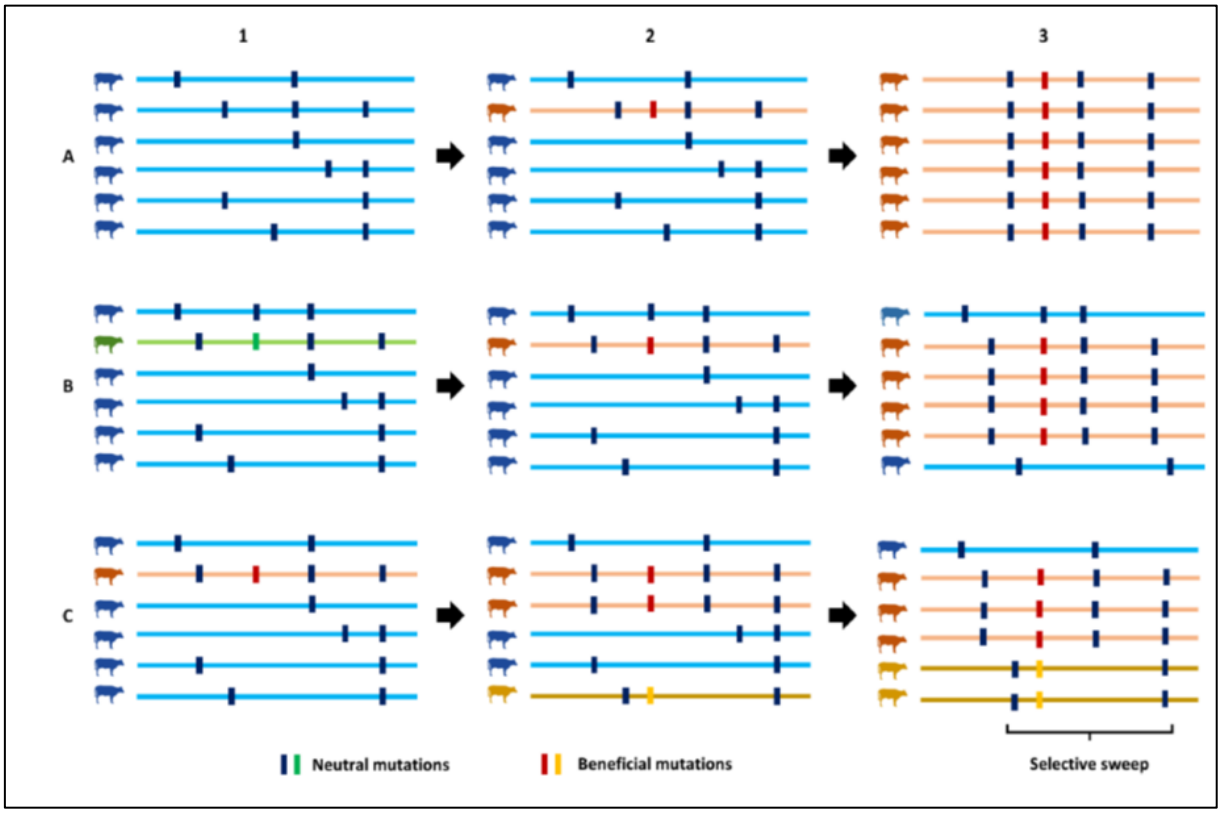

Figura 2. Tipos de varreduras seletivas. A) Varredura seletiva rígida/clássica: onde seis sequências de DNA de uma população com alelos de segregação neutra (azul) antes da seleção; 2) ocorre uma mutação benéfica na segunda sequência (vermelho) e a variabilidade genética é percebida em torno do alelo favorável; 3) Durante o processo seletivo nas gerações subsequentes, o alelo benéfico aumenta em frequência e finalmente atinge a fixação na população. Isso reduz a variação genética a montante e a jusante do alelo benéfico (ou seja, varredura seletiva). B) Varredura seletiva suave devido à variação genética permanente: 1) seis sequências de DNA de uma população com mutações neutras (verde e azul); 2) o alelo neutro que segrega em uma população (verde) torna-se benéfico (vermelho) devido a mudanças ambientais ou genéticas; 3) a seleção leva à fixação dos alelos benéficos na população, mas deixa alguma variação genética ao seu redor. C) Varredura suave de origem múltipla (devido a mutações independentes recorrentes): 1) ocorrência da primeira mutação benéfica

(vermelho) na segunda sequência de DNA 2) durante a seleção, o alelo benéfico (vermelho) aumenta em frequência junto com os sítios neutros associados. A segunda mutação benéfica (amarela) ocorre em outro background genômico no mesmo lócus. 3) Ambas as mutações benéficas em antecedentes genéticos diferentes aumentam em frequência e nenhuma consegue atingir a fixação. Adaptada de Saravanan *et al*. (2020).

2.6. Métodos para detecção das assinaturas de seleção

A metodologia baseada na variabilidade local reduzida se concentra na identificação de regiões genômicas com menor variação em relação à média do genoma (SARAVANAN *et al*., 2020), através de métodos como as ROHs que são amplamente utilizadas para avaliar os níveis de endogamia genômica, estrutura populacional e histórico demográfico em populações pecuárias (CURIK; FERENČAKOVIĆ; SÖLKNER, 2014). Com base na teoria da carona, uma varredura seletiva deve ter trechos de loci homozigotos que exibem maior homozigose do que a média do genoma (ALMEIDA *et al*., 2019; SARAVANAN *et al*., 2020).

A ROH pode ser usado para identificar assinaturas de seleção, pois os indivíduos que passaram pelo processo seletivo exibirão longos períodos de homozigose em torno do lócus alvo (FORUTAN *et al*., 2018; REBELATO; CAETANO, 2018; SARAVANAN *et al*., 2020). Outras análises estatísticas são eficazes para capturar assinaturas de seleção dentro das populações (Figura 3), e incluem a razão de verossimilhança composta (CLR, NIELSEN *et al*., 2005).

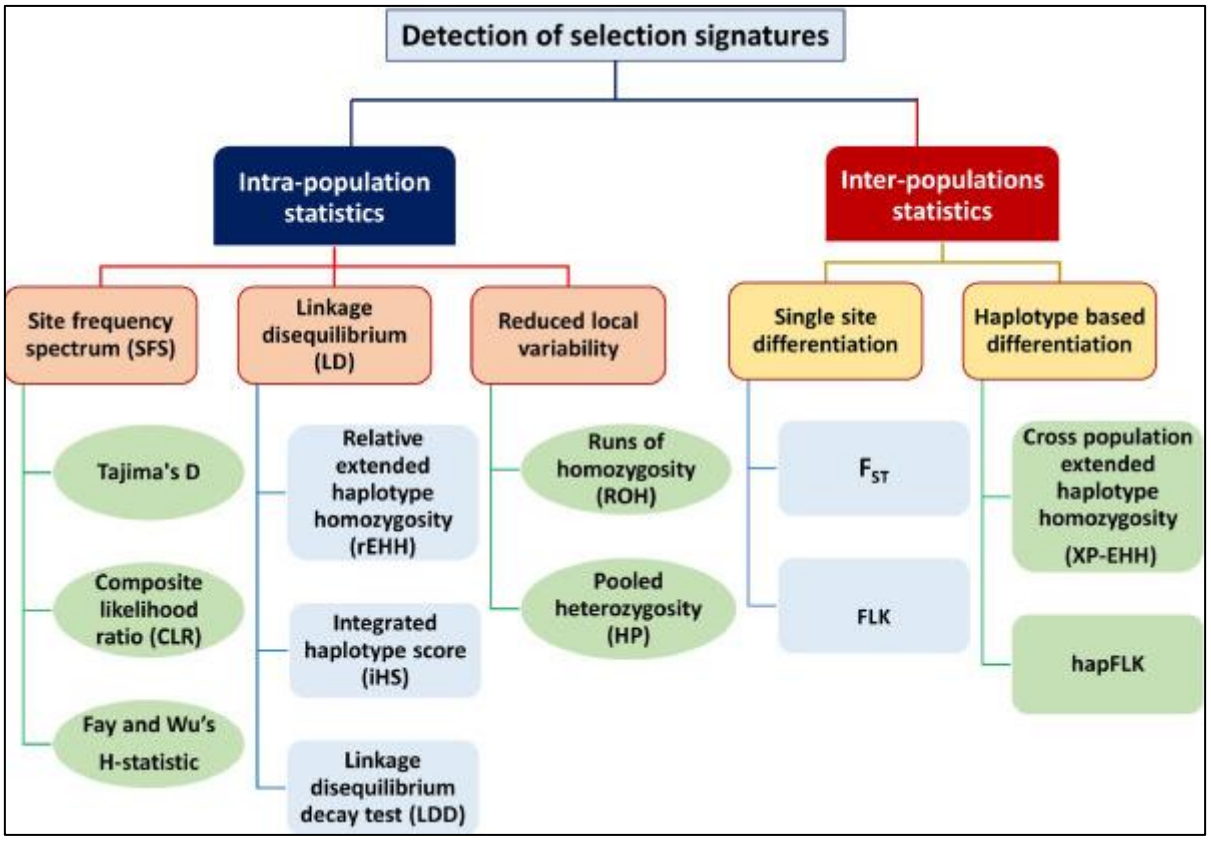

Figura 3. Classificação de diferentes abordagens comumente usadas para a detecção de assinaturas de seleção em populações pecuárias. Adaptada de Saravanan *et al*. (2020).

2.7. Softwares para análise da ancestralidade

Os softwares mais utilizados por pesquisadores, particularmente aqueles interessados em estrutura populacional e inferência histórica, normalmente apresentam resultados de mistura juntamente com outros métodos que fazem diferentes suposições de modelagem. Estes incluem o TreeMix (PICKRELL; PRITCHARD, 2012), ADMIXTUREGRAPH (LEPPÄLÄ; NIELSEN; MAILUND, 2017), fineSTRUCTURE (LAWSON *et al*., 2012).

Os softwares STRUCTURE e ADMIXTURE são populares porque fornecem ao usuário uma visão ampla da variação nos dados genéticos, ao mesmo tempo em que permitem a possibilidade de diminuir o zoom em detalhes sobre indivíduos específicos ou grupos rotulados.

3. Hipóteses

A raça Hereford tem mais segmentos homozigóticos no seu DNA, em comparação a raça Braford, por ser uma raça pura; as ilhas de ROH e regiões genômicas homozigotas compartilhadas possuem genes relacionados a produção animal, o coeficiente de endogamia baseado nas ROHs captura níveis mais profundos da autozigosidade individual.

A análise de ancestralidade baseada na baixa variabilidade local identificou assinaturas de seleção no genoma do Braford; as regiões das assinaturas de seleção são regiões associadas à QTLs de características importantes de produção; a raça Braford apresenta maior composição genômica taurina, por ser a raça de maior fração gênica na sua composição.

4. Objetivos

Comparar os padrões de autozigosidade genômica entre raças de bovinos Hereford e Braford; identificar ilhas ROH e regiões genômicas homozigóticas compartilhadas para prospectar genes relevantes dentro dessas regiões genômicas; calcular o coeficiente de endogamia genômica com base na ROH e na matriz de relação genômica, e a partir do coeficiente baseado em pedigree.

Identificar assinaturas de seleção em Braford usando dados de SNP de alta densidade através das corridas de homozigose; associar assinaturas de seleção com QTLs; identificar composição genômica ancestral dos animais Braford.

CAPÍTULO II – Assessment of autozygosity in Brazilian Hereford and Braford cattle breeds through runs of homozygosity[1]

[1] Artigo submetido a revista Livestock Science 07 novembro de 2022.

Assessment of autozygosity in Brazilian Hereford and Braford cattle breeds through runs of homozygosity

D. U. Tyska[1], G. S. Campos[2], E. Peripolli[2], K. A. R. de Souza[1], F. F. Cardoso[3], J. Braccini Neto[1]

[1]Animal Science Department, University Federal do Rio Grande do Sul (UFRGS), Rio Grande do Sul State, Av. Bento Gonçalves, 7712, District Agronomia – Porto Alegre – CEP:91540-000.

[2]Animal Science Department, School of Agricultural and Veterinary Sciences, São Paulo State, University (Unesp), Via de acesso Paulo Donato Castellane s/n. Jaboticabal, SP CEP 14884-900, Brazil

[3]Animal science research program, Animal Science Department, University Federal de Pelotas, Pelotas CEP 96010-900, RS, Brazil. Embrapa Pecuária Sul, Bagé CEP 96401-970, RS, Brazil

Abstract Graphic

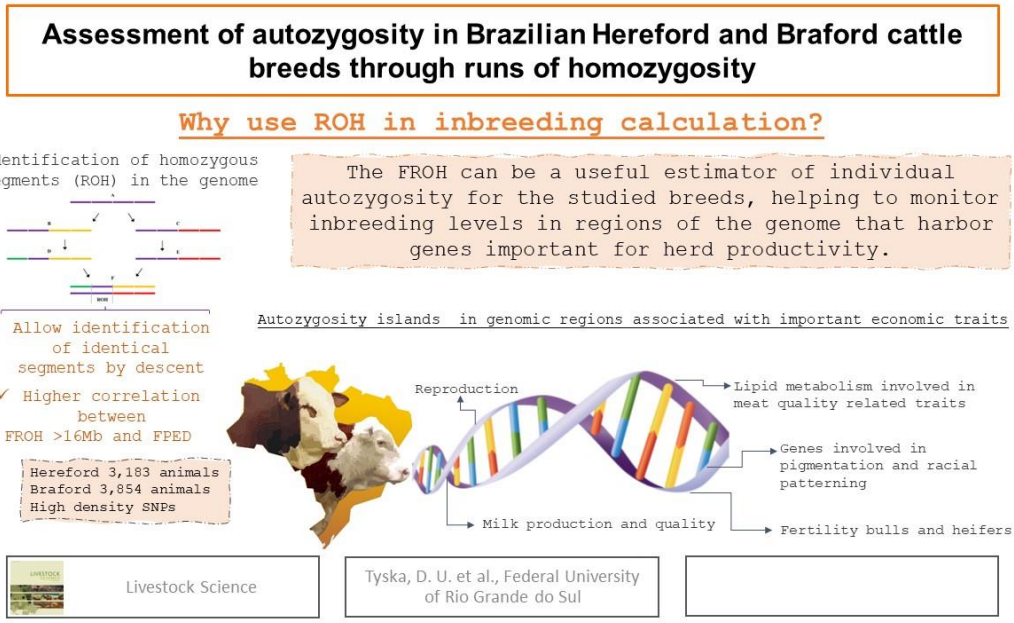

Abstract

Runs of homozygosity (ROH) are continuous homozygous segments of the DNA that can be used to infer about population structure and genomic inbreeding coefficients. ROH were evaluated in Hereford and Braford cattle breeds to assess inbreeding levels, characterize ROH patterns, and regions of the genome with a high frequency of ROH as well as to identify candidate genes within these homozygous regions. After genotype imputation in FImpute software and quality control, a total of 3,183 animals and 371,571 SNPs in the Hereford breed and 3,854 animals and 494,481 SNPs in the Braford breed were used for subsequent analyses. PLINK software was used to identify ROH and the autozygosity islands. A total of 531,992 ROH were identified (n=329,971 Hereford and n=202,021 Braford). The average ROH length was 3.17 Mb (±3.58) and 2.92 Mb (±3.43) for the Hereford and Braford cattle breeds, respectively. ROH_{Short} (1-4 Mb) were predominant through the genome for both cattle breeds. Autozygosity islands

were evident in genomic regions associated with important economic traits, and some of them overlapped in between the breeds (n=14). Genes within the enriched terms ($p<0.05$) for the Braford cattle were mainly associated with milk quality-related traits, reproduction, and lipid metabolism involved in meat quality-related traits (i.e., marbling, dorsal fat thickness, and loin eye area). For the Hereford cattle, the genes were mainly involved in the expression of pigmentation and coat traits of the breed, milk production/quality, lactation persistence, and molecular functions related to the fertility of bulls and heifers. Many of these genes and pathways were described in both breeds, such as the genes involved in marbling traits, meat quality, and carcass weight. Shared homozygous regions within and between the breeds were also noticeable throughout the genome and harbored several genes and QTLs which functions have been mainly associated with body weight, carcass quality, feed efficiency, fertility, and susceptibility to bovine respiratory diseases. Inbreeding coefficients in the Hereford population were calculated using the pedigree (F_{PED}: 0.003), genomic relationship matrix (F_{GRM}: 0.263), and ROH ($F_{ROH\text{-}Mean}$: 0.132). In Braford animals, the mean values were 0.001 (F_{PED}), 0.215 (F_{GRM}), and 0.061 ($F_{ROH\text{-}Mean}$). The highest correlation between inbreeding coefficients was between $F_{ROH>16Mb}$ and F_{PED} (0.33) for the Hereford population and F_{ROH_mean} and F_{GRM} (0.44) for the Braford population. The correlation between $F_{ROH>16Mb}$ and F_{PED} evidenced the superficiality of the pedigree, corroborating to the concept that F_{ROH} can capture deeper levels of individual autozygosity.

Keywords: *Bos taurus*, beef cattle, ROH hotspots, genomic inbreeding, ROH

1. Introduction

There are 224,6 million cattle heads in Brazil (IBGE, 2021), making the country the second largest beef producer in the world. (ABIEC, 2022). The subtropical climate of the southern region of Brazil favors the breeding of taurine cattle breeds (*Bos taurus taurus*), such as Hereford. This breed was the predominant British cattle breed in Brazil until the 1980s. Studies encompassing diversity and inbreeding within the breed in open (Piccoli *et al*., 2020, 2014) and closed (Cleveland *et al*., 2005; Sumreddee *et al*., 2020, 2019) populations are extremely important. It aims to obtain parameters for directing or redirecting the selection of economically important traits and for controlling the loss of genetic diversity.

Using pedigree data from the National Breeders Association (National Breeders Association - Herd Book Collares), Piccoli *et al*. (2014) described a high effective population size and low inbreeding levels. These results may reflect the continuous flow of animals and semen imported from various origins, however, these inbreeding levels calculated through the pedigree may not reflect the reality, considering the depth of pedigree and the lack of information from the genealogy of these imported breeders. Furthermore, the FPED considers the probability that a pair of alleles are IBD from the expected values, where the accuracy of the coefficients obtained is dependent on the depth and integrity of the pedigree (Ron *et al*., 1996). The authots Blott *et al*., (1998) demonstrated how Canadian and British Herefords become more related over time due to the expansion of reproductive technologies, implying the reduction of global genetic diversity (Cleveland *et al*., 2005).

Seeking for animals with better adaptive and productive traits in tropical conditions, crosses between zebu (*Bos taurus indicus*) and taurine cattle breeds are commonly used, giving rise to composite breeds such as the Braford (Piccoli *et al*., 2020). In Brazil, the Braford breed emerged from experiments coordinated by the Hereford Breeding Association and Embrapa Pecuária Sul. The Braford cattle have a mosaic genome due to crosses and backcrosses to obtain 5/8 Hereford and 3/8 zebu, in which Brahman cows from the USA were initially used,

and currently, some breeders use Nellore animals in the development of the breed (ABHB, 2020). The composite breed exploits the hybrid vigor due to the genetic distance of these founding breeds (González *et al*., 2022). The genetic diversity and population history of a given population can be studied through homozygous patterns within the genome (Biscarini *et al*., 2020; Eusebi *et al*., 2020; Freitas *et al*., 2021; Lozada-Soto *et al*., 2021; Saravanan *et al*., 2020).

Runs of homozygosity (ROH) are adjoining lengths of homozygous genotypes present in the genome due to parental transmission of identical by descendant haplotypes (Purfield *et al*., 2012). Their extent and frequency within the genome can inform about the individual's ancestry and population background (Purfield *et al*., 2012). Long ROH stretches can be found where homozygous genotypes occur in an unbroken sequence, indicating recent inbred mattings (Zhang *et al*., 2015a). ROH segments also tend to recombine and mutate over generations, interrupting the long chromosomal segments and resulting in decreased size, indicating ancient inbreeding (Curik *et al*., 2014).

As the ROH length is inversely proportional to the number of generations from the common ancestor (Howrigan *et al*., 2011), it can be used as an estimate of the animal's genomic autozygosity proportion or inbreeding coefficient (*F*) (Curik *et al*., 2014; McQuillan *et al*., 2008). When compared to the inbreeding coefficient based on the genomic relationship matrix, it has the advantage of distinguishing the autozygotic segments that are identical by state (IBS) from those identical by descent (IBD), not overestimating the *F* value (Baes *et al*., 2019; Howrigan *et al*., 2011). Further, it can be calculated regardless the pedigree depth.

The pattern and frequency of ROH allow an understanding of how artificial selection shape the genome autozygosity (Metzger *et al*., 2015; Peripolli *et al*., 2018a; Szmatoła *et al*., 2016) as these segments are not randomly distributed. Regions of homozygosity shared by many individuals (hotspots/ROH islands) are likely triggered by selection pressure events around the gene expression loci and/or quantitative traits (QTL) fixed in the genome over generations (Sonesson *et al*., 2010; Zavarez *et al*., 2015; Zhang *et al*., 2015a). Therefore, characterizing autozygosity patterns within the genome can help breeding programs to better

elucidate past or recent inbreeding events more accurately (Reverter *et al*., 2017), reveal genes/QTLs associated within such genomic regions that impact livestock production systems and economically important traits, and support the long-term sustainability of breeding programs through the preservation of genetic diversity (Purfield *et al*., 2012; Zavarez *et al*., 2015).

The objective of this study was to: (I) compare the genome-wide autozygosity patterns between Hereford and Braford cattle breeds; (II) identify ROH islands and shared homozygous genomic regions to prospect relevant genes within these genomic regions; and (III) calculate the genomic inbreeding coefficient based on ROH and the genomic relationship matrix, and from the pedigree-based coefficient.

2. Material and Methods

2.1. Ethics statement

Prior approval from the animal care and use committee was not required in this study since the information was obtained from a pre-existing database provided by the Brazilian Agricultural Research Corporation (Embrapa Pecuária sul, Bagé/RS) and Delta G genetic breeding program.

2.2. Animals

The genotype dataset consisted of 3,247 samples from Hereford animals (1,459 males and 1,788 females) and 3,924 samples Braford animals (2,727 males and 1,197 females), totaling 7,171 genotyped samples. Animals were genotyped with the *Illumina High-Density Bovine Bead Chip Array* (HD; Illumina Inc., San Diego, USA) containing 777K markers (n=114 Hereford and n=117 Braford); *GeneSeek Genomic Profiler HD-150K* (150k,Illumina Inc., San Diego, CA, USA) containing 150K markers (n=163 Hereford); *BovineSNP50 Bead Chip* (50 K; Illumina, San Diego, USA) containing 50K markers (n=2,212 Hereford and n=3548 Braford); *GGP-LD BeadChip*® (30k,Illumina Inc., San Diego, CA, USA)

containing roughly 30K markers (n=722 Hereford and n=186 Braford); and *Illumina BovineLD* (27k,Illumina Inc., San Diego, CA, USA) containing 27K markers (n=36 Hereford and n=73 Braford).

2.3. Data quality control and imputation

The quality control (QC) of the genotypes was implemented using the R/SNPStats package (Clayton, 2014). The goal of QC is to remove any data that may introduce bias or noise in the analysis, such as samples with low genotyping rates or SNPs with high missingness or deviation from Hardy-Weinberg equilibrium (HWE). Markers with a call rate lower than 0.90, located on sex chromosomes, or with a highly significant deviation from the Hardy-Weinberg equilibrium ($p<10\text{-}7$) were removed from the dataset. For markers located in the same genomic position or those highly correlated ($r> 0,98$), the ones with the highest MAF (minimum allele frequency) were retained. For the samples, a call rate of 0.90 was also applied and for animals that were genotyped in different panels, only the information from the highest density panel was kept, resulting in 3,183 Hereford animals and 3,854 Braford animals.

After the QC, imputation was implemented using the FIMPUTE 2.2 software (Sargolzaei *et al*., 2011), and all genotypes were imputed from the lowest density to the highest density panel. The panel in HD contained reference bulls used in the herds. The number of SNPs retained for subsequent analysis after the editing process was 371,571 for the Hereford breed and 494,481 for the Braford breed.

2.4. ROH detection and classification

ROH were identified for each animal using the PLINK v1.90 software (Purcell *et al*., 2007). This software examines each individual chromosome through a sliding window with a hit rate of at least 0.05. The minimum length of an ROH was established as 1000 kb, containing 30 consecutive homozygous SNPs, with up to two heterozygotes genotypes being allowed, requiring a

minimum density of one homozygous SNP every 120 kb, and a maximum distance of 100 kb between two consecutive homozygous SNPs. A minimum ROH length of 1000 kb was set as small segments occur predominantly throughout the genome due to linkage disequilibrium, and greater is the chance of being false positives (Maja Ferenčaković *et al*., 2013; Purfield *et al*., 2012).

ROH were classified into five length classes: $ROH_{1\text{-}2Mb}$, $ROH_{2\text{-}4Mb}$, $ROH_{4\text{-}8Mb}$, $ROH_{8\text{-}16Mb}$, $ROH_{>16Mb}$, respectively. Further, ROH were classified as short (ROH_{Short}), medium (ROH_{Medium}), and long (ROH_{Long}) segments as follows: ROH_{Short} (1-2 Mb and 2-4 Mb), ROH_{Medium} (4-8 Mb), and ROH_{Long} (8-16 Mb and >16Mb).

2.5. Autozygosity islands and shared ROH regions

To identify genomic regions the genome characterized by a high occurrence of ROH (autozygosity islands), a file generated by the PLINK software which specifies how many times each SNP appeared in an ROH was used. Subsequently, the top 1% of the most frequent SNPs within a ROH were selected, and the genomic regions were identified as autozygosity islands by considering consecutive SNPs. In these regions, a 100 Kb window was used in the chromosomal position, and it was intersected with the CattleQTL database (Hu *et al*., 2016). To search for overlapping genes within these regions, the autozygosity islands were aligned to the ARS-UDC 1.2 reference genome using the Ensembl cow gene set 94 releases (Howe *et al*., 2021). Database for Annotation, Visualization, and Integrated Discovery (DAVID) v.2021q2 tool (Huang *et al*., 2009, 2008) was used to identify overrepresented gene ontology (GO) terms and Kyoto Encyclopedia of Genes and Genomes (KEGG) pathways by Fisher's test ($p<0.05$) (Kim, 2017). The DAVID enrichment analysis was performed separately for each cattle breed.

2.6. Genomic and pedigree inbreeding coefficients

Genomic inbreeding coefficient based on ROH (F_{ROH}) was estimated for every animal according to the methodology proposed by McQuillan *et al*. (2008): $F_{ROHi} = \frac{\sum_{j=1}^{n} L_{ROHj}}{L_{total}}$, where $\sum_{j=1}^{n} L_{ROHj}$ is the sum of all ROH lengths across the genome for the *i*th animal and L_{total} is the total length of the autosomal genome covered by markers (2,487.574 Mb). For each animal, F_{ROH} ($F_{ROH1–2\ Mb}$, $F_{ROH2–4\ Mb}$, $F_{ROH4–8\ Mb}$, $F_{ROH8\text{-}16\ Mb}$, and $F_{ROH>16\ Mb}$) was calculated based on five ROH lengths: 1-2Mb, 2-4Mb, 4-8Mb, 8-16Mb, >16Mb respectively.

A second measure of genomic inbreeding was calculated using the Genomic relationship matrix (**G**) (F_{GRM}). To obtain the F_{GRM}, the elements of the matrix **G** were computed using the preGSf90 software (Aguilar and Misztal, 2008) calculated according to VanRaden (2008): $G = \frac{ZZ'}{2\sum_{i=1}^{n} pi(1-pi)}$, where **Z** is a genotype matrix, which can be obtained through **Z**=**M**-**P**. The matrix **M** specifies which alleles each individual inherited: markers coded as 0, 1, or 2 for alternative homozygous, heterozygous, and reference homozygous allele, respectively. The matrix **P** specifies elements of the column l that are equal to 2 (pi), where pi is the frequency of the reference allele at the locus. It was assumed pi = 0,5 fixed. The diagonal elements of the matrix **G** represent the relationship of an animal with itself and, therefore, the F_{GRM} for individual *i* was taken as **G**ii−1.

The pedigree-based inbreeding coefficient (F_{PED}) was calculated using the renumf90 software (Aguilar and Misztal, 2008). The pedigree dataset was provided by the Brazilian Agricultural Research Corporation (Embrapa Pecuária Sul, Bagé, Rio Grande do Sul, Brazil) and Delta G genetic Breeding program (Conexão Delta G, Dom Pedrito, Rio Grande do Sul, Brazil). The dataset contained information from 1,637,637 animals, with an average depth of four generations and a maximum of nine. Kruskall-Walli's test ($p<0.05$) (Frey, 2018) method was used to estimate the correlations between the inbreeding measures.

3. Results

3.1. ROH detection and classification

A total of 531,992 ROH were detected, in which 329,971 were described for Hereford animals and 202,021 for Braford animals, with an average length of 3.17 Mb (±3.58) and 2.92 Mb (±3.43), respectively (Tab.1). In the Hereford breed, 78.7% of the segments were smaller than 4 Mb (ROH_{Short}), covering only 0.16% of the genome, and 6.1% of were larger than 8 Mb (ROH_{Long}). In the Braford breed, 82% were ROH_{Short} and 5.1% ROH_{Long}. It is worth mentioning that, in both breeds, short segments covered only 0.16% of the genome, while the long ones covered 1.42%.

Table 1. Descriptive statistics of runs of homozygosity number (n ROH) and mean length (Standard deviation in brackets) for five ROH length in Hereford and Braford cattle breeds.

Class	Hereford			Braford		
	n ROH	(%)	Mean length	*n* ROH	(%)	Mean length
$ROH_{1-2\ Mb}$	162,929	49.38	1.38 (0.28)	110,643	54.77	1.36 (0.28)
$ROH_{2-4\ Mb}$	96,598	29.28	2.81 (0.56)	54,923	27.19	2.79 (0.56)
$ROH_{4-8\ Mb}$	50,437	15.29	5.50 (1.10)	26,145	12.94	5.45 (1.09)
$ROH_{8-16\ Mb}$	15,859	4.81	10.67 (2.13)	8,027	3.97	10.62 (2.10)
$ROH_{>16\ Mb}$	4,148	1.26	24.66 (10.31)	2,283	1.13	24.99 (10.77)

The autosomes that displayed the highest number of ROH in both breeds were on *Bos taurus autosome* (BTA) 1, BTA2, BTA6, and BTA7, corresponding to approximately 23% of all ROH identified (Figure 1). In the Hereford breed, the BTA1 displayed the highest number of ROH (*n*=18,236), in which 72% of them were ROH_{Short} (ROH_{1-2Mb} and $ROH_{2-4\ Mb}$) and 9.5% ROH_{Large} (ROH8-16Mb and $ROH_{>16\ Mb}$), with the longest ones covering up to 63% of the chromosome. In the Braford breed, the BTA6 displayed the highest number of ROH (*n*=11,532), in which 74% of them were ROH_{Short} (ROH_{1-2Mb} and ROH_{2-4Mb}) and 7% ROH_{Large} ($ROH_{8-16\ Mb}$ and $ROH_{>16\ Mb}$), with the longest ones covering up

to 82% of the chromosome. In the Hereford and Braford population, 89% and 68% of the animals, respectively, presented at least one ROH larger than 10 Mb in length.

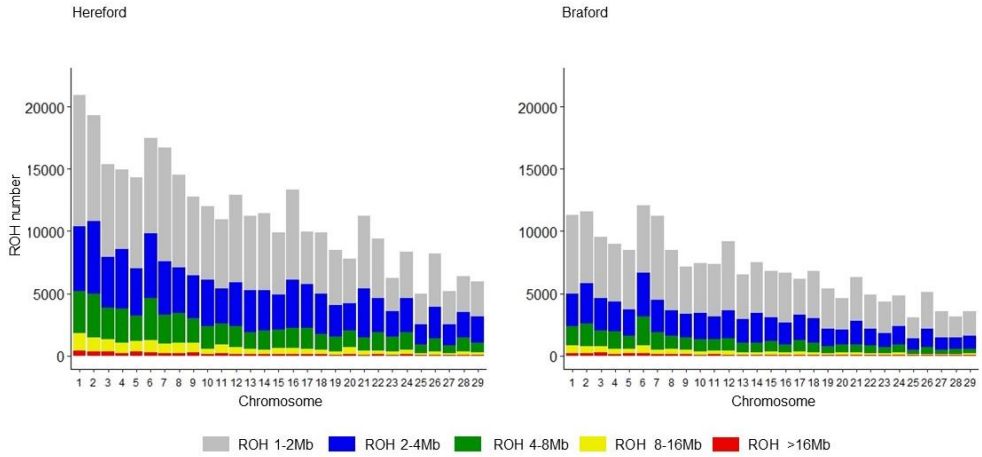

Figure 1. Distribution of the number runs of homozygosity (ROH) in the Hereford (Left) and Braford (Right) cattle breeds for each chromosome in five different ROH length: grey ($ROH_{1–2\ Mb}$), blue ($ROH_{2–4\ Mb}$), green ($ROH_{4–8Mb}$), yellow ($ROH_{8\text{-}16\ Mb}$), and red ($ROH_{>16\ Mb}$).

Hereford animals exhibited an average of 103±10.9 ROH per animal with an average length of 328±66.71 Mb. It should be mentioned that 64% of the population had more than 100 ROH, and 2.39% of these animals displayed more than 20% of the genome covered by ROH and 7.16% less than 10% of the genome covered by them. Braford individuals exhibited 52±13.20 ROH per animal (152.86±58.40 Mb in length). Only 0.1% of the Braford population presented more than 20% of the genome in homozygosity and 94.21% of the individuals showed less than 10% of the genome covered by ROH (Figure 2).

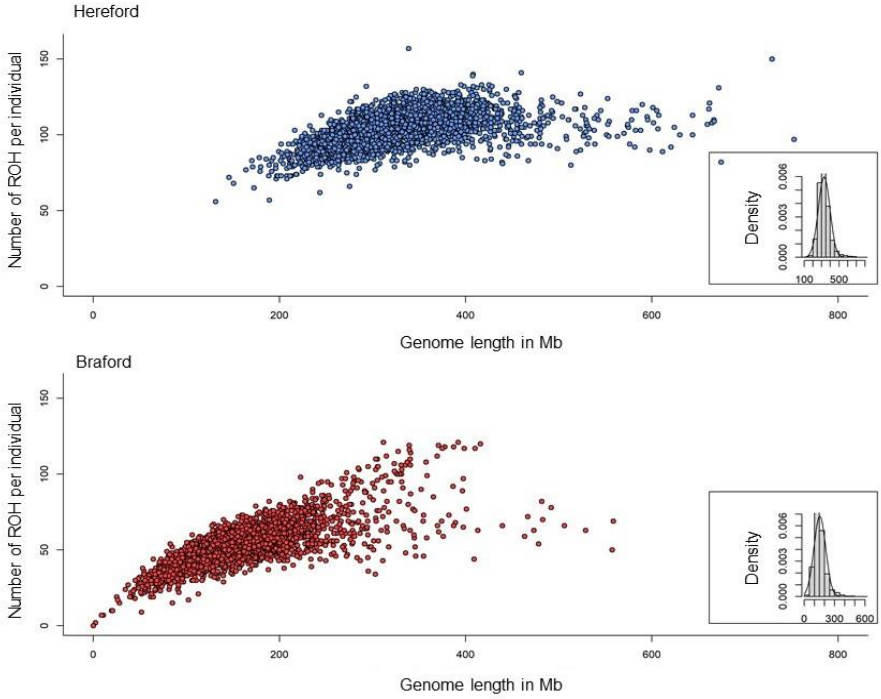

Figure 2. Number runs of homozygosity (ROH) greater than 1 Mb per animal (y-axis) and the total genome size (x-axis) covered by homozygous segments in Hereford (Blue) and Braford (Red) cattle breeds.

3.2. Autozygosity islands and shared ROH regions

ROH islands were identified by taking 1% of the most shared SNPs within a ROH, which corresponds to a frequency threshold of 0.35 (Hereford) and 0.34 (Braford) (Figure 3). A total of 17 autozygosity islands were detected for each breed, and most of the islands overlapped in between the breeds (*n=14*, Supplementary material Table 1). Non-overlapping autozygosity islands were observed for Hereford animals on BTA8 (105,854,420:106,558,356 bp) and BTA9 (19,573,725:20,378,144 bp). For Braford animals, three non-overlapping autozygosity islands were described scattered on BTA1 (78,344,736:78,483,776 bp), BTA12 (69,672,038:71,014,915 bp), and BTA23 (51,620:1.150,966 bp).

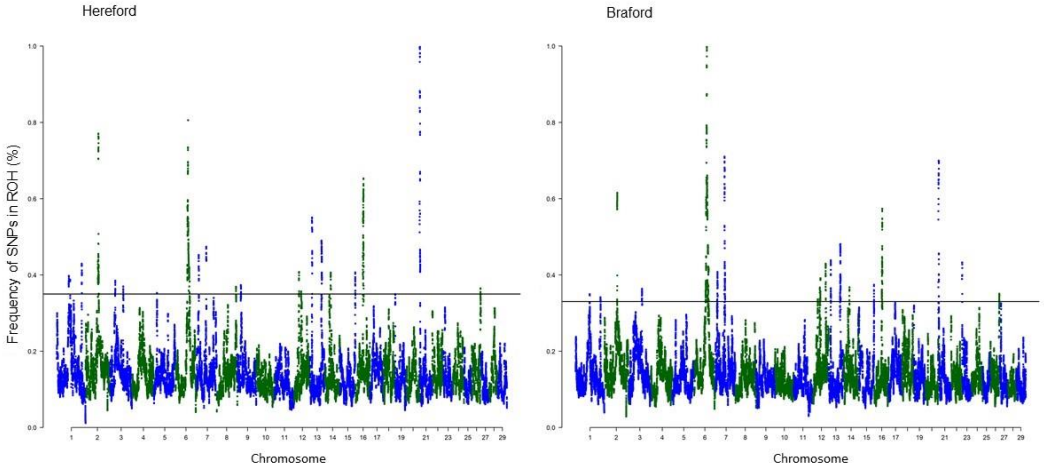

Figure 3. Manhattan plot illustrating the frequency of overlapping homozygous segments in Hereford (Left) and Braford (Right) cattle breeds. The horizontal line represents the top 1% of the most frequent SNPs within a ROH. SNPs above the threshold line correspond to the autozygosity islands.

Besides the autozygosity islands described herein, regions throughout the genome with a high frequency of overlapping ROH within the cattle populations were also described (Supplementary material Table 2), with sharing frequency values varying from 31 to 94%.

3.3. Functional annotation of genes and QTLs located within the autozygosity islands and shared ROH regions

The autozygosity islands harbored a set of genes that covered several molecular functions, biological processes, cellular components, as well as KEGG pathways (Supplementary material Table 3). A set of significant GO terms ($p \leq 0.05$) found in the Hereford breed were associated with milk production traits and fertility in cattle. Among them, we can highlight the Calcium ion cellular homeostasis (GO:0006874) with the main genes located on BTA1, Calcium ion binding (GO:0005509), Cation transport ATPase activity (GO:0019829), Integral component of the plasma membrane (GO:0005887), and Outer side of the plasma membrane (GO:0009897). The KEGG pathways clustered three genes

(*KIT*, *MTOR* and *PDGFRA*) related to Central carbon metabolism in cancer and the Cancer pathway harbored the gene *NRAS* on BTA3.

The Braford cattle displayed the biological process cellular response to reactive oxygen species (GO:0034614) and revealed the *SRC* gene on BTA13 involved in production and milk quality. The homophilic cell adhesion via plasma membrane adhesion molecules (GO:0007156) encompassed the *PCDHA13* gene on BTA7 also related to milk production. The microtubule cell component (GO:0005874) has been linked to lactogenesis and the *CSPP1* gene related to reproduction. The KEGG pathways 'cancer' clustered nine genes located on BTA2, BTA3, BTA6, BTA7, and BTA16. The molecular function lipid binding (GO:0008289), present in both breeds, grouped genes related to marbling traits and meat quality as well as the KEGG pathways serotonergic synapse and endocytosis.

Analyzing the most shared regions between the two cattle breeds, the region on BTA21 (12,664:6,1036,423 bp) shared by 94% of the Hereford individuals and by 31% of the Braford individuals (BTA21 – 12,664:44,239,499 bp) harbored 12 QTLs associated with average daily gain (QTL:164012) (Akanno *et al*., 2018), body weight (QTL:164342) (Akanno *et al*., 2018), metabolic body weight (QTL:154024) (Abo-Ismail *et al*., 2018), residual feed intake (QTL:154025) (Abo-Ismail *et al*., 2018), dry matter intake (QTL:154023)(Abo-Ismail *et al*., 2018), carcass weight (QTL:191340) (Wang *et al*., 2020) , lean meat yield (QTL:164059) (Akanno *et al*., 2018), longissimus muscle area (QTL:11743) (MacNeil and Grosz, 2002), shear force (QTL:20812) (McClure *et al*., 2012), yield grade (QTL:11752) (MacNeil and Grosz, 2002), pregnancy rate QTL:6496500 (Akanno *et al*., 2018), and bovine respiratory disease susceptibility (QTL:160305) (Neupane *et al*., 2018).

The region on BTA2 (21,184,643:122,822,251 bp) identified in 72% of Hereford individuals has been related to 10 QTLs, including average daily gain (QTL:164320) (Akanno *et al*., 2018), body weight (QTL:164342) (Akanno *et al*., 2018), body weight gain (QTL:69169) (Snelling *et al*., 2010), metabolic body weight (QTL:188989) (Zhang *et al*., 2020), dry matter intake (QTL:154023) (Abo-Ismail *et al*., 2018), residual feed intake (QTL:154025) (Abo-Ismail *et al*., 2018),

shear force (QTL:20812) (McClure *et al*., 2012), longissimus muscle area (QTL:164057) (Akanno *et al*., 2018), bovine coronavirus susceptibility (QTL:221240) (Kiser and Neibergs, 2021), and calving ease (QTL:24614) (Saatchi *et al*., 2014).

3.4. Inbreeding coefficients

Inbreeding coefficients were obtained through three different approaches: (i) based on runs of homozygosity (F_{ROH}) for different length sizes; (ii) using the genomic relationship matrix (F_{GRM}), and (iii) based on the pedigree records (F_{PED}). In the Hereford population, 93%, 70%, and 55% of the individuals presented inbreeding values lower than the mean for F_{PED}, F_{GRM}, and $F_{ROH\text{-}mean}$, respectively. In the Braford population, this percentage was 98% (F_{PED}), 40% (F_{GRM}), and 59% ($F_{ROH\text{-}mean}$). Overall, $F_{ROH\text{-}mean}$, $F_{ROH\ 1\text{-}2\ Mb}$, $F_{ROH\ 2\text{-}4\ Mb}$, $F_{ROH\ 4\text{-}8\ Mb}$, and $F_{ROH\ 8\text{-}16\ Mb}$ did not differ from one another by the Kruskall-Walli's test ($p<0.05$) in the Hereford breed, while the $F_{ROH\text{-}mean}$ differed from the other segments lengths in the Braford breed. It is worth mentioning that F_{PED} and F_{ROH} differed from one another ($p<0.05$) in both breeds.

Table 2. Descriptive statistics of the inbreeding coefficients based on the pedigree (F_{PED}), genomic relationship matrix (F_{GRM}), and runs of homozygosity (F_{ROH}) for different lengths ($F_{ROH1–2\ Mb}$, $F_{ROH2–4\ Mb}$, $F_{ROH\ 4–8\ Mb}$, $F_{ROH\ 8\text{-}16\ Mb}$, and $F_{ROH\ >16\ Mb}$).

Coefficients[1]	Hereford					Braford				
	Mean	Minimum	Maximum	SD[1]	n[2]	Mean	Minimum	Maximum	SD[1]	n[2]
F_{PED}	0.003[a]	0	0.156	0.015	2,930	0.001[a]	0	0.25	0.01	3,761
F_{GRM}	0.263[b]	0	0.407	0.059	3,045	0.215[b]	0	0.369	0.049	3,727
$F_{ROH\text{-}Mean}$	0.132[c]	0.053	0.303	0.026	3,183	0.061[c]	0.001	0.224	0.023	3,853
$F_{ROH\ 1\text{-}2\ Mb}$	0.028[c]	0.012	0.051	0.004	3,183	0.016[d]	0.099	0.365	0.004	3,853
$F_{ROH\ 2\text{-}4\ Mb}$	0.034[c]	0.104	0.057	0.007	3,183	0.016[d]	0	0.05	0.006	3,852
$F_{ROH\ 4\text{-}8\ Mb}$	0.035[c]	0.006	0.074	0.01	3,183	0.015[d]	0	0.063	0.008	3,816
$F_{ROH\ 8\text{-}16\ Mb}$	0.021[c]	0	0.073	0.011	3,142	0.009[f]	0	0.059	0.007	3,224
$F_{ROH\ >16\ Mb}$	0.013[d]	0	0.176	0.019	2,013	0.006[g]	0	0.154	0.012	1,400

[1]SD= standard deviation, [2]n= number of genotyped animals. Different letters within the column is significantly different from one another by the Kruskall-Walli's test.

When comparing Hereford and Braford cattle breeds, they differed from one another ($p<0.05$, Table 3), in which Hereford animals displayed a higher inbreeding coefficient than did the Braford.

Table 3. Comparison of the inbreeding coefficients based on the pedigree (F_{PED}), genomic relationship matrix (F_{GRM}), and runs of homozygosity (F_{ROH}) for different lengths ($F_{ROH\ 1–2\ Mb}$, $F_{ROH2–4\ Mb}$, $F_{ROH\ 4–8\ Mb}$, $F_{ROH\ 8\text{-}16\ Mb}$, and $F_{ROH\ >16\ Mb}$) between Hereford and Braford cattle breeds.

Coefficients[1]	F_{PED}	F_{GRM}	$F_{ROH\text{-}Mean}$	$F_{ROH\ 1\text{-}2\ Mb}$	$F_{ROH\ 2\text{-}4\ Mb}$	$F_{ROH\ 4\text{-}8\ Mb}$	$F_{ROH\ 8\text{-}16\ Mb}$	$F_{ROH\ >16\ Mb}$
Hereford	0.003[a]	0.263[a]	0.132[a]	0.028[a]	0.034[a]	0.035[a]	0.021[a]	0.013[a]
Braford	0.001[b]	0.215[b]	0.061[b]	0.016[b]	0.016[b]	0.149[b]	0.009[b]	0.006[b]

Different letters within the column are significantly different from one another ($p<0.05$) by the Friedman test ($p<0.05$).

In the Hereford breed, the $F_{ROH\text{-}Mean}$ had a low correlation with F_{GRM} (0.29) and F_{PED} (0.26). F_{PED} had the highest correlation with $F_{ROH\ 8\text{-}16\ Mb}$ (Figure 4). In the Braford breed, the correlation between the $F_{ROH\text{-}mean}$ and F_{GRM} (0.44) was moderate. Further, F_{PED} correlations were very low when comparing with F_{GRM} and F_{ROH} (Figure 5).

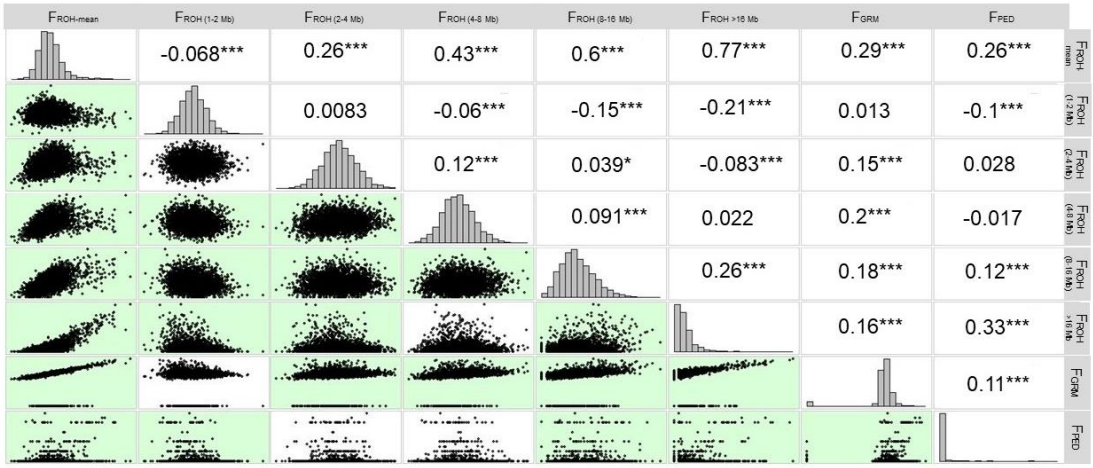

Figure 4. Scatter plot (lower panel) and correlations (upper panel) of inbreeding coefficients based on the pedigree (F_{PED}), genomic relationship matrix (F_{GRM}), and runs of homozygosity (F_{ROH}) for different lengths ($F_{ROH\ 1–2\ Mb}$, $F_{ROH2–4\ Mb}$, $F_{ROH\ 4–8\ Mb}$, $F_{ROH\ 8\text{-}16\ Mb}$, and $F_{ROH\ >16\ Mb}$) for the Hereford cattle breed. *$p<0.05$, ***$p<0.001$.

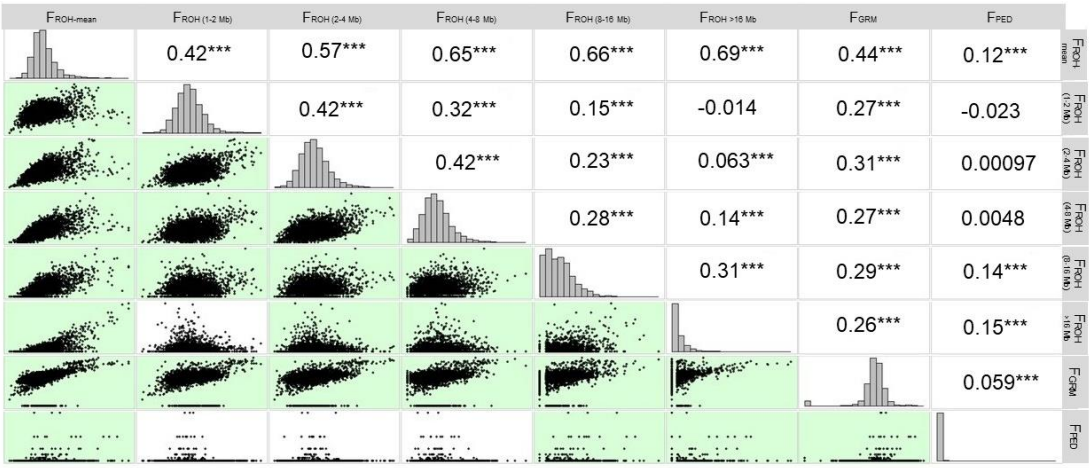

Figure 5. Scatter plot (lower panel) and correlations (upper panel) of inbreeding coefficients based on the pedigree (F_{PED}), genomic relationship matrix (F_{GRM}), and runs of homozygosity (F_{ROH}) for different lengths ($F_{ROH\ 1–2\ Mb}$, $F_{ROH2–4\ Mb}$, $F_{ROH\ 4–8\ Mb}$, $F_{ROH\ 8\text{-}16\ Mb}$, and $F_{ROH\ >16\ Mb}$) for the Braford cattle breed. ***p<0.001.

4. Discussion

4.1. ROH detection and classification

Our results strongly support those obtained by other authors for different cattle breeds. The presence of ROH_{Short} was evident throughout the genome (79% Hereford and 82% Braford), as described for other taurine cattle breeds (Purfield *et al*., 2012; Zhao *et al*., 2021) and indicine (Peripolli *et al*., 2018a). According to Ferenčaković *et al*., (2013), the analysis is more sensitive when using a high-density SNP array, and it allows identifying short and less biased ROH. $ROH_{2\text{-}4\ Mb}$ correspond to inbreeding events approximately 22 generations ago (Howrigan *et al*., 2011), which corroborates the arrival of the first Hereford animals in southern Brazil in 1907 (ABHB, 2020). Further, $ROH_{Short\ (1\text{-}2\ Mb)}$ describes inbreeding events even much further back than 50 generations ago, probably stemming from the breed's formation that originated in the mid-1700s in Hereford-shire, UK (Blott *et al*., 1998).

Braford animals exhibited fewer segments per individual 52±13.2, which were shorter (average 152.86 Mb) compared to Hereford animals (103±11 ROH of 328 Mb on average). The crossing between indicine and taurine animals

increases genetic diversity and contributes to the interruption of long stretches of homozygous genotypes within individuals (Purfield *et al*., 2012), however, the persistence and frequency of these segments in crossed populations still needs to be better elucidated (Peripolli *et al*., 2020). The average ROH length in the Hereford breed is relatively shorter than that described by Sumreddee *et al*. (2019) in a Hereford strain from the United States, which is more closed and inbred herd (89 ROH and 574.7 Mb). The ROH length identified in Braford animals is lower than that reported by Peripolli *et al*. (2020) in Montana crossbreed cattle (with an average size of 7,73 Mb)

Other studies with beef cattle, including Hereford, also showed a higher frequency of ROH on BTA1 (Gurgul *et al*., 2016; Mastrangelo *et al*., 2016; Purfield *et al*., 2012). In Braford, the highest frequency was on BTA6. The number of ROH is positively correlated with the length of the autosomes (Zhao *et al*., 2020).

The high ROH frequency in these chromosomes can be explained by the directional selection applied in these populations, in which nucleotides linked to favorable mutations have their frequencies increased during selection and their variability reduced over time, forming ROH hotspots/islands (Purfield *et al*., 2012). Inspecting BTA1 and BTA6, other studies have located QTLs related to weight gain and residual food consumption (Lu *et al*., 2013), genes involved in milk production (Jiang *et al*., 2019), and Hereford coat pattern (Pausch *et al*., 2012). All these traits are part of the improvement program applied to these breeds (ABHB, 2020).

4.2. Functional annotation of genes located within the autozygosity islands

Autozygosity islands were distributed throughout the genome in both cattle breeds, and many of these regions were found to overlap likely due to the Braford racial makeup, in which 5/8 derive from the Hereford breed. The functional enrichment analysis made it possible to understand the functions of the biological system (Peñagaricano *et al*., 2013), in which genes were grouped according to their function (Milano, 2018; Tang *et al*., 2018) allowing a better interpretation of the data, as described below:

(I) Biological process: (a) Dendritic morphogenesis (GO:0048813) encompassed the *PREX2* gene (BTA7), which has been associated with QTL carcass weight in Hanwoo beef cattle (Li *et al*., 2017), an important trait for beef cattle such as Hereford and Braford. (b) (b) Homophilic cell adhesion via plasma membrane adhesion molecules (GO:0007156) was significant for both cattle breeds, however the *PCDHA13* (BTA7) gene was only described for the Braford breed. Such gene is associated with milk production characteristics in Holstein cattle (*Bos taurus taurus*) (Cole *et al*., 2011)(c) Cellular response to reactive oxygen species (GO:0034614), with emphasis on the *SRC* gene (BTA13), which is also related to QTLs for milk production and quality in Holstein cattle (Cole *et al*., 2011). Such milk-related traits can be attributed to the heterosis, that allowed Braford cows to increase milk production and quality (Leal *et al*., 2018).

(II) Cellular component: (a) Outer side of the plasma membrane (GO:0009897) was significant for the Hereford breed, in which the *KIT* gene has been associated with QTLs linked to eye area pigmentation in Fleckvieh cattle (Pausch *et al*., 2012). Eye area pigmentation is an important trait of adaptation, and it is part of the selection objectives of the Hereford breed (Reimann *et al*., 2018). (b) Microtubule (GO:0005874) was significant for the Braford breed, in which the *CSPP1* gene (BTA14) was related to reproductive traits in Holstein bulls and cows (Cochran *et al*., 2013; Ortega *et al*., 2017). (c) Integral component of the plasma membrane (GO:0005887) was significant for the Hereford breed, highlighting the *ADGRL3* (BTA6) gene for traits associated with milk production and quality (Jiang *et al*., 2019).

(III) Molecular function: (a) Lipid binding (GO:0008289), which was present in both breeds. Its function has been associated with marbling, dorsal fat thickness, and rib eye area in Hanwoo cattle (Yoon and Ko, 2016). The *BPIFB1, BPIFA3, BPIFA1, BPIFB5,*

BPIFA2B, and *BPIFA2C* genes (BTA13) encompassing this molecular function were also identified within the ROH islands in Nellore bulls with extreme phenotypes for fatty acid composition of intramuscular fat (Schettini *et al*., 2022). The *DBI* gene is involved in meat quality-related traits, fatty acid oxidation, biosynthesis, and lipid storage (Edea *et al*., 2020). (b) Calcium ion binding (GO:0005509) in Hereford cattle was associated with bull fertility (Peñagaricano *et al*., 2013); the *ADGRE3 gene* (BTA7) is associated with fertility in Holstein heifers (Galliou *et al*., 2020); the *ADGRL3* gene (BTA6) is related to milk production and protein QTLs in US Holstein cattle (Jiang *et al*., 2019). Previous studies suggest that the *MASP2* gene (BTA16) has a relationship with milk quality and mastitis (Zhang *et al*., 2019), in addition to participating in the immune function. Besides, its lower expression has been reported in Holstein animals susceptible to pneumococcal meningitis (Chen *et al*., 2019).

(IV) Metabolic pathways: (a) Central carbon metabolism in cancer KEGG pathway (Hereford) and Cancer KEGG pathway (Braford), identified the *KIT* and *PDGFRA* genes (BTA6) and the *MTOR* gene (BTA16). Their main functions are associated with cell proliferation regulation, including tumor proliferation, metastasis, and neovascularization (Ma *et al*., 2018). The coat pattern in cattle is largely influenced by the allele series at the spotting locus that includes the s^H allele, which maps to the same region as the *KIT* gene, suggesting that the presence of the *KIT* gene with the s^H allele is responsible for the expression of the Hereford coat pattern (Pausch *et al*., 2012). Previous studies carried out by Gross end MacNeil (1999), suggest that the combination of the s^H allele with the *KIT* gene can alter the expression of nearby genes, causing mutations, anemia, and ocular squamous cell carcinoma. It is known that the absence of ocular pigmentation is directly associated with the incidence of ocular carcinoma (Pausch *et al*.,

2012). Therefore, researchers are looking for animals more adapted to ultraviolet radiation exposure since this trait has a high direct additive genetic variance (46%) (Reimann *et al*., 2018). This conserved region on BTA6 that harbors the *KIT* gene has already been described by other authors as a strong hotspot of selection signatures in cattle (Adebambo, 2001; Durkin *et al*., 2012; Fariello *et al*., 2014; Hayes *et al*., 2010; Henkel *et al*., 2019; Ma *et al*., 2015; Qanbari and Simianer, 2014). It should be noted that the coat uniformity is strongly selected by the breeders and monitored by the cattle associations, seeking for animals within the purity standards of the breed; (b) Serotonergic synapse KEGG pathway harbored the *CACNA1A* gene (BTA7), which has been associated with heifer conception rate and pregnancy rate in dairy cows (Gaddis *et al*., 2016). Further, the *GABRB1* gene (BTA6) is a candidate gene that affects sensory attributes, such as meat color in Nellore cattle (Marín-Garzón *et al*., 2021). It is also related to carcass conformation score in Piedmontese cattle (Pegolo *et al*., 2020) and live weight in Simmental cattle (Fan *et al*., 2015); (c) Endocytosis KEGG pathway was significant for both breeds, in which the *PDGFRA* gene (BTA6) plays an important role in regulating many biological processes, including embryonic development, angiogenesis, and cell proliferation and differentiation (Ma *et al*., 2018).

The region on BTA2 shared by 72% of Hereford individuals harbors QTLs associated with body weight traits (MacNeil and Grosz, 2002), feed intake (Seabury *et al*., 2017), and meat quality (MacNeil and Grosz, 2002; Wang *et al*., 2020). The SNPrs29015781 was present in this region, described by Sollero *et al*., (2017) in Hereford and Braford cattle when selecting marker SNPs to predict tick resistance.

The BTA6 region (17,798,998:112,785,714 bp) displayed the highest share within the Braford animals (33%), and it also overlapped with the Hereford cattle. This region was found to harbor 37 QTLs, which have been associated

with fertility traits in Nellore (Irano *et al*., 2016) and Brahman (Hawken *et al*., 2012) cattle. In Hereford cattle, this region was associated with body weight QTLs at birth and weaning and weight gain (Snelling *et al*., 2010). It is also worth mentioning that the region on BTA7 (20,731,094:88,787,004) shared by 32% of Braford individuals contains QTLs associated with weight gain in beef cattle (Collis *et al*., 2012), feed efficiency in Nelore cattle (Brunes *et al*., 2021), meat quality in Brahman cattle (Barendse *et al*., 2008; Leal-Gutiérrez *et al*., 2019), shear force in Hereford, Brahman and Nellore cattle (Bolormaa *et al*., 2011; McClure *et al*., 2012; Pinto *et al*., 2010), body weight in Brahman heifers (Porto-Neto *et al*., 2015), fat thickness in the loin eye area in Nellore cattle (Martins *et al*., 2021; Santana *et al*., 2015), reproductive and sexual precocity traits in Nellore and Brahman cattle (Hawken *et al*., 2012; Melo *et al*., 2018), and bovine respiratory disease in beef feedlot cattle (Neupane *et al*., 2018).

The region on BTA13 (213,132:83,457,015 bp) shared by 52% of the Hereford animals showed 134 QTLs associated with average daily gain in beef cattle (Zhang *et al*., 2020), 18 QTLS with bovine respiratory disease susceptibility (Neupane *et al*., 2018), 163 QTLs with body weight gain traits (Snelling *et al*., 2010) and residual consumption in beef cattle (Zhang *et al*., 2020), and four QTLs involved in tick resistance (Sollero *et al*., 2017).

On BTA16 (195,314:75,997,329 bp), the region found to be shared by 56% of the Hereford animals encompassed QTLs involved in weight gain (Abo-Ismail *et al*., 2018; Snelling *et al*., 2010), meat quality and yield (Abo-Ismail *et al*., 2014; Bolormaa *et al*., 2011; Saatchi *et al*., 2014; Snelling *et al*., 2010), bovine respiratory disease susceptibility (Neupane *et al*., 2018), tick resistance (Sollero *et al*., 2017), and feed intake (Abo-Ismail *et al*., 2018; Zhang *et al*., 2020).

Shared by 94% of Hereford animals and 31% of Braford animals, the region on BTA21 (12,664:61,036,423 bp) was associated with 61 QTLs mainly involved in Brahman cattle fertility traits (Frischknecht *et al*., 2017; Hawken *et al*., 2012; Melo *et al*., 2019, 2018; Saatchi *et al*., 2014), carcass quality (Akanno *et al*., 2018; Fernandes *et al*., 2016; Santana *et al*., 2015), weight gain (Akanno *et al*., 2018; Oliveira *et al*., 2014; Snelling *et al*., 2010), feed efficiency (Abo-Ismail

et al., 2018; Seabury *et al*., 2017), and susceptibility to bovine respiratory diseases (Neupane *et al*., 2018).

These results indicate that many SNPs contribute to the variation and differentiation of these traits, in which each QTL explains only a fraction of the phenotypic variation of complex traits that are controlled by a series of genes (Ibeagha-Awemu *et al*., 2008). These conserved and shared regions are important for understanding the selection, in which several authors (Szmatoła *et al*., 2019; Xu *et al*., 2019; Zhang *et al*., 2015b) suggest that ROH hotspots shared between individuals are caused by selection, which probably acted to keep regions originating from IBD (identical by descent) segments conserved. Given that these QTLs indicate traits that were and are under intense selection in both breeds, such as the historical selection to fix the S^H allele responsible for the coat color phenotype in the Hereford and Braford breeds (5/8 Hereford), ingestion traits and body weight gain, loin eye area, have already been reported in other studies in these breeds (Biegelmeyer *et al*., 2016; Grosz and MacNeil, 1999).

4.3. Inbreeding coefficients

The average F_{ROH} value (0.132) for the Hereford breed is lower than those obtained by Sumreddee *et al*. (2019) and Pilon *et al*. (2021), with $F_{ROH\text{-}mean}$ of 0.229 and 0.32 in a Hereford strain from the United States, respectively. However, the average autozygotic proportion of the Hereford genome is comparatively high as those described in Brown Swiss cattle (M. Ferenčaković *et al*., 2013) $F_{ROH\text{-}mean}$ of 15%. Several studies in cattle have shown a negative effect of inbreeding on productive traits (Baes *et al*., 2019; Cleveland *et al*., 2005; Leroy, 2014; Mc Parland *et al*., 2008; Pariacote *et al*., 1998; Reverter *et al*., 2017; Santana *et al*., 2010; Sumreddee *et al*., 2021, 2019)

The $F_{ROH\text{-}mean}$ value (0.061) for the Braford breed is lower than that reported in Brahman ($F_{ROH\text{-}mean}$ 0.530) and tropical composite ($F_{ROH\text{-}mean}$ 0.423) cattle using a 700k panel (Reverter *et al*., 2017).

The F_{PED} estimates usually does not show the real relationship among individuals since it is estimated from statistical expectations of the probable IBD

genomic proportion (Zavarez *et al*., 2015). It should be noted that the highest correlations for F_{PED} were described for $F_{ROH>16\ Mb}$, in which the length of the ROH and the pedigree depth are the two main factors controlling the correlation between them (Sumreddee *et al*., 2019).

The Hereford F_{PED} value (0.003) was lower than that found by Piccoli *et al*. (2014) who also worked with Hereford samples (*n=245,942* animals), finding an average F_{PED} of 0.0116. The mean value of F_{PED} (0.001) for the Braford breed was lower than that found by Peripolli *et al*. (2020) in Montana cattle and it was higher than the mean value of 0.0006 found by Lopa (2015) in the Brazilian Braford cattle breed. The F_{PED} in the Braford breed was also lower than the mean value found here for the Hereford breed (0.003). Estimates of inbreeding in Braford animals reflect the fact that it is a composite breed (Kelleher *et al*., 2017; Lopa, 2015), in which the introduction of new animals to explore the complementarity between breeds allows different genetic combinations leading to a decrease in inbreeding, in addition to breaking the long segments of ROH (Peripolli *et al*., 2020).

The F_{GRM} and $F_{ROH\text{-}Mean}$ differed ($p<0.05$) within the breeds. Such result was expected since the F_{GRM} captures all homozygous segments in the genome, in which the calculations to obtain the **G** matrix depend on the allele frequencies, being sensitive compared to methods based on chromosome segments such as F_{ROH} (Zhang *et al*., 2015a). Low correlations between F_{GRM} and F_{PED} for both cattle breeds described herein corroborate to previous studies that reported weak or no correlations between these two estimators (Gurgul *et al*., 2016; Marras *et al*., 2015; Peripolli *et al*., 2018; Purfield *et al*., 2012; Sumreddee *et al*., 2019; Zhang *et al*., 2015a).

5. Final considerations

Runs of homozygosity allow a more accurate understanding of the proportion of the homozygous genome. Hereford animals showed more and larger ROH segments when compared to Braford animals, as they are a pure breed and are more subject to inbreeding. The Braford population had fewer ROH when compared to other composite breeds due to crosses to obtain the degree of blood. The autozygosity islands were distributed throughout the genome in both cattle breeds, and many of these regions were found to overlap between them. The ROH islands and shared ROH regions encompassed a relevant number of genes and QTLs related to traits of economic importance, i.e., meat quality, body weight, milk production and fertility, as well as genes that express the racial pattern of these breeds. These findings provide evidence that ROH patterns can be used to track regions of genomic hotspots that harbor selection signatures. The low correlation between F_{PED} and short F_{ROH} evidenced the superficiality of the pedigree, corroborating to the concept that F_{ROH} can capture deeper levels of individual autozygosity. Inbreeding estimates suggest that F_{ROH} can be a useful estimator of individual autozygosity for the studied breeds, helping to monitor inbreeding levels in regions of the genome that harbor important genes for herd productivity.

Acknowledgment

The present work was carried out with the support of the Coordination for the Improvement of Higher Education Personnel - Brazil (CAPES) – Financing code 001. The authors thanks to the Empresa Brasileira de Pesquisa Agropecuária - Embrapa Pecuária Sul (Bagé/RS) and Delta G connection for providing the datasets.

REFERENCES

ABHB - ASSOCIAÇÃO BRASILEIRA DE HEREFORD E BRAFORD. **As raças Hereford e Braford**. Bagé: ABHB, 2020. Disponível em: https://www.abhb.com.br/. Acesso em: 14 nov. 2022.

ABIEC – ASSOCIAÇÃO BRASILEIRA DAS INDÚSTRIAS EXPORTADORAS DE CARNES. **Beef report 2022:** perfil da pecuária no Brasil. São Paul: ABIEC, 2022. Disponível em: https://www.abiec.com.br/publicacoes/beef-report-2022/. Acesso em: 16 set. 2022.

ABO-ISMAIL, M. K. *et al*. Development and validation of a small SNP panel for feed efficiency in beef cattle. **Journal of Animal Science**, Champaign, v. 96, n. 2, p. 375–397, 2018. Disponível em: https://doi.org/10.1093/jas/sky020. Acesso em: 05 set 2022.

ADEBAMBO, O. A. The Muturu: a rare sacred breed of cattle in Nigeria. **Animal Genetic Resources Information**, v. 31, p. 27-36, 2001. Disponível em: https://doi.org/10.1017/s1014233900001450. Acesso em: 15 set 2021.

AGUILAR, I.; MISZTAL, I. Technical note: Recursive algorithm for inbreeding coefficients assuming nonzero inbreeding of unknown parents. **Journal of Dairy Science**, Champaign, v. 91, n. 4, p. 1669-1672, 2008. Disponível em: https://doi.org/10.3168/jds.2007-0575. Acesso em: 01 out 2022.

AKANNO, E. C. *et al*. Genome-wide association scan for heterotic quantitative trait loci in multi-breed and crossbred beef cattle. **Genetics Selection Evolution**, Paris, v. 50, n. 1, [art.] 48, 2018. Disponível em: https://doi.org/10.1186/s12711-018-0405-y. Acesso em: 10 nov. 2021.

BAES, C. F. *et al.* Symposium review: the genomic architecture of inbreeding: How homozygosity affects health and performance. **Journal of Dairy Science**, Champaign, v. 102, n. 3, p. 2807–2817, 2019.

BARENDSE, W. *et al*. Variation at the Calpain 3 gene is associated with meat tenderness in zebu and composite breeds of cattle. **BMC Genetics**, London, v. 9, [art.] 41, 2008. Disponível em: https://doi.org/10.1186/1471-2156-9-41. Acesso em:01 out. 2020.

BIEGELMEYER, P. *et al*. Linkage disequilibrium, persistence of phase and effective population size estimates in Hereford and Braford cattle. **BMC Genetics**, London, v. 17, n. 1, [art.] 32, 2016.

BISCARINI, F. *et al*. Insights into genetic diversity, runs of homozygosity and heterozygosity-rich regions in maremmana semi-feral cattle using pedigree and genomic data. **Animals**, Basel, v. 10, n. 12, [art.] 2285, 2020.

BLOTT, S. C.; WILLIAMS, J. L.; HALEY, C. S. Genetic variation within the Hereford breed of cattle. **Animal Genetics**, Oxford, v. 29, n. 3, p. 202-211, 1998. Disponível em: https://doi.org/10.1046/j.1365-2052.1998.00326.x. Acesso em: 02 dez. 2020.

BOLORMAA, S. *et al*. Detection of chromosome segments of zebu and taurine origin and their effect on beef production and growth. **Journal of Animal Science**, Champaign, v. 89, n. 7, p. 2050-2060, 2011. Disponível em: https://doi.org/10.2527/jas.2010-3363. Acesso em: 02 out. 2021.

BRUNES, L.C. *et al.* Weighted single-step genome-wide association study and pathway analyses for feed efficiency traits in Nellore cattle. **Journal of Animal Breeding and Genetics**, Berlin, v. 138, n. 1, p. 23-44, 2021. Disponível em: https://doi.org/10.1111/jbg.12496. Acesso em: 03 mar 2022.

CHEN, S. *et al*. Genetic variants of fatty acid elongase 6 in Chinese Holstein cow. **Gene**, Amsterdam, v. 670, p. 123-170, 2018.

CLAYTON, D. **SNPSTATS:** SnpMatrix and XSnpMatrix Classes and Methods. [Vienna]: R Package Documentation, 2014.

CLEVELAND, M. A. *et al*. Changes in inbreeding of U.S. Herefords during the twentieth century. **Journal of Animal Science**, Champaign, v. 83, n. 5, p. 992-1001, 2005. Disponível em: https://doi.org/10.2527/2005.835992x. Acesso em: 02 abr. 2021.

COCHRAN, S. D. *et al*. Discovery of single nucleotide polymorphisms in candidate genes associated with fertility and production traits in Holstein cattle. **BMC Genetics**, London, v. 14, [art.] 49, 2013.

COLE, J. B. *et al*. Genome-wide association analysis of thirty one production, health, reproduction and body conformation traits in contemporary U.S. Holstein cows. **BMC Genomics**, London, v. 12, [art.] 408, 2011.

COLLIS, E. *et al*. Genetic variants affecting meat and milk production traits appear to have effects on reproduction traits in cattle. **Animal Genetics**, Oxford, v. 43, p. 442–446, 2012. Disponível em: https://doi.org/10.1111/j.1365-2052.2011.02272.x. Acesso em:16 nov. 2022.

CURIK, I.; FERENČAKOVIĆ, M.; SÖLKNER, J. Inbreeding and runs of homozygosity: a possible solution to an old problem. **Livestock Science**, Amsterdam, v. 166, n. 1, p. 26–34, 2014.

DURKIN, K. *et al*. Serial translocation by means of circular intermediates underlies colour sidedness in cattle. **Nature**, London, v. 482, n. 7383, p. 81-84, 2012. Disponível em: https://doi.org/10.1038/nature10757. Acesso em: 18 nov 2022.

EDEA, Z. *et al*. Signatures of positive selection underlying beef production traits in Korean cattle breeds. **Journal of Animal Science and Technology**, Seoul, v. 62, n. 3, p. 293-305, 2020. Disponível em: https://doi.org/10.5187/JAST.2020.62.3.293. Acesso em:14 out. 2022.

EUSEBI, P. G.; MARTINEZ, A.; CORTES, O. Genomic tools for effective conservation of livestock breed diversity. **Diversity**, Basel, v. 12, n. 1, [art.] 8, 2020. Disponível em: https://doi.org/10.3390/d12010008. Acesso em: 01 mar. 2021.

FAN, H. *et al*. Pathway-based genome-wide association studies for two meat production traits in simmental cattle. **Scientific Reports**, London, v. 5, [art.] 18389, 2015. Disponível em: https://doi.org/10.1038/srep18389. Acesso em: 05 dez. 2021.

FARIELLO, M. I. *et al*. Selection signatures in worldwide sheep populations. **PLoS One**, San Francisco, v. 9, n. 8. [art.] e103813, 2014. Disponível em: https://doi.org/10.1371/journal.pone.0103813. Acesso em: 22 set. 2021.

FERENČAKOVIĆ, M.; SÖLKNER, J.; CURIK, I. Estimating autozygosity from high-throughput information: effects of SNP density and genotyping errors. **Genetics Selection Evolution**, Paris, v. 45, [art.] 42, 2013.

FERNANDES JÚNIOR, G.A. *et al*. Genome scan for postmortem carcass traits in nellore cattle. **Journal of Animal Science**, Champaign, v. 94, n. 10, p. 4087-4095, 2016. Disponível em: https://doi.org/10.2527/jas.2016-0632. Acesso em:25 nov 2021.

FREITAS, P. H. F. *et al*. Genetic diversity and signatures of selection for thermal stress in cattle and other two bos species adapted to divergent climatic conditions. **Frontiers in Genetics**, Lausanne, v.12, [art.] 604823, 2021. Disponível em: https://doi.org/10.3389/fgene.2021.604823. Acesso em: 24 abr. 2022.

FRISCHKNECHT, M. *et al*. Genome-wide association studies of fertility and calving traits in Brown Swiss cattle using imputed whole-genome sequences. **BMC Genomics**, London, v. 18, n. 1, [art.] 910, 2017. Disponível em: https://doi.org/10.1186/s12864-017-4308-z. Acesso em: 11 maio 2021.

GADDIS, K. L.; NULL, D. J.; COLE, J. B. Explorations in genome-wide association studies and network analyses with dairy cattle fertility traits. **Journal of Dairy Science**, Champaign, v. 99, n. 8, p. 6420-6435, 2016. Disponível em: Disponível em: https://doi.org/10.3168/jds.2015-10444. Acesso em: 19 jul. 2021.

GALLIOU, J. M. *et al*. Identification of loci and pathways associated with heifer conception rate in U.S. holsteins. **Genes**, Basel, v. 11, n. 7, [art.] 767, 2020.

GONZÁLEZ, A. R. M. *et al*. Process of introduction of australian braford cattle to south america: configuration of population structure and genetic diversity evolution. **Animals**, Basel, v. 12, n. 3, [art.] 275, 2022.

GROSZ, M. D.; MACNEIL, M. D. The “spotted” locus maps to bovine chromosome 6 in a Hereford-cross population. **Journal of Heredity**, Cary, v. 90, n. 1, p. 233-236, 1999. Disponível em: https://doi.org/10.1093/jhered/90.1.233. Acesso em: 15 abr. 2021.

GURGUL, A. *et al*. Identification of genome-wide selection signatures in the Limousin beef cattle breed. **Journal of Animal Breeding and Genetics**, Berlin, v. 133, p. 264–276, 2016a. Disponível em: https://doi.org/10.1111/jbg.12196. Acesso em: 15 dez. 2021.

GURGUL, A. *et al.* The use of runs of homozygosity for estimation of recent inbreeding in Holstein cattle. **Journal of Applied Genetics**, Cheshire, v. 57, n. 4, p. 527-530, 2016b. Disponível em: https://doi.org/10.1007/s13353-016-0337-6. Acesso em: 19 set. 2021.

HAWKEN, R. J. *et al*. Genome-wide association studies of female reproduction in tropically adapted beef cattle. **Journal of Animal Science**, Champaign, v. 90, n. 5, p. 1398-1410, 2012. Disponível em: https://doi.org/10.2527/jas.2011-4410. Acesso em: 12 set. 2021.

HAYES, B. J. *et al*. Genetic architecture of complex traits and accuracy of genomic Prediction: Coat colour, Milk-fat percentage, and type in holstein cattle as contrasting model traits. **PLoS Genetics**, San Francisco, v. 6, n. 9, [art.] e1001139, 2010. Disponível em: https://doi.org/10.1371/journal.pgen.1001139. Acesso em: 16 set. 2021.

HENKEL, J. *et al*. Selection signatures in goats reveal copy number variants underlying breed-defining coat color phenotypes. **PLoS Genetics**, San Francisco, v. 15, n. 12, [art.] e1008536, 2019. Disponível em: https://doi.org/10.1371/journal.pgen.1008536. Acesso em: 14 out. 2020.

HOWE, K. L. *et al.* Ensembl 2021. **Nucleic Acids Research**, Oxford, v. 49, n. D1, p. D884-D891, 2021. Disponível em: https://doi.org/10.1093/nar/gkaa942. 01 fev. 2022. Acesso em: 15 out. 2021.

HOWRIGAN, D. P.; SIMONSON, M. A.; KELLER, M. C. Detecting autozygosity through runs of homozygosity: a comparison of three autozygosity detection algorithms. **BMC Genomics**, London, v. 12, [art.] 460, 2011.

HU, Z. L.; PARK, C. A.; REECY, J. M. Developmental progress and current status of the Animal QTLdb. **Nucleic Acids Research**, Oxford, v. 44, n. D1, p. D827-833, 2016. Disponível em: https://doi.org/10.1093/nar/gkv1233. Acesso em: 09 jan. 2022.

HUANG, D. W.; SHERMAN, B. T.; LEMPICKI, R. A. Systematic and integrative analysis of large gene lists using DAVID bioinformatics resources. **Nature Protocols**, London, v. 4, p. 44–57, 2009. Disponível em: https://doi.org/10.1038/nprot.2008.211. Acesso em: 06 jan. 2022.

IBEAGHA-AWEMU, E. M.; KGWATALALA, P.; ZHAO, X. A critical analysis of production-associated DNA polymorphisms in the genes of cattle, goat, sheep, and pig. **Mammalian Genome**, New York, v. 19, n. 9, p. 591-617, 2008. Disponível em: https://doi.org/10.1007/s00335-008-9141-x. Acesso em: 18 nov 2022.

IBGE – INSTITUTO BRASILEIRO DE GEOGRAFIA E ESTATÍSTICA. Diretoria de Pesquisas, Coordenação de Estatísticas Agropecuárias. **Pesquisa da Pecuária Municipal 2021**, Rio de Janeiro, v. 49, p.1-12, 2021. Disponível em: https://biblioteca.ibge.gov.br/visualizacao/periodicos/84/ppm_2021_v49_br_informativo.pdf. Acesso em: 26 set. 2022.

IRANO, N. *et al*. Genome-wide association study for indicator traits of sexual precocity in Nellore cattle. **PLoS One**, San Francisco, v. 11, n. 8, [art.] e015950, 2016. Disponível em: https://doi.org/10.1371/journal.pone.0159502. Acesso em:15 nov. 2021.

JIANG, J. *et al*. A large-scale genome-wide association study in U.S. Holstein cattle. **Frontiers in Genetics**, Lausanne, v. 10, [art.] 412, May 2019.

KELLEHER, M. M. *et al*. Inference of population structure of purebred dairy and beef cattle using high-density genotype data. **Animal**, Cambridge, v. 11, n. 1, p. 15–23, Jan. 2017.

KIM, H.-Y. Statistical notes for clinical researchers: chi-squared test and Fisher's exact test. **Restorative Dentistry & Endodontics**, Seoul, v. 42, n. 2, p. 152-155, 2017.

KISER, J. N.; NEIBERGS, H. L. Identifying loci associated with bovine corona virus infection and bovine respiratory disease in dairy and feedlot cattle. **Frontiers in Veterinary Science**, Lausanne, v. 8, [art.] 679074, 2021. Disponível em: https://doi.org/10.3389/fvets.2021.679074. Acesso em: 15 set 2022.

LEAL, W. S. *et al*. Direct and maternal breed additive and heterosis effects on growth traits of beef cattle raised in southern Brazil. **Journal of Animal Science**, Champaiggn, v. 96, n. 7, p. 2536-2544, 2018. Disponível em: https://doi.org/10.1093/jas/sky160. Acesso em: 01 fev 2021.

LEAL-GUTIÉRREZ, J. D. *et al*., Genome wide association and gene enrichment analysis reveal membrane anchoring and structural proteins associated with meat quality in beef. **BMC Genomics**, London, v. 20, [art.] 151, 2019.

Disponível em: https://doi.org/10.1186/s12864-019-5518-3. Acesso em: 16 fev 2021.

LEROY, G. Inbreeding depression in livestock species: review and meta-analysis. **Animal Genetics**, Oxford, v. 45, n. 5, p. 618-628, 2014. Disponível em: https://doi.org/10.1111/age.12178. Acesso em:16 mar 2020.

LI, Y. *et al*. A whole genome association study to detect additive and dominant single nucleotide polymorphisms for growth and carcass traits in Korean native cattle, Hanwoo. **Asian-Australasian Journal of Animal Sciences**, Seoul, v. 30, n. 1, p. 8-19, 2017. Disponível em: Disponível em: https://doi.org/10.5713/ajas.16.0170. Acesso em: 19 maio 2020.

LOPA, Thais Maria Bento Pires. **Estudo da estrutura populacional da raça Braford com base no pedigree**. 2015. 59 f. Dissertação (Mestrado em Ciência Animal) - Universidade Federal do Pampa, Campus Uruguaiana, Uruguaiana, 2015.

LOZADA-SOTO, E. A. *et al*. Trends in genetic diversity and the effect of inbreeding in American Angus cattle under genomic selection. **Genetics Selection Evolution**, Paris, v. 53, n. 1, [at.] 50, 2021. Disponível em: https://doi.org/10.1186/s12711-021-00644-z. Acesso em: 15 abr 2022.

Lu LU, D. *et al*. Genome-wide association analyses for carcass quality in crossbred beef cattle. **BMC Genetics**, London, v. 14, [art.] 80, 2013. Disponível em: https://doi.org/10.1186/1471-2156-14-80. Acesso em: 19 jun 2021.

MA, N. *et al*. Analyzing the molecular mechanism of the tissue specificity of gastrointestinal stromal tumors by using bioinformatics approaches. **Journal of BUON**, Nicosia, v. 23, n. 4, p. 1149-1155, 2018.

MA, Y. *et al*. A genome scan for selection signatures in pigs. **PLoS One**, San Francisco, v. 10, n. 3, [art.] e0116850, 2015. Disponível em: https://doi.org/10.1371/journal.pone.0116850. Acesso em: 16 jul 2021.

MACNEIL, M. D.; GROSZ, M. D. Genome-wide scans for QTL affecting carcass traits in Hereford x composite double backcross populations. **Journal of Animal Science**, Champaign, v. 80, n. 9, p. 2316-2324, 2002. Disponível em: https://doi.org/10.1093/ansci/80.9.2316. Acesso em: 19 jul 2021.

MARÍN-GARZÓN, N. A. *et al*. Genome-wide association study identified genomic regions and putative candidate genes affecting meat color traits in Nellore cattle. **Meat Science**, Oxford, v. 171, [art.] 108288, 2021. Disponível em: https://doi.org/10.1016/j.meatsci.2020.108288. Acesso em: 25 jul 2021.

MARRAS, G. *et al*. Analysis of runs of homozygosity and their relationship with inbreeding in five cattle breeds farmed in Italy. **Animal Genetics**, Oxford, v. 46, n. 2, p. 110–121, Apr. 2015.

MARTINS, R. *et al.* Genome-wide association study and pathway analysis for fat deposition traits in nellore cattle raised in pasture–based systems. **Journal of Animal Breeding and Genetics**, Berlin, v. 138, n. 3, p. 360-378, 2021. Disponível em: https://doi.org/10.1111/jbg.12525. Acesso em: 28 nov. 2022.

MASTRANGELO, S. *et al*. Genomic inbreeding estimation in small populations: evaluation of runs of homozygosity in three local dairy cattle breeds. **Animal**, Cambridge, v. 10, p. 746–754, 2016. Disponível em: https://doi.org/10.1017/S1751731115002943. Acesso em: 20 nov. 2021.
MCCLURE, M. C. *et al*. Genome-wide association analysis for quantitative trait loci influencing Warner-Bratzler shear force in five taurine cattle breeds. **Animal Genetics**, Oxford, v. 43, n. 6, p. 662-673, 2012. Disponível em: https://doi.org/10.1111/j.1365-2052.2012.02323.x. Acesso em: 15 set 2020.

MCPARLAND, S. *et al*. Inbreeding effects on postweaning production traits, conformation, and calving performance in Irish beef cattle. **Journal of Animal Science**, Champaign, v. 86, n. 12, p. 3338-3347, 2008. Disponível em: https://doi.org/10.2527/jas.2007-0751. Acesso em: 15 set 2020.

MCQUILLAN, R. *et al*. Runs of homozygosity in european populations. **American Journal of Human Genetics**, Cambridge, v. 83, n. 3, p. 359–372, 2008.

MELO, T. P. *et al.* Multitrait meta-analysis identified genomic regions associated with sexual precocity in tropical beef cattle. **Journal of Animal Science**, Champaign, v. 96, n. 10, p. 4087-4099, 2018. Disponível em: https://doi.org/10.1093/jas/sky289. Acesso em: 15 set. 2020.

MELO, T. P. *et al.* Multitrait meta-analysis identified genomic regions associated with sexual precocity in tropical beef cattle. **Journal of Animal Science**, Champaign, v. 96, n. 10, p. 4087-4099, 2018. Disponível em: https://doi.org/10.1093/jas/sky289. Acesso em: 15 set. 2020.

METZGER, J. *et al*. Runs of homozygosity reveal signatures of positive selection for reproduction traits in breed and non-breed horses. **BMC Genomics**, London, v. 16, [art.] 764, 2015.

MILANO, M. Gene prioritization tools. **Encyclopedia of Bioinformatics and Computational Biology: ABC of Bioinformatics**, Amsterdam, v. 1, p. 907-914, 2018. Disponível em: https://doi.org/10.1016/B978-0-12-809633-8.20406-8. Acesso em: 12 set 2021.

NEUPANE, M.; KISER, J. N.; NEIBERGS, H. L. Gene set enrichment analysis of SNP data in dairy and beef cattle with bovine respiratory disease. **Animal Genetics**, Oxford, v. 49, n. 6, p. 527-538, 2018.

OLIVEIRA, P. S. N. *et al*. Identification of genomic regions associated with feed efficiency in Nelore cattle. **BMC Genetics**, London, v. 15, [art.] 100, 2014. Disponível em: https://doi.org/10.1186/s12863-014-0100-0. Acesso em: 01 set. 2022.

ORTEGA, M. S. *et al*. Association of single nucleotide polymorphisms in candidate genes previously related to genetic variation in fertility with phenotypic measurements of reproductive function in Holstein cows. **Journal of Dairy Science**, Champaign, v. 100, n. 5, p. 3725-3734, 2017.

PARIACOTE, F.; VAN VLECK, L. D.; MACNEIL, M. D. Effects of Inbreeding and heterozygosity on preweaning traits in a closed population of herefords under selection. **Journal of Animal Science**, Champaign, v. 76, n. 5, p. 1303-1310, 1998. Disponível em: https://doi.org/10.2527/1998.7651303x. Acesso em:16 nov. 2020.

PAUSCH, H. *et al*. Identification of QTL for UV-protective eye area pigmentation in cattle by progeny phenotyping and genome-wide association analysis. **PLoS ONE**, San Francisco, v. 7, n. 5, [art.] e36346, 2012.

PEGOLO, S. *et al.* Genome-wide association and pathway analysis of carcass and meat quality traits in Piemontese young bulls. **Animal**, Cambridge, v. 14, n. 2, p. 243-252, 2020. Disponível em: https://doi.org/10.1017/S1751731119001812. Acesso em: 16 set 2021.

PEÑAGARICANO, F. *et al*. Inferring quantitative trait pathways associated with bull fertility from a genome-wide association study. **Frontiers in Genetics**, Lausanne, v. 3, [art.] 307, 2013. Disponível em: https://doi.org/10.3389/fgene.2012.00307. Acesso em:15 out 2021.

PERIPOLLI, E. *et al*. Assessment of runs of homozygosity islands and estimates of genomic inbreeding in Gyr (*Bos indicus*) dairy cattle. **BMC Genomics**, London, v. 19, [art.] 34, [p. 1–13], 2018b.

PERIPOLLI, E. *et al*. Autozygosity islands and ROH patterns in Nellore lineages: Evidence of selection for functionally important traits. **BMC Genomics**, London, v. 19, [art.] 680, 2018a.

PERIPOLLI, E. *et al*. Genome-wide scan for runs of homozygosity in the composite Montana Tropical® beef cattle. **Journal of Animal Breeding and Genetics**, Berlin, v. 137, n. 2, p. 155-165, 2020.

PICCOLI, M. L. *et al*. Accuracy of genome-wide imputation in Braford and Hereford beef cattle. **BMC Genetics**, London, v. 15, [art.] 157, 2014. Disponível em: https://doi.org/10.1186/s12863-014-0157-9. Acesso em: 19 set. 2020.

PICCOLI, M.L., *et al.* Comparison of genomic prediction methods for evaluation of adaptation and productive efficiency traits in Braford and Hereford cattle. Livestock Science, 231, [art.] 103864, 2020. https://doi.org/10.1016/J.LIVSCI.2019.103864. Acesso em, 15 jan. 2021.

PILON, B. *et al*. Inbreeding calculated with runs of homozygosity suggests chromosome-specific inbreeding depression regions in line 1 Hereford. **Animals**, Basel, v. 11, n. 11, [art.] 3105, Oct. 2021.

PINTO, L. F. *et al.* Association of SNPs on CAPN1 and CAST genes with tenderness in Nellore cattle. **Genetics and Molecular Research**, Ribeirão Preto, v. 9, n. 3, p. 1431-1442, 2010. Disponível em: https://doi.org/10.4238/vol9-3gmr881. Acesso em: 22 set. 2021.

PORTO-NETO, L. R. *et al*. Genome-wide association for the outcome of fixed-time artificial insemination of Brahman heifers in Northern Australia. **Journal of Animal Science**, Champaign, v. 93, n. 11, p. 5119-5127, 2015. Disponível em: https://doi.org/10.2527/jas.2015-9401. Acesso em: 12 nov 2021.

PURCELL, S. *et al*. Plink: a tool set for whole-genome association and population-based linkage analyses. **American Journal of Human Genetics**, Baltimore, v. 81, n. 3, p. 559–575, 2007.

PURFIELD, D. C. *et al*. Runs of homozygosity and population history in cattle. **BMC Genetics**, London, v. 13, [art.] 70, 2012.

QANBARI, S.; SIMIANER, H. Mapping signatures of positive selection in the genome of livestock. **Livestock Science**, Amsterdam, v. 166, p. 133–143, 2014. Disponível em: https://doi.org/10.1016/j.livsci.2014.05.003. Acesso em: 15 jul 2022.

REIMANN, F. A. *et al*. Genetic parameters and accuracy of traditional and genomic breeding values for eye pigmentation, hair coat and breed standard in Hereford and Braford cattle. **Livestock Science**, Amsterdam, v. 213, p. 44–50, 2018. Disponível em: https://doi.org/10.1016/J.LIVSCI.2018.04.007. Acesso em: 11 out 2021.

REVERTER, A. *et al*. Genomic inbreeding depression for climatic adaptation of tropical beef cattle. **Journal of Animal Science**, Champaign, v. 95, n. 9, p. 3809-3821, 2017.

RON, M. *et al*. Misidentification rate in the israeli dairy cattle population and its implications for genetic improvement. **Journal of Dairy Science**, Champaign, v. 79, n. 4, p. 676-681, 1996. Disponível em: https://doi.org/10.3168/jds.S0022-0302(96)76413-5. Acesso em: 16 jul 2021.

SAATCHI, M. *et al.* Large-effect pleiotropic or closely linked QTL segregate within and across ten US cattle breeds. **BMC Genomics**, London, v. 15, n. 1,

[art.] 442, 2014. Disponível em: https://doi.org/10.1186/1471-2164-15-442. Acesso em: 15 jul. 2021.

SANTANA Jr. M. L. *et al*. Effect of inbreeding on growth and reproductive traits of Nellore cattle in Brazil. **Livestock Science** 131. 2010. Disponível em: https://doi.org/10.1016/j.livsci.2010.04.003. Acesso em: 25 mar 2020.

SANTANA, M. H. A. *et al*. A genomewide association mapping study using ultrasound-scanned information identifies potential genomic regions and candidate genes affecting carcass traits in Nellore cattle. **Journal of Animal Breeding and Genetics**, Berlin, v. 132, n. 6, p. 420-427, 2015. Disponível em: https://doi.org/10.1111/jbg.12167. Acesso em: 19 abr. 2020.

SARAVANAN, K. A. *et al*. Selection signatures in livestock genome: A review of concepts, approaches and applications. **Livestock Science**, Amsterdam, v. 241, [art.] 104257, Nov. 2020.

SARGOLZAEI, M.; CHESNAIS, J.; SCHENKEL, F. S. FImpute-An efficient imputation algorithm for dairy cattle populations. **Journal of Dairy Science**, Champaign, v. 94, 421, 2011.

SCHETTINI, G. P. *et al*. Transcriptome profile reveals genetic and metabolic mechanisms related to essential fatty acid content of intramuscular longissimus thoracis in nellore cattle. **Metabolites**, Basel, v. 12, n. 5, [art.] 471, 2022. Disponível em: https://doi.org/10.3390/METABO12050471. Acesso em: 15 dez. 2022.

SEABURY, C. M. *et al*. Genome-wide association study for feed efficiency and growth traits in U.S. beef cattle. **BMC Genomics**, London, v. 18, n. 1, [art.] 386, 2017.

SNELLING, W. M. *et al*. Genome-wide association study of growth in crossbred beef cattle. **Journal of Animal Science**, Champaign, v. 88, n. 3, p. 837-848, 2010.

SOLLERO, B. P. *et al.* Tag SNP selection for prediction of tick resistance in Brazilian Braford and Hereford cattle breeds using Bayesian methods. **Genetics Selection Evolution**, Paris, v. 49, [art.] 49, 2017.

SONESSON, A. K.; WOOLLIAMS, J. A.; MEUWISSEN, T. H. E., 2010. Maximising genetic gain whilst controlling rates of genomic inbreeding using genomic optimum contribution selection. *In*: WORLD CONGRESS ON GENETICS APPLIED TO
LIVESTOCK PRODUCTION, 9., 2010. **Proceedings of the** […]. Leipzig: German Society for Animal Science, 2010. Abstract no. 892.

SUMREDDEE, P. *et al*. Grid search approach to discriminate between old and recent inbreeding using phenotypic, pedigree and genomic information. **BMC Genomics**, London, v. 22, n. 1, [art.] 538, 2021. Disponível em: https://doi.org/10.1186/s12864-021-07872-z. Acesso em: 03 mar. 2022.

SUMREDDEE, P. *et al*. Inbreeding depression in line 1 Hereford cattle population using pedigree and genomic information. **Journal of Animal Science**, Champaign, v. 97, n. 1, p. 1-18, 2019. Disponível em: https://doi.org/10.1093/jas/sky385. Acesso em: 05 mar. 2021.

SUMREDDEE, P. *et al*. Runs of homozygosity and analysis of inbreeding depression. **Journal of Animal Science**, Champaign, v. 98, n. 12, [art.] skaa361, 2020.

SZMATOŁA, T. *et al*. A comprehensive analysis of runs of homozygosity of eleven cattle breeds representing different production types. **Animals**, Basel, v. 9, n. 12, [art.] 1024, 2019. Disponível em: https://doi.org/10.3390/ani9121024. Acesso em: 15 set. 2021.

SZMATOŁA, T. *et al*. Characteristics of runs of homozygosity in selected cattle breeds maintained in Poland. **Livestock Science**, Amsterdam, v. 188, p. 72–80, June 2016.

TANG, H. *et al*. **GOTaxon:** Representing the evolution of biological functions in the Gene Ontology. ArXiv. [Ithaca, NY]: Cornell University, 2018.

VANRADEN, P. M. Efficient methods to compute genomic predictions. **Journal of Dairy Science**, Champaign, v. 91, n. 11, p. 4414-4423, 2008. Disponível em: https://doi.org/10.3168/jds.2007-0980. Acesso em: 11 mar. 2021.

WANG, Y. *et al*. Genetic architecture of quantitative traits in beef cattle revealed by genome wide association studies of imputed whole genome sequence variants: II: carcass merit traits. **BMC Genomics**, London, v. 21, n. 1, [art.] 36. 2020.

XU, L. *et al.* Genomic patterns of homozygosity in chinese local cattle. **Scientific Reports**, London, v. 9, [art.] 16977, 2019. Disponível em: https://doi.org/10.1038/s41598-019-53274-3. Acesso em: 11 abr. 2020.

YOON, D.; KO, E. P5061 association study between SNPs of the genes within bovine QTLs and meat quality of Hanwoo. **Journal of Animal Science**, Champaign, v. 94, p. 145, 2016. Disponível em: https://doi.org/10.2527/jas2016.94supplement4145x. Acesso em: 11 nov. 2021.

ZAVAREZ, L. B. *et al.* Assessment of autozygosity in Nellore cows (*Bos indicus*) through high-density SNP genotypes. **Frontiers in Genetics**, Lausanne, v. 6, [art.] 5, Jan. 2015.

ZHANG, F. *et al*. Genetic architecture of quantitative traits in beef cattle revealed by genome wide association studies of imputed whole genome sequence variants: I: feed efficiency and component traits. **BMC Genomics**, London, v. 21, n. 1, [art.] 36, 2020. Disponível em: https://doi.org/10.1186/s12864-019-6362-1. Acesso em: 15 set. 2021.

ZHANG, H. *et al*. Polymorphisms of MASP2 gene and its relationship with mastitis and milk production in Chinese Holstein cattle. **Biotechnology and Biotechnological Equipment**, Sofia, v. 33, n. 1, p. 589-596, 2019. Disponível em: https://doi.org/10.1080/13102818.2019.1596755. Acesso em: 26 set. 2021.

ZHANG, Q. *et al.* Estimation of inbreeding using pedigree, 50k SNP chip genotypes and full sequence data in three cattle breeds. **BMC Genetics**, London, v. 16, [art.] 88, 2015a. Disponível em: https://doi.org/10.1186/s12863-015-0227-7. Acesso em: 15 abr. 2021.

ZHANG, Q. *et al*., Guldbrandtsen, B., Bosse, M., Lund, M.S., Sahana, G. Runs of homozygosity and distribution of functional variants in the cattle genome. **BMC Genomics**, London, v. 16, [art.] 542, 2015b. Disponível em: https://doi.org/10.1186/s12864-015-1715-x. Acesso em: 15 abr. 2021.

ZHAO, G. *et al*. Genome-wide assessment of runs of homozygosity in chinese wagyu beef cattle. **Animals**, Basel, v. 10, n. 8, [art.] 1425, 2020.

ZHAO, G. *et al*. Runs of homozygosity analysis reveals consensus homozygous regions affecting production traits in Chinese Simmental beef cattle. **BMC Genomics**, London, v. 22, [art.] 678, 2021.

COMPLEMENTARY MATERIAL

Table 1. Autozygosity islands based on runs of homozygosity (ROH) in Hereford and Braford cattle breeds

Islands (chromosomal position)	Gene ontology			Genes[1]	P-value	Size (Mb)	n SNP
HEREFORD							
1:65430768:73692348	GO:0005789	GOTERM_CC_DIRECT	endoplasmic reticulum membrane	*A0A3Q1MMR1_BOVIN, SEC22_A, NRROS, PIGX, SLC51A*	9,8E-3	826	149
	GO:0005829	GOTERM_CC_DIRECT	cytosol	*IQCG, SENP5, CSTA, DTX3L, FAM162A, GTF2E1, LSG1, PAK2, PARP14, RUBCN*	3,5E-2		
1:137609909:138640707	GO:0071277	GOTERM_BP_DIRECT	cellular response to calcium ion	*A0A3Q1MMF8_BOVIN, A0A3Q1MGA0_BOVIN, A0A3Q1MV40_BOVIN, CPNE4*	3,0E-7	1.03	97
	GO:0005886	GOTERM_CC_DIRECT	plasma membrane	*A0A3Q1MMF8_BOVIN, A0A3Q1MGA0_BOVIN, A0A3Q1MV40_BOVIN, CPNE4*	4,8E-2		
	GO:0005544	GOTERM_MF_DIRECT	calcium-dependent phospholipid binding		1,0E-7		
2:68474051:72842275	GO:0003341	GOTERM_BP_DIRECT	cilium movement	*G3MZ93_BOVIN, CFAP221*	2,1E-2	4.37	475
	GO:0032091	GOTERM_BP_DIRECT	negative regulation of protein binding	*RALB, EPB41L5*	3,5E-2		
	GO:0032869	GOTERM_BP_DIRECT	cellular response to insulin stimulus	*INHBB, INSIG2*	3,7E-2		

	GO:0009267	GOTERM_BP_DIRECT	cellular response to starvation	*RALB, INHBB*	3,7E-2		
	GO:0032092	GOTERM_BP_DIRECT	positive regulation of protein binding	*RALB, EPB41L5*	4,2E-2		
	GO:0008092	GOTERM_MF_DIRECT	cytoskeletal protein binding	*EPB41L5, PTPN4*	2,0E-2		
6:65635995:78634046	GO:0002244	GOTERM_BP_DIRECT	hematopoietic progenitor cell differentiation	*KIT, RESTB, PDGFRA*	4,7E-3	13	1070
	GO:0006893	GOTERM_BP_DIRECT	Golgi to plasma membrane transport	*EXOC1L, EXOC1*	2,7E-2		
	GO:0006378	GOTERM_BP_DIRECT	mRNA polyadenylation	*A0A3Q1M6L3_BOVIN, FIP1L1*	4,5E-2		
	GO:0000145	GOTERM_CC_DIRECT	exocyst	*EXOC1L, EXOC1*	2,1E-2		
	GO:0005887	GOTERM_CC_DIRECT	integral component of plasma membrane	*ATP10D, KIT, ADGRL3, GABRB1, PDGFRA*	2,3E-2		
		KEGG_PATHWAY	Huntington disease	*RESTA, RESTB, POLR2B*	3,8E-2		
7:51976376:53021077	GO:0007156	GOTERM_BP_DIRECT	homophilic cell adhesion via plasma membrane adhesion molecules	*PCDHGA3, PCDHGA5, PCDHGC4, A0A3Q1LSE9_BOVIN, A0A3Q1LTT5_BOVIN, A0A3Q1ML27_BOVIN, G3MYJ3_BOVIN, G3MYX2_BOVIN, PCDHA13, PCDHB1, LOC104968820, PCDHGA8, PCDHGB4, PCDHGC3*	5,5E-27	1.04	75

GO:0007155	GOTERM_BP_DIRECT	cell adhesion	*PCDHGA3, PCDHGA5, PCDHGC4, A0A3Q1LSE9_BOVIN, A0A3Q1LTT5_BOVIN, A0A3Q1ML27_BOVIN, G3MYJ3_BOVIN, G3MYX2_BOVIN, PCDHA13, PCDHB1, LOC104968820, PCDHGC3*	5,2E-17
GO:0005887	GOTERM_CC_DIRECT	integral component of plasma membrane	*PCDHGA3, PCDHGA5, PCDHGC4, A0A3Q1LSE9_BOVIN, A0A3Q1LTT5_BOVIN, A0A3Q1ML27_BOVIN, G3MYJ3_BOVIN, G3MYX2_BOVIN, PCDHA13, PCDHB1, LOC104968820, PCDHGC3*	8,6E-13
GO:0005509	GOTERM_MF_DIRECT	calcium ion binding	*PCDHGA3, PCDHGA5, PCDHGC4, A0A3Q1LSE9_BOVIN, A0A3Q1LTT5_BOVIN, A0A3Q1ML27_BOVIN, G3MYJ3_BOVIN, G3MYX2_BOVIN, PCDHA13, PCDHB1, LOC104968820, PCDHGA8, PCDHGB4, PCDHGC3*	1,7E-18

7:10649679:11641000	GO:0007189	GOTERM_BP_DIRECT	adenylate cyclase-activating G-protein coupled receptor signaling pathway	*G5E558_BOVIN, LOC112447333, ADGRE3, PTGER1*	3,5E-5	0.99	98
	GO:0007166	GOTERM_BP_DIRECT	cell surface receptor signaling pathway	*G5E558_BOVIN, LOC112447333, ADGRE3, ADGRL1*	1,2E-4		
	GO:0032496	GOTERM_BP_DIRECT	response to lipopolysaccharide	*PALM3, PTGER1*	4,0E-2		
	GO:0043197	GOTERM_CC_DIRECT	dendritic spine	*GIPC1, PRKACA*	4,0E-2		
	GO:0004930	GOTERM_MF_DIRECT	G-protein coupled receptor activity	*G5E558_BOVIN, LOC112447333, ADGRE3, ADGRL1*	2,1E-2		
		KEGG_PATHWAY	Retrograde endocannabinoid signaling	*NDUFB7, PRKACA*	5,0E-2		
8:105.854.420:106.558.356	not found					0.7	173
9:19.573.725:20.378.144	not found					0.8	96
12:25.727.678:38.005.041	not found					12.28	119
13:10.790.497:12.078.256	not found					1.29	89
13:63590679:65666579	GO:0000045	GOTERM_BP_DIRECT	autophagosome assembly	*MAP1LC3A, TP53INP2*	4,7E-2	2.07	259

14:30.638.513:31.703.574	not found					1.07	139
15:83797100:84568491	GO:0016021	GOTERM_CC_DIRECT	integral component of membrane	*A0A3Q1MRM5_BOVIN, OR4A2C, OR4A2I, OR4C160*	4,0E-2	0.77	41
	GO:0004984	GOTERM_MF_DIRECT	olfactory receptor activity	*A0A3Q1MRM5_BOVIN, OR4A2C, OR4A2I, OR4C160*	1,9E-4		
	GO:0004930	GOTERM_MF_DIRECT	G-protein coupled receptor activity	*A0A3Q1MRM5_BOVIN, OR4A2C, OR4A2I, OR4C160*	3,4E-4		
16:41602177:45629162	GO:0001558	GOTERM_BP_DIRECT	regulation of cell growth	*CLSTN1, MTOR, MAD2L2*	5,1E-4	4.02	447
	GO:0003085	GOTERM_BP_DIRECT	negative regulation of systemic arterial blood pressure	*NPPA, NPPB*	8,6E-3		
	GO:0007168	GOTERM_BP_DIRECT	receptor guanylyl cyclase signaling pathway	*NPPA, NPPB*	9,7E-3		
	GO:0006182	GOTERM_BP_DIRECT	cGMP biosynthetic process	*NPPA, NPPB*	9,7E-3		
	GO:0019934	GOTERM_BP_DIRECT	cGMP-mediated signaling	*NPPA, NPPB*	1,6E-2		
	GO:0008217	GOTERM_BP_DIRECT	regulation of blood pressure	*NPPA, UTS2*	4,4E-2		
	GO:00085829	GOTERM_CC_DIRECT	cytosol	*ERRFI1, FBXO2, CASZ1, CTNNBIP1, EXOSC10, MTOR, MTHFR, MAD2L2*	1,2E-2		

	GO:0005179	GOTERM_MF_DIRECT	hormone activity	*NPPA, NPPB. UTS2*	4,9E-3		
	GO:0051427	GOTERM_MF_DIRECT	hormone receptor binding	*NPPA, NPPB*	6,2E-3		
	GO:0001540	GOTERM_MF_DIRECT	beta-amyloid binding	*FBXO2, CLSTN1*	4,8E-2		
		KEGG_PATHWAY	HIF-1 signaling pathway	*ENO1, MTOR, NPPA*	1,6E-2		
21:11664:3225908	GO:0050871	GOTERM_BP_DIRECT	positive regulation of B cell activation	*A0A3Q1M458_BOVIN, A0A3Q1MI29_BOVIN, A0A3Q1ML26_BOVIN, G3N188_BOVIN, LOC100300716, LOC104968484,*	1,3E-13	3.21	208
	GO:0006910	GOTERM_BP_DIRECT	phagocytosis, recognition	*A0A3Q1M458_BOVIN, A0A3Q1MI29_BOVIN, A0A3Q1ML26_BOVIN, G3N188_BOVIN, LOC100300716, LOC104968484,*	1,6E-13		
	GO:0006911	GOTERM_BP_DIRECT	phagocytosis, engulfment	*A0A3Q1M458_BOVIN, A0A3Q1MI29_BOVIN, A0A3Q1ML26_BOVIN, G3N188_BOVIN, LOC100300716, LOC104968484,*	1,1E-12		
	GO:0006958	GOTERM_BP_DIRECT	complement activation, classical pathway	*A0A3Q1M458_BOVIN, A0A3Q1MI29_BOVIN, A0A3Q1ML26_BOVIN, G3N188_BOVIN, LOC100300716, LOC104968484,*	2,4E-12		

GO:0050853	GOTERM_BP_DIRECT	B cell receptor signaling pathway	*A0A3Q1M458_BOVIN, A0A3Q1MI29_BOVIN, A0A3Q1ML26_BOVIN, G3N188_BOVIN, LOC100300716, LOC104968484,*	4,7E-12
GO:0042742	GOTERM_BP_DIRECT	defense response to bacterium	*A0A3Q1M458_BOVIN, A0A3Q1MI29_BOVIN, A0A3Q1ML26_BOVIN, G3N188_BOVIN, LOC100300716, LOC104968484,*	1,2E-9
GO:0045087	GOTERM_BP_DIRECT	innate immune response	*A0A3Q1M458_BOVIN, A0A3Q1MI29_BOVIN, A0A3Q1ML26_BOVIN, G3N188_BOVIN, LOC100300716, LOC104968484,*	7,1E-8
GO:0042571	GOTERM_CC_DIRECT	immunoglobulin complex, circulating	*A0A3Q1M458_BOVIN, A0A3Q1MI29_BOVIN, A0A3Q1ML26_BOVIN, G3N188_BOVIN, LOC100300716, LOC104968484,*	2,9E-14
GO:0009897	GOTERM_CC_DIRECT	external side of plasma membrane	*A0A3Q1M458_BOVIN, A0A3Q1MI29_BOVIN, A0A3Q1ML26_BOVIN, G3N188_BOVIN, LOC100300716, LOC104968484,*	6,5E-8
GO:0034987	GOTERM_MF_DIRECT	immunoglobulin receptor binding	*A0A3Q1M458_BOVIN, A0A3Q1MI29_BOVIN, A0A3Q1ML26_BOVIN, G3N188_BOVIN, LOC100300716, LOC104968484,*	5,3E-14

GO:0003823	GOTERM_MF_DIRECT	antigen binding	*A0A3Q1M458_BOVIN, A0A3Q1MI29_BOVIN, A0A3Q1ML26_BOVIN, G3N188_BOVIN, LOC100300716, LOC104968484,*	1,2E-13
	KEGG_PATHWAY	Asthma	*LOC100300716, LOC104968484*	4,3E-3
	KEGG_PATHWAY	Primary immunodeficiency	*LOC100300716, LOC104968484*	4,7E-3
	KEGG_PATHWAY	African trypanosomiasis	*LOC100300716, LOC104968484*	4,9E-3
	KEGG_PATHWAY	Allograft rejection	*LOC100300716, LOC104968484*	6,4E-3
	KEGG_PATHWAY	Intestinal immune network for IgA production	*LOC100300716, LOC104968484*	6,4E-3
	KEGG_PATHWAY	Fc epsilon RI signaling pathway	*LOC100300716, LOC104968484*	7,8E-3
	KEGG_PATHWAY	Autoimmune thyroid disease	*LOC100300716, LOC104968484*	8,1E-3
	KEGG_PATHWAY	Viral myocarditis	*LOC100300716, LOC104968484*	8,7E-3
	KEGG_PATHWAY	Leishmaniasis	*LOC100300716, LOC104968484*	8,7E-3
	KEGG_PATHWAY	B cell receptor signaling pathway	*LOC100300716, LOC104968484*	9,4E-3
	KEGG_PATHWAY	Fc gamma R-mediated phagocytosis	*LOC100300716, LOC104968484*	1,1E-2
	KEGG_PATHWAY	Dilated cardiomyopathy	*LOC100300716, LOC104968484*	1,1E-2
	KEGG_PATHWAY	Rheumatoid arthritis	*LOC100300716, LOC104968484*	1,2E-2

KEGG_PATHWAY	Staphylococcus aureus infection	*LOC100300716, LOC104968484*	1,2E-2
KEGG_PATHWAY	Hematopoietic cell lineage	*LOC100300716, LOC104968484*	1,2E-2
KEGG_PATHWAY	NF-kappa B signaling pathway	*LOC100300716, LOC104968484*	1,2E-2
KEGG_PATHWAY	Amoebiasis	*LOC100300716, LOC104968484*	1,3E-2
KEGG_PATHWAY	Phospholipase D signaling pathway	*LOC100300716, LOC104968484*	1,7E-2
KEGG_PATHWAY	Yersinia infection	*LOC100300716, LOC104968484*	1,7E-2
KEGG_PATHWAY	Natural killer cell mediated cytotoxicity	*LOC100300716, LOC104968484*	1,7E-2
KEGG_PATHWAY	Phagosome	*LOC100300716, LOC104968484*	1,9E-2
KEGG_PATHWAY	Systemic lupus erythematosus	*LOC100300716, LOC104968484*	2,1E-2
KEGG_PATHWAY	Transcriptional misregulation in cancer	*LOC100300716, LOC104968484*	2,2E-2
KEGG_PATHWAY	Tuberculosis	*LOC100300716, LOC104968484*	2,3E-2
KEGG_PATHWAY	Epstein-Barr virus infection	*LOC100300716, LOC104968484*	2,6E-2
KEGG_PATHWAY	Neutrophil extracellular trap formation	*LOC100300716, LOC104968484*	2,7E-2
KEGG_PATHWAY	Calcium signaling pathway	*LOC100300716, LOC104968484*	2,8E-2
KEGG_PATHWAY	Coronavirus disease - COVID-19	*LOC100300716, LOC104968484*	3,1E-2
KEGG_PATHWAY	PI3K-Akt signaling pathway	*LOC100300716, LOC104968484*	4,2E-2

26:48.519.593:48.968.839	not found					0.45	45
BRAFORD							
1:137757809:138338924	GO:0071277	GOTERM_BP_DIRECT	cellular response to calcium ion	*A0A3Q1MMF8_BOVIN, A0A3Q1MGA0_BOVIN, A0A3Q1MV40_BOVIN, CPNE4*	7,5e-8	0.14	30
	GO:0005886	GOTERM_CC_DIRECT	plasma membrane		1,5e-2		
	GO:0005544	GOTERM_MF_DIRECT	calcium-dependent phospholipid binding	*A0A3Q1MMF8_BOVIN, A0A3Q1MGA0_BOVIN, A0A3Q1MV40_BOVIN, CPNE4*	2,6e-8		
1:137.758.809:138.337.924	not found					0.58	107
2:70971542:72174132	GO:0003341	GOTERM_BP_DIRECT	cilium movement	*G3MZ93_BOVIN, CFAP221*	1,2E-2	1.2	636
	GO:0032091	GOTERM_BP_DIRECT	negative regulation of protein binding	*RALB, EPB41L5*	1,9E-2		
	GO:0009267	GOTERM_BP_DIRECT	cellular response to starvation	*RALB, INHBB*	2,0E-2		
	GO:0032092	GOTERM_BP_DIRECT	positive regulation of protein binding	*RALB, EPB41L5*	2,3E-2		
	GO:0008092	GOTERM_MF_DIRECT	cytoskeletal protein binding	*EPB41L5, PTPN4*	9,8E-3		
3:71.907.596:73.031.262	not found					1.12	130

6:62661045:80236506	GO:0002244	GOTERM_BP_DIRECT	hematopoietic progenitor cell differentiation	*KIT, RESTB, PDGFRA*	5,0E-3	17.57	2524
	GO:0006893	GOTERM_BP_DIRECT	Golgi to plasma membrane transport	*EXOC1L, EXOC1*	2,8E-2		
	GO:0006378	GOTERM_BP_DIRECT	mRNA polyadenylation	*A0A3Q1M6L3_BOVIN, FIP1L1*	4,6E-2		
	GO:0000145	GOTERM_CC_DIRECT	exocyst	*EXOC1L, EXOC1*	2,2E-2		
	GO:0005887	GOTERM_CC_DIRECT	integral component of plasma membrane	*ATP10D, KIT, ADGRL3, GABRB1, PDGFRA*	2,6E-2		
		KEGG_PATHWAY	Huntington disease	*RESTA, RESTB, POLR2B*			
7:9138073:11614756	GO:0007189	GOTERM_BP_DIRECT	adenylate cyclase-activating G-protein coupled receptor signaling pathway	*G5E558_BOVIN, LOC100337213, LOC112447333, ADGRE3, PTGER1*	4,1E-7	3.47	219
	GO:0007166	GOTERM_BP_DIRECT	cell surface receptor signaling pathway	*G5E558_BOVIN, LOC100337213, LOC112447333, ADGRE3, ADGRL1*	2,1E-6		
	GO:0016021	GOTERM_CC_DIRECT	integral component of membrane	*A0A3Q1MBA0_BOVIN, G3N1S1-BOVIN, A0A3Q1LV00-BOVIN, LOC112447333, ADGRL1, ADGRL1, OR7A102, OR7A10B, OR7A112, OR7A78, OR7A83, OR7A88, OR7A91, OR7A96, OR7A97, OR7A99, PTGER1*	1,2E-3		

	GO:0004930	GOTERM_MF_DIRECT	G-protein coupled receptor activity	*A0A3Q1MBA0_BOVIN, G3N1S1_BOVIN, A0A3Q1LV00_BOVIN, G5E558_BOVIN, LOC100337213, LOC112447333, ADGRE3, ADGRL1, OR7A102, OR7A10B, OR7A112, OR7A78, OR7A83, OR7A88, OR7A91, OR7A96, OR7A97, OR7A99*	1,2E-15		
	GO:0004984	GOTERM_MF_DIRECT	olfactory receptor activity	*A0A3Q1MBA0_BOVIN, G3N1S1_BOVIN, A0A3Q1LV00_BOVIN, OR7A102, OR7A10B, OR7A112, OR7A78, OR7A83, OR7A88, OR7A91, OR7A96, OR7A97, OR7A99*	9,3E-10		
		KEGG_PATHWAY	Olfactory transduction	*OR7A10B, OR7A112, OR7A78, OR7A83, OR7A88, OR7A91, OR7A96, OR7A97, OR7A99, PRKACA*	1,9E-6		
7:49550981:53021077:1	GO:0007156	GOTERM_BP_DIRECT	homophilic cell adhesion via plasma membrane adhesion molecules	*PCDHA2, PCDHGA3, PCDHGA5, PCDHGC4, A0A3Q1LSE9_BOVIN, A0A3Q1LTT5_BOVIN, A0A3Q1ML27_BOVIN, G3MYJ3_BOVIN, G3MYX2_BOVIN, G5E6K8_BOVIN, PCDHA13, PCDHA4,*	3,4E-27	2.47	118

			LOC104968501, PCDHB1, LOC104968820, PCDHGA8, PCDHGB4, PCDHGC3	
GO:0007155	GOTERM_BP_DIRECT	cell adhesion	*PCDHA2, PCDHGA3, PCDHGA5, PCDHGC4, A0A3Q1LSE9_BOVIN, A0A3Q1LTT5_BOVIN, A0A3Q1ML27_BOVIN, G3MYJ3_BOVIN, G3MYX2_BOVIN, G5E6K8_BOVIN, PCDHA13, PCDHA4, LOC104968501, PCDHB1, LOC104968820, PCDHGC3*	5,5E-17
GO:0045947	GOTERM_BP_DIRECT	negative regulation of translational initiation	*EIF4EBP3, PAIP2*	2,1E-2
GO:0005887	GOTERM_CC_DIRECT	integral component of plasma membrane	*PCDHA2, PCDHGA3, PCDHGA5, PCDHGC4, A0A3Q1LSE9_BOVIN, A0A3Q1LTT5_BOVIN, A0A3Q1ML27_BOVIN, G3MYJ3_BOVIN, G3MYX2_BOVIN, G5E6K8_BOVIN, PCDHA13, PCDHA4, LOC104968501, PCDHB1, LOC104968820, PCDHGC3*	1,1E-10

	GO:0005509	GOTERM_MF_DIRECT	calcium ion binding	*PCDHA2, PCDHGA3, PCDHGA5, PCDHGC4, A0A3Q1LSE9_BOVIN, A0A3Q1LTT5_BOVIN, A0A3Q1ML27_BOVIN, G3MYJ3_BOVIN, G3MYX2_BOVIN, G5E6K8_BOVIN, PCDHA13, PCDHA4, LOC104968501, PCDHB1, LOC104968820, PCDHGA8, PCDHGB4, PCDHGC3*	8,1E-16		
	GO:0000900	GOTERM_MF_DIRECT	translation repressor activity, nucleic acid binding	*PAIP2, PURA*	1,8E-2		
12:25907504:41753726	GO:1990349	GOTERM_BP_DIRECT	gap junction-mediated intercellular transport	*GJA3, GJB2, GJB6*	6,8E-5	15.84	217
	GO:0007267	GOTERM_BP_DIRECT	cell-cell signaling	*GJA3, GJB2, GJB6*	4,8E-3		
	GO:0016264	GOTERM_BP_DIRECT	gap junction assembly	*GJB2, GJB6*	8,6E-3		
	GO:0010644	GOTERM_BP_DIRECT	cell communication by electrical coupling	*GJB2, GJB6*	1,1E-2		
	GO:0055085	GOTERM_BP_DIRECT	transmembrane transport	*GJA3, GJB2, GJB6*	3,0E-2		
	GO:0005922	GOTERM_CC_DIRECT	connexin complex	*GJA3, GJB2, GJB6*	5,9E-4		

	GO:0005634	GOTERM_CC_DIRECT	nucleus	*N4BP2L2, CDX2, CENPJ, XPO4, HSPH1, HMGB1, KATNAL1, LATS2, MAB21L1, PSPC1, SACS, USP12, ZMYM5*	4,2E-2		
	GO:0005243	GOTERM_MF_DIRECT	gap junction channel activity	*GJA3, GJB2, GJB6*	6,3E-4		
	GO:1903763	GOTERM_MF_DIRECT	gap junction channel activity involved in cell communication by electrical coupling	*GJB2, GJB6*	7,9E-3		
	GO:0019838	GOTERM_MF_DIRECT	growth factor binding	*FLT1, FLT3*	4,1E-2		
12:69671038:71015915:1	GO:0055085	GOTERM_BP_DIRECT	transmembrane transport	*G5E5W7_BOVIN, LOC784305*	7,5E-3	1.34	71
	GO:0016021	GOTERM_CC_DIRECT	integral component of membrane	*G3MW11_BOVIN, G5E5T3_BOVIN, G5E5W7_BOVIN, LOC784305*	4,0E-2		
	GO:0042626	GOTERM_MF_DIRECT	ATPase activity, coupled to transmembrane movement of substances	*G3MW11_BOVIN, G5E5T3_BOVIN, G5E5W7_BOVIN, LOC784305*	8,5E-8		
	GO:0005524	GOTERM_MF_DIRECT	ATP binding	*G3MW11_BOVIN, G5E5T3_BOVIN, G5E5W7_BOVIN, LOC784305*	4,8E-4		
13:10.790.497:12.082.391	not found					1.29	212

13:62.782.981:65.656.937	not found					2.87	340
14:30.652.577:31.613.097	not found					0.96	157
15:83.917.720:84.094.741	not found					0.18	9
16:42270958:45633090	GO:0001558	GOTERM_BP_DIRECT	regulation of cell growth	*CLSTN1, MTOR*	2,4E-2	3.36	326
21:162560:2274918	GO:0050871	GOTERM_BP_DIRECT	positive regulation of B cell activation	*A0A3Q1M458_BOVIN, A0A3Q1MI29_BOVIN, A0A3Q1ML26_BOVIN, G3N188_BOVIN, LOC100300716, LOC104968484*	1,3E-13	2.24	74
	GO:0006910	GOTERM_BP_DIRECT	phagocytosis, recognition	*A0A3Q1M458_BOVIN, A0A3Q1MI29_BOVIN, A0A3Q1ML26_BOVIN, G3N188_BOVIN, LOC100300716, LOC104968484*	1,6E-13		
	GO:0006911	GOTERM_BP_DIRECT	phagocytosis, engulfment	*A0A3Q1M458_BOVIN, A0A3Q1MI29_BOVIN, A0A3Q1ML26_BOVIN, G3N188_BOVIN, LOC100300716, LOC104968484*	1,1E-12		

GO:0006958	GOTERM_BP_DIRECT	complement activation, classical pathway	*A0A3Q1M458_BOVIN, A0A3Q1MI29_BOVIN, A0A3Q1ML26_BOVIN, G3N188_BOVIN, LOC100300716, LOC104968484*	2,4E-12
GO:0050853	GOTERM_BP_DIRECT	B cell receptor signaling pathway	*A0A3Q1M458_BOVIN, A0A3Q1MI29_BOVIN, A0A3Q1ML26_BOVIN, G3N188_BOVIN, LOC100300716, LOC104968484*	4,7E-12
GO:0042742	GOTERM_BP_DIRECT	defense response to bacterium	*A0A3Q1M458_BOVIN, A0A3Q1MI29_BOVIN, A0A3Q1ML26_BOVIN, G3N188_BOVIN, LOC100300716, LOC104968484*	1,2E-9
GO:0045087	GOTERM_BP_DIRECT	innate immune response	*A0A3Q1M458_BOVIN, A0A3Q1MI29_BOVIN, A0A3Q1ML26_BOVIN, G3N188_BOVIN, LOC100300716, LOC104968484*	7,1E-8
	KEGG_PATHWAY	Asthma	*LOC100300716, LOC104968484*	4,3E-3
	KEGG_PATHWAY	Primary immunodeficiency	*LOC100300716, LOC104968484*	4,7E-3
	KEGG_PATHWAY	African trypanosomiasis	*LOC100300716, LOC104968484*	4,9E-3
	KEGG_PATHWAY	Allograft rejection	*LOC100300716, LOC104968484*	6,4E-3
	KEGG_PATHWAY	Intestinal immune network for IgA production	*LOC100300716, LOC104968484*	6,4E-3

KEGG_PATHWAY	Fc epsilon RI signaling pathway	*LOC100300716, LOC104968484*	7,8E-3
KEGG_PATHWAY	Autoimmune thyroid disease	*LOC100300716, LOC104968484*	8,1E-3
KEGG_PATHWAY	Leishmaniasis	*LOC100300716, LOC104968484*	8,7E-3
KEGG_PATHWAY	Viral myocarditis	*LOC100300716, LOC104968484*	8,7E-3
KEGG_PATHWAY	B cell receptor signaling pathway	*LOC100300716, LOC104968484*	9,4E-3
KEGG_PATHWAY	Fc gamma R-mediated phagocytosis	*LOC100300716, LOC104968484*	1,1E-2
KEGG_PATHWAY	Dilated cardiomyopathy	*LOC100300716, LOC104968484*	1,1E-2
KEGG_PATHWAY	Rheumatoid arthritis	*LOC100300716, LOC104968484*	1,2E-2
KEGG_PATHWAY	Staphylococcus aureus infection	*LOC100300716, LOC104968484*	1,2E-2
KEGG_PATHWAY	Hematopoietic cell lineage	*LOC100300716, LOC104968484*	1,2E-2
KEGG_PATHWAY	NF-kappa B signaling pathway	*LOC100300716, LOC104968484*	1,2E-2
KEGG_PATHWAY	Amoebiasis	*LOC100300716, LOC104968484*	1,3E-2
KEGG_PATHWAY	Phospholipase D signaling pathway	*LOC100300716, LOC104968484*	1,7E-2
KEGG_PATHWAY	Yersinia infection	*LOC100300716, LOC104968484*	1,7E-2
KEGG_PATHWAY	Natural killer cell mediated cytotoxicity	*LOC100300716, LOC104968484*	1,7E-2
KEGG_PATHWAY	Phagosome	*LOC100300716, LOC104968484*	1,9E-2

		KEGG_PATHWAY	Systemic lupus erythematosus	*LOC100300716, LOC104968484*	2,1E-2	
		KEGG_PATHWAY	Transcriptional misregulation in cancer	*LOC100300716, LOC104968484*	2,2E-2	
		KEGG_PATHWAY	Tuberculosis	*LOC100300716, LOC104968484*	2,3E-2	
		KEGG_PATHWAY	Epstein-Barr virus infection	*LOC100300716, LOC104968484*	2,6E-2	
		KEGG_PATHWAY	Neutrophil extracellular trap formation	*LOC100300716, LOC104968484*	2,7E-2	
		KEGG_PATHWAY	Calcium signaling pathway	*LOC100300716, LOC104968484*	2,8E-2	
		KEGG_PATHWAY	Coronavirus disease - COVID-19	*LOC100300716, LOC104968484*	3,1E-2	
		KEGG_PATHWAY	PI3K-Akt signaling pathway	*LOC100300716, LOC104968484*	4,2E-2	
23:51.620:1.150.966	not found				1.1	54
26:48.344.472:49.691.984	not found				1.35	223

[1]ARS-UCD1.2 Assembly of the *Bos taurus* genome

Table 2. Gene content of runs of homozygosity (ROH) overlapping regions in the Hereford (HH) and Braford (BO) cattle breeds

Breed	BTA[1]	Sharing frequency	Position[2] (bp)	Length (bp)	Genes
HH	2	0.72	21,184,643:122,822,251	101,637,610	*ABCB11, ABI2, ACSL3, ACTR3, ACVR1, ACVR1C, AK2, ALP1, AOX1, AOX2, AOX4, ARPC2, ATF2, ATIC, BCS1L, BMPR2, BZW1, CAB39, CASP8, CATIP, CCL20, CD24, CD28, CD302, CDK5R2, CFLAR, CGC, CHN1, CHRNA1, CHRND, CHRNG, CNOT9, COL4A3, COPS7B, CPS1, CREB1, CTLA4, CYP27A1, DARS, DBI, DPP10, EIF4E2, EPB41L5, ERMN, FABP3, FZD7, GLI2, GPBAR1, GRB14, HSPE1, IFIW1, ITM2C, LAPTM5, LOC100125266, LOC516378, LOC538702, LYPD1, MAP2, MAP3K19, MARCKSL1, MARS2, MCM6, METTL8, MTMR9, MYO1B, NABP1, NIF3L1, NMI, NOP58, NR4A2, OLA1, ORC4, PEF1, PIKFYVE, PLCD4, PNKD, PRPF40A, PSMD1, PTP4A2, PTPN4, RPRM, SCN1A, SCN7A, SCN9A, SKC11A1, SLC11A1, SMARCAL1, SNRNP40, SPATS2L, SPEG, STK16, STK36, STK39, STRADB, TLK1, TRIM62, TSN, TUBA1D, VIL1, WNT10A, WNT6, XRCC5, YARS, ZRANB3*
HH	6	0.75	17,798,998:112,785,714	94,986,717	*ADGRL3, ADH4, ADH5, ADH6, ADH7, AFP, ALB, AMTN, ANXA3, AREG, ATP10D, BDH2, BMP3, BPAT3, BST1, C6H4orf19, CD38, CHRNA9, COPS4, CSN1S1, CSN1S2, CSN3, CXCL13, CXCL2, CXCL3, CXCL5, CXCL8, CXL3, CXL5, CYTL1, DCDS1, DCK, DMP1, DRD5, ENAM, ENOPH1, EREG, FGF5, GABRB1, GBA3, GRO1, HPGDS, HSTN, KIT, KLB, LAP3, LIAS, MED28, MTHFD2L, NSUN7, ODAM, PAICS, PDGFRA, PF4, PGM2, PI4K2B, POLR2B, PPA2, PPP3CA, RBPJ, SEPT11, SLIT2, SNCA, SOD3, SRD5A3, TRMT10A, ZCCHC4*

BO	6	0.33	15,050,230:112,169,109	97,118,880	*COPS4, CHRNA9, ADGRL3, ADH4, ADH5, ADH6, ADH7, AFP, ALB, AMTN, ANXA3, AREG, ATP10D, BDH2, BMP3, BST1, C1QTNF7, C6H4oRF19, CD38, CDS1, CFI, CSCL2, CSCL3, CSCL5, CSCL8, CSN1S1, CSN1S2, CSN1S3, CSN3, CXCL13, CXCL2, CXCL3, CXCL5, CXCL8, CYTL1, DCK, DKK2, DMP1, DRD5, ENAM, ENOPH1, EREG, ETNPPL, FGF5, GABRB1, GBA3, GBAT3, GRO1, HPGDS, HSTN, KIT, KLB, LAP3, LEF1, LIAS, LIT, MBP3, MED28, MTHFD2L, NSUN7, NUDT9, ODAM, PAICS, PAPSS1, PDGFRA, PF4, PGM2, PI4K2B, PLA2G12A, PLA2G12A, POLR2B, PPA2, PPP3CA, RBPJ, SEPT11, SLIT2, SNCA, SOD3, SRD5A3, TRMT10A, ZCCHC4*
BO	7	0.32	20,731,094:88,787,004	68,055,911	*AFAP1L1, APC2, AZU1, BSG, CATSPER3, CDHR2, CTNNA1, CYSTM1, DIRAS1, EFNA2, EGR1, G3BP1, GABRA1, GABRA6, GABRAG2, GABRG2, GNG7, GRIA1, GRK6, HINT1, LOC100299275, LOC508626, LOC517722, LOC524160, LOC524985, LOC526765, LOC787898, MADCAM1, MFAP3, MISP, OR2G2, OR2G3, OR2M4, OR2R12, OR2T11, OR2T12, OR2T2, OR2W3, OR6F1, OR6T1, PCDHA13, PCDHA6, PCDHB1, PCDHB11, PCDHGC3, PRTN3, RASA1, REEP2, REEP6, RELL2, RGS14, SLC39A3, SPINK5, SPINK6, SPINK7, STK11, TCF7, UBE2B, ZNF346*
HH	13	0.52	213,132:83,457,015	83,243,884	*20ALPHA-HSD, ACSS2, ACTR5, ADIG, ADRA1D, AKR1C3, AKR1C4, ANGPT4, ARFGEF2, ARFRP1, ARMC3, ARMC4, ASIP, AURKA, AVP, BANF2, BMI1, BMP2, BMP7, BPI, BPIFA1, BPIFA2A, BPIFA2B, BPIFA2C, BPIFA3, BPIFB1, BPIFB2, BPIFB3, BPIFB4, BPIFB5, BPIFB6, CACNB2, CALML5, CD40, CDS2, CFAP61, CHGB, CHMP4B, COMMD3, CSE1L, CSNK2A1, CST7, CST8, CTCFL, CTNNBL1, DBNDD2, DEFB123, DHX35, DSTN, DTD1, DYNLRB1, EPB41L1, ERGIC3, EYA2, FAM83D, FKBP1A, GAD2, GCNT7, GDAP1L1, GDI2, GINS1, GMEB2, GNAS, HCK, HNF4A, HSPA14, ID1, IDI1, IL2RA, ITCH, ITGB1, ITIH5, KIF3B, KIF5B, KIZ, LAMA5, LAMP5, LARP4B, LBP, LOC100295842, LOC100337056, LOC100850808, LOC404103, LOC407163, LOC505033, LOC512548, LOC527068, LOC531692, LOC617402, LOC782061, LOC782884, LOC785762, MAP1LC3A, MAP3K8, MAPRE1, MASTL, MCM10, MEIG1, MGC133636, MMP9, MYBL2, MYH7B, MYL9, MYLK2, NCOA3, NNAT, NRP1, NSFL1C, NXT1, OPTN, PABPC1L, PARD3, PARD6B, PCSK2, PDYN, PFDN4, PHF20, PI3, PKIG, PLCB1, PLCB4, PLCG1, POFUT1, POLR3F, PRKCQ, PSMA7, PTK6, PTPN1, PYGB, REM1, RGS19, RNF114, RPRD1B, SDCBP2,*

					SEC23B, SGK2, SLC2A10, SNAI1, SNAP25, SNRPB, SPEF1, SRC, SRMS, STAM, STK4, STMN3, SUV39H2, SYS1, THNSL1, TPX2, TTLL9, TTPAL, TUBAL3, UBE2C, UPF2, VIM, VSTM2L, WFDC10A, WFDC2, WISP23, XKR7, XRN2, YWHAB, ZNF438
HH	16	0.56	195,314:75,997,329	75,802,016	*AKT3, ATP1B1, C4BPA, C4BPB, CAPN2, CASP9, CD55, CDK11B, CLSTN1, CNTN2, CR2, DEGS1, DFFA, DVL1, EXOSC10, F13B, FASLG, FBXO2, FH, FMO1, FMO2, FMO3, FMO4, GNB1, HES5, ICMT, IL19, IL20, IL24, KCNH1, LAMB3, LAMC1, LAMC2, LOC517828, MARC1, MARC2, MASP2, MIA3, MTHFR, MTOR, NEK2, NOL9, PFKFB2, PLA2G4A, PLEKHG5, PRG4, PSEN2, RASSF5, RRP15, SOAT1, TGFB2, TNFRSF18, TNFRSF25, TNFRSF4, TNFRSF9, TNN, TOR1AIP1, UBE2J2, XCL1, XCL2*
HH	21	0.94	12,664:61,036,423	61,023,760	*BRMS1L, BTBD1, CYP11A1, CYP1A1, EDC3, IGF1R, ISG20, MORF4L1, PSMA4, PSMA6, SIN3A, SNRPA1*
BO	21	0.31	12,664:44,239,499	44,226,836	*BTBD1, CEMIP, CYP11A1, CYP1A1, EDC3, GZMB, IGF1R, ISG20, LOC509956, PCSK6, PSMA4, SEMA4B, SEMA7A, SNRPA1*

[1] BTA: *Bos taurus autosome*, [2]ARS-UCD1.2 Assembly of the *Bos taurus* genome

Table3. Gene ontology (GO) terms and Kyoto Encyclopedia of Genes and Genomes (KEGG) enriched by Fisher's test (p<0.05) in Hereford (HH) and Braford (BO) cattle breeds retrived from the autozygosity islands set of genes.

	Genes[1] (BTA[2])	*P-value*	Breeds
Biological Process			
(GO:0048813)		0.005	
Dendritic morphogenesis	*RERE (16)*		HH/BO
	CACNA1A (7)		HH/BO
	DCLK1 (12)		HH/BO
	PREX2 (14)		HH/BO
(GO:0007156)		0.008	
Homophilic cell adhesion via plasma membrane adhesion molecules	*CLSTN1 (16)*		HH/BO
	PCDHA6 (7)		HH/BO
	PCDHB1 (7)		HH/BO
	PCDHB11 (7)		HH/BO
	PCDHGC3 (7)		HH/BO
	PCDHA13 (7)		BO
(GO:0006874)		0.008	
Calcium ion cellular homeostasis	*ATP13A3 (1)*		HH
	ATP13A4 (1)		HH
	ATP13A5 (1)		HH
	CASR (1)		HH
	TMEM165 (6)		HH
(GO:0034614)		0.012	
Cellular response to reactive oxygen species	*SRC (13)*		BO
	PDGFRA (6)		BO
	ROMO1 (13)		BO
(GO:1902857)		0.045	
Positive adjustment of non-moving primary eyelash assembly	*CEP135 (6)*		BO
	CENPJ (12)		BO
Cell Component			

(GO:0005773)		0.010	
Vacuole	*LOC519145 (15)*		HH/BO
	LOC613282 (15)		HH/BO
	GLB1L3 (15)		HH/BO
(GO:0009897)		0.016	
Outer side of the plasma membrane	*CD86 (1)*		HH
	KIT (6)		HH
	TNFRSF9 (16)		HH
	MS4A1 (15)		HH
	MS4A2 (15)		HH
	PDGFRA (6)		HH
	TLR4 (8)		HH
(GO:0098793)		0.028	
Pre-synapse	*ADGRL1 (6)*		HH
	CACNA1A (7)		HH
	SYT6 (3)		HH
	STX (3)		HH
(GO:0005874)		0.031	
Microtubule	*CSPP1 (14)*		BO
	DYNLRB1 (13)		BO
	KIF20A (7)		BO
	KIF3B (13)		BO
	MAP1LC3A (13)		BO
	MAPRE1 (13)		BO
(GO:0005887)		0.037	
Integral component of the plasma membrane	*ATP13A3 (1)*		HH
	LOC523484 (2)		HH
	ATP13A4 (1)		HH
	ATP13A5 (1)		HH
	STEAP3 (2)		HH
	TNFRSF9 (16)		HH
	ADGRL3 (6)		HH
	GABRB1 (6)		HH
	MMP24 (13)		HH
	MS4A1 (15)		HH
	MS4A2 (15)		HH
	PDGFRA (6)		HH
	PTGER1 (7)		HH
	SLC10A4 (6)		HH

	SLC2A5 (16)		HH
	SLC4A9 (7)		HH
	TSPAN2 (3)		HH
	TLR4 (8)		HH
(GO:0030425)		0.050	
Dendrite	*LOC523484 (2)*		HH
	CACNA1A (7)		HH
	MTOR (16)		HH
	PSD2 (7)		HH
	PURA (7)		HH
	STX3 (15)		HH
Molecular Function			
(GO:0019829)		0.001	
Cation transport ATPase activity	*ATP13A3 (1)*		HH
	ATP13A4 (1)		HH
	ATP13A5 (1)		HH
(GO:0004565)		0.002	
beta-galactosidase activity	*LOC519145 (15)*		HH/BO
	LOC613282 (15)		HH/BO
	GLB1L3 (15)		HH/BO
(GO:0008289)		0.003	
Lipid binding			
	BPIFA1 (13)		HH/BO
	BPIFA3 (13)		HH/BO
	BPIFA2A (13)		BO
	BPIFA2B (13)		HH/BO
	BPIFA2C (13)		BO
	BPIFB1 (13)		HH/BO
	BPIFB2 (13)		BO
	BPIFB3 (13)		BO
	BPIFB4 (13)		BO
	BPIFB5 (13)		HH/BO
	BPIFB6 (13)		BO
	DBI (2)		HH/BO
(GO:0005509)		0.034	
Calcium ion binding			
	ADGRE3 (7)		HH

	ADGRL3 (6)		HH
	CASQ2 (3)		HH
	CLSTN1 (16)		HH
	MASP2 (16)		HH
	MYL9 (13)		HH
	PCDHA13 (7)		HH
	PCDHA6 (7)		HH
	PCDHB1 (7)		HH
	PCDHB11 (7)		HH
	PCDHGC3 (7)		HH
	SYT6 (3)		HH
KEGG pathways			
Central carbon metabolism in cancer		0.027	
	KIT (6)		HH
	MTOR (16)		HH
	PDGFRA (6)		HH
Cancer pathways		0.028	
	KIT (6)		BO
	RALB (2)		BO
	CTNNA1 (7)		BO
	MTOR (16)		BO
	PDGFRA (6)		BO
	GLI2 (2)		BO
	WNT8A (7)		BO
	PTGER1 (7)		BO
	PRKACA (3, 7)		BO
	NRAS (3)		HH
Serotonergic synapse		0.033	
	LOC523484 (2)		HH
	CACNA1A (7)		HH/BO
	NRAS (3)		HH
	PRKACA (3,7)		HH/BO
	GABRB1 (6)		HH/BO
	SRC (13)		BO
Endocytosis		0.041	
	CHMP4B (13; 26)		HH/BO
	ITCH (13)		HH/BO
	VPS26B (15)		HH/BO

	PDGFRA (6)	HH/BO
	PSD2 (7)	HH/BO
	SRC (13)	BO

[1] BTA: *Bos taurus autosome*, [2]ARS-UCD1.2 *Bos taurus* genome assembly

CAPÍTULO III- Population structure and detection of selection signatures in the genome of the Brazilian Braford composite breed

Population structure and detection of selection signatures in the genome of the Brazilian Braford composite breed

Abstract

The bovine genome, as well as that of other domestic species, carries evolutionary marks, these resulting from natural and artificial selection. Chromosomal regions with high homozygosity in the population are called selection signatures and are used to identify loci subject to selection. Associating the selection signatures with Quantitative trait loci regions, which are regions of the genome responsible for the expression of phenotypes of interest, can contribute to a better understanding of the traits that are under artificial selection. Therefore, the aim of the study was to identify and characterize selection signatures in Braford cattle through runs of homozygosity. Data from High-Density SNPs of 7,149 cattle of the Hereford-Embrapa, Braford, Braham, Nellore, and Hereford USA breeds were used, after quality control the data base contained 310,816 common SNPs. To determine the regions of low diversity, PLINK v1.90 software was used to calculate ass ROHs, where 1% of the most frequent SNPs were used to determine the regions of selection signatures. The ADMIXTURE software was used to calculate the probability of ancestry of the founding breeds of the Braford. Principal component analysis showed that the Braford is genetically closer to the Hereford, and their dispersion suggests that Brafords are becoming a distinct breed. The ancestry of the genome covered by the Braford SNPs maintained an average percentage expected by its racial composition 3/8 Zebu. Nineteen islands of homozygosity were identified, and these regions contained QTLs of selected traits in the breeds. The QTLs related to selected productive traits in the founding breeds were identified in the regions of the ROH islands; as well as biological processes involved in the expression of phenotypes of interest. The detections of selection signatures with QTLs related to meat production demonstrate that the objective of producing a composite animal focused on beef production left marks in the genome of these populations.

Key words: Ancestry, *Bos taurus, Bos indicus,* complementarity of breeds, favorable alleles, runs of homozygosity

1. Introduction

The bovine genome, as well as that of other domestic species, carries evolutionary marks, these arisitng from natural and artificial selection (GIBBS *et al*., 2009). The artificial selection has strongly affected numerous traits for many generations, both in the domestication of animals and in the formation of breeds, making this species adapt to different environmental conditions, displaying distinct production characteristics (YURCHENKO *et al*., 2018).

The two bovine subspecies most used by breeders in the world, *Bos taurus taurus and Bos. taurus indicus*, produce hybrids well adapted to a wide variety of environments and production systems (GONZÁLEZ *et al*., 2022). The objective of producing a product with the rusticity and adaptive traits of the zebu breeds, combined with the meat quality of the taurine breeds (PEACOCK *et al*., 1981), a cross between Hereford bulls and Brahman cows was developed in the United States in mid-1947, giving rise to the Braford synthetic breed. (GONZÁLEZ *et al*., 2022).

In Brazil, crossings to obtain the Braford breed emerged in the 1980s, coordinated by the Hereford Breeders Association and the Rio Grande do Sul, Brazil, using a limited pool of Nellore bulls in the formation of the breed, efforts are currently being made to increase the diversity of this population with the introduction of foreign lineages formed with Brahman cattle (BIEGELMEYER *et al*., 2016). In Fig.1, demonstration of possible crossings to obtain the Braford composite breed.

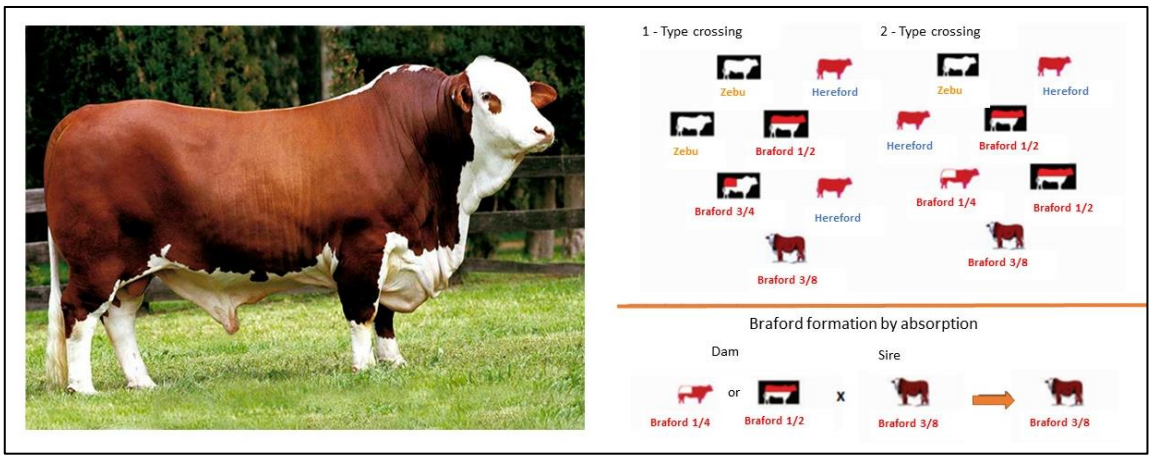

Figure 1. Illustration of three crossing schemes to form the Braford Breed 5/8 (Taurus - red) and 3/8 (Zebu - white), adapted, photo credits from Associação Brasileira de Hereford e Braford (2018).

The selection process for productive traits causes a change in the allele (or gene) frequency in specific loci of the genome, establishing a strong linkage disequilibrium that is defined as a high degree of association between alleles at different loci, where certain combinations of alleles occur more often together than would be expected by chance. The regions close to these selected advantageous sites are dragged which results in the “selective sweep effect”, retaining not only the favorable allele but a region close to it (FAY; WU, 2000). These chromosomal regions with high homozygosity in the population are called selection signatures, genomic footprints, or selective sweeps (HAASL; PAYSEUR, 2016), and are used to identify loci subject to selection (KREITMAN, 2000).

One of the ways to analyze these marks in the genome is through the reduction of local variability, using runs of homozygosity (ROH) (WILLIAMS *et al*., 2016). Therefore, genomic regions with a high frequency of ROH in the population, called ROH islands, are used to detect the association between genes and traits of interest (SZMATOŁA *et al*., 2016), because when an SNP is identified in several individuals, it can be inferred that it is not a sequencing error or a mutation found in a single individual, but a signature in that population (WILLIAMS *et al*., 2016). Both ROH islands and selection signatures can be used to identify regions of the genome that have been subject to recent selective

pressures. However, ROH islands are more specific in detecting the effects of inbreeding or sweeps while selection signatures detect more general signals of natural selection (PURFIELD *et al*., 2017).

Associating the selection signatures with regions of Quantitative trait loci (QTLs), which are regions of the genome responsible for the expression of phenotypes of interest, can contribute to a better understanding of the traits that are under selection (GRIGOLETTO *et al*., 2019). The genetic effects of crossbreeding composite breeds through the identification of probable ancestry (Paim *et al*., 2020a), can shed light on the genomic composition and contribution (Taurus and Zebu) to the compounds. Therefore, the aim of the study was (I) to identify selection signatures in Braford using high-density SNP data through homozygous runs, (II) to associate selection signatures with QTL, (III) to identify the ancestral genomic composition of composite Braford.

2. Material e métodos

2.1. Ethics statement

Prior approval from the animal care and use committee was not required in this study since the information was obtained from a pre-existing database provided by the Brazilian Agricultural Research Corporation (Embrapa Pecuária Sul, Bagé, Rio Grande do Sul, Brazil) and Delta G genetic breeding program.

2.2. Animals

Where 3,854 Braford animals, 3,183 Hereford animals from the Delta G connection genetic improvement program, provided by the Brazilian Agricultural Research Corporation (EMBRAPA). Animals were genotyped with the *Illumina High-Density Bovine Bead Chip Array* (HD; Illumina Inc., San Diego, USA) containing 777K markers (n=114 Hereford and n=117 Braford); *GeneSeek Genomic Profiler HD-150K* (150k,Illumina Inc., San Diego, CA, USA) containing 150K markers (n=163 Hereford); *BovineSNP50 Bead Chip* (50 K; Illumina, San Diego, USA) containing 50K markers (n=2,148 Hereford and n=3,478 Braford);

GGP-LD BeadChip® (30k,Illumina Inc., San Diego, CA, USA) containing roughly 30K markers (n=722 Hereford and n=186 Braford); and *Illumina BovineLD* (27k,Illumina Inc., San Diego, CA, USA) containing 27K markers (n=36 Hereford and n=73 Braford).

The genotype bank of possible haplotype donor breeds, or probable founder population, genotypes were imported into the HD panel (http://widde.toulouse.inra.fr/widde/), of 35 Hereford animals, 31 Nelore, 46 Brahman (SEMPÉRÉ *et al*., 2015) with no direct relationship with Braford Brazil individuals. All SNP panels were from the arrays the Illumina *High-Density Bovine Bead Chip Array* (HD; Illumina Inc., San Diego, USA). To identify the founding races, Taurus (Hereford$_{\text{-Embrapa}}$ and Hereford individuals from the Widde bank) and Zebu (Brahman and Nelore) were named.

2.3. Data quality control and imputation

The quality control (QC) of the genotypes was implemented using the R/SNPStats package (Clayton, 2014). Markers with a call rate lower than 0.90, located on sex chromosomes, or with a highly significant deviation from the Hardy-Weinberg equilibrium ($p<10\text{-}7$) were removed from the dataset. For markers located in the same genomic position or those highly correlated ($r> 0,98$), the ones with the highest MAF (minimum allele frequency) were retained. For the samples, a call rate of 0.90 was also applied and for animals that were genotyped in different panels, only the information from the highest density panel was kept.

After the QC, imputation was implemented using the FIMPUTE 2.2 software (Sargolzaei *et al*., 2011), and all genotypes were imputed from the lowest density to the highest density panel. The number of SNPs common in the two banks and the rest of this editing process was 310,816 SNPs, contains 7149 cattle.

2.4. Genetic relationship between individuals

The assessment of population stratification was estimated through principal component analysis (PCA) in the PLINK v.1.09 (PURCELL *et al*., 2007), through the genetic distance between individuals, based on state identity matrices (IBS). For the graphic part, the statistical software R was used (http://www.R-project.org/).

2.5. ROH detection and classification

To obtain the runs of homozygosity, the bank with 7149 animals and 310,816 SNPs was used. The ROH were identified for each animal using the PLINK v1.90 software (Purcell *et al*., 2007) This software examines each individual chromosome through a sliding window (Ferenčaković *et al*., 2017; Purfield *et al*., 2012).

Table 1. PLINK parameters for run of homozygosity (ROH) analysis.

Parameter	**Value**	**Definition**
-homozyg-snp	30	Minimum number of SNP required to consider a ROH
-homozyg-kb	1000	Size (Kb) of the sliding window
-homozyg-density	120	Minimum density required to consider a ROH;
-homozyg-gap	1000	Maximum size (Kb) between two SNP to be considered in the same ROH;
-homozyg-window-snp	50	Number of SNP present in the sliding window;
-homozyg-window-het	2	Number of heterozygous SNP allowed in a ROH;
-homozyg-window-threshold	0.05	Threshold to determine a roh;

2.6. Inbreeding coefficient calculated based on the ROH

A genomic inbreeding coefficient based on ROH (F_{ROH}) was estimated for every animal according to the methodology proposed by McQuillan *et al*. (2008): $F_{ROHi} = \frac{\sum_{j=1}^{n} L_{ROHj}}{L_{total}}$, where $\sum_{j=1}^{n} L_{ROHj}$ is the sum of all ROH lengths across the genome for the *i*th animal and L_{total} is the total length of the autosomal genome

covered by markers (2,487.574 bp). For each animal, F_{ROH} ($F_{ROH1–2\ Mb}$, $F_{ROH2–4\ Mb}$, $F_{ROH4–8\ Mb}$, $F_{ROH8\text{-}16\ Mb}$, and $F_{ROH>16\ Mb}$) was calculated based on five ROH lengths: 1-2Mb, 2-4Mb, 4-8Mb, 8-16Mb, >16Mb respectively.

2.7. Autozygosity islands and shared ROH regions

In this analysis, the database containing all individuals (7149 cattle) was used. To identify genomic regions the genome characterized by a high occurrence of ROH (autozygosity islands), a file generated by the PLINK software which specifies how many times each SNP appeared in an ROH was used. Subsequently, the top 1% of the most frequent SNPs within a ROH were selected, and the genomic regions were identified as autozygosity islands by considering consecutive SNPs. In these regions, a 100 Kb window was used in the chromosomal position, and it was intersected with the CattleQTL database (Hu *et al*., 2016). To search for overlapping genes within these regions, the autozygosity islands were aligned to the ARS-UDC 1.2 reference genome using the Ensembl cow gene set 94 releases (Howe *et al*., 2021). Database for Annotation, Visualization, and Integrated Discovery (DAVID) v.2021q2 tool (Huang *et al*., 2009) was used to identify overrepresented gene ontology (GO) terms and Kyoto Encyclopedia of Genes and Genomes (KEGG) pathways by Fisher's test ($p<0.05$) (KIM, 2017). The DAVID enrichment analysis was performed separately for each cattle breed.

The --homozyg-group parameter was used to obtain information on the overlapping of ROH (pools), an overlapping region being considered that which was shared by at least 50% of the individuals in the bank, using an internal script in R to verify the overlap. Subsequently, the gene research and search for QTLs in these regions was carried out.

2.8. Ancestry of Braford compounds

Braford individuals were classified into three subgroups, according to the expected racial composition in the crosses, Braford 1/2 (expected 0.50% Zebu composition), Braford 3/8 (expected 0.37% Zebu composition), and Braford 1/4 (expected 0.25% Zebu composition) to perform ancestry analysis. To perform the ancestry analysis, 50 Hereford-Embrapa individuals, 50 Braford 3/8 animals, were drawn at random. The correlating SNPs were pruned using PLINK software (--indep-pairwise 50 10 0.15).

The database after the editions remained with Herefords-Embrapa - HH (n=50), Brafords 3/8 – BO 3/8 (n=50), Braford 1/4 – BO1/4 (n=31), Braford 1/2 – BO 1/2 (n=16), Nellore - NEL (n=31), Brahman - BRM (n=46) and Hereford-Widde - HFD (n=35), totaling 259 animals with 29512 SNPs.

For cluster analysis, k=2 was defined, where it represents the Braford's Taurine and Zebu ancestry. The Braford genome covered by SNPs were (ALEXANDER; NOVEMBRE; LANGE, 2009) which evaluated using the software ADMIXTURE v. 1.3.0 uses the maximum likelihood estimates of the mixing coefficients through the frequency of ancestral alleles. In addition, each island was analyzed separately for brand ancestry, compared to the expected proportion of taurine and zebu origin of the three Braford compositions. For graphical and statistical visualization, a script was prepared in the R software (http://www.R-project.org/).

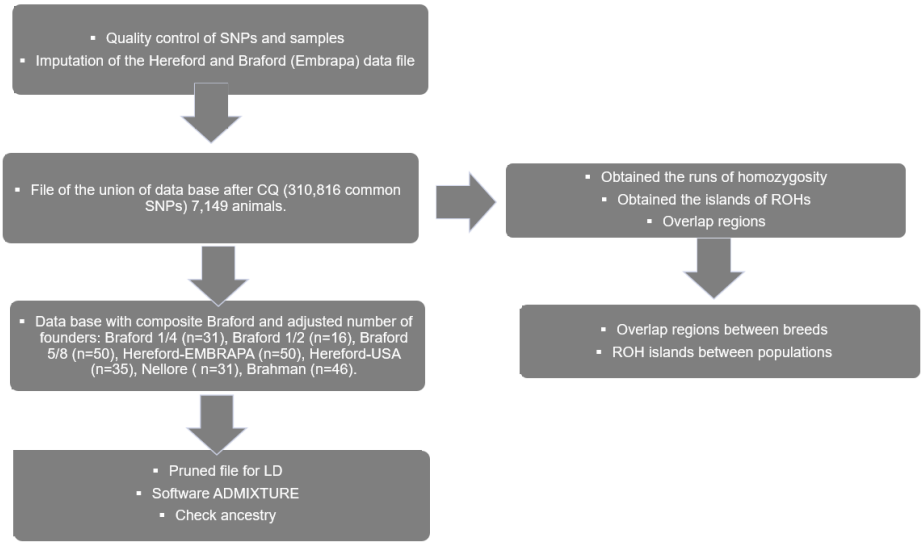

Figure 2. Plot of scheme of the proposed analyzes.

3. Results

3.1. Principal component analysis

Principal component analysis (PCA) using the founding breeds of the Braford, revealed cluster separation between animals according to their Taurine and Zebuine origin observed at the distance from the horizontal axis, where the Braford as expected by its genetic composition is closer to the Hereford. In component 2, a segregation of the Braford animals according to their bloodline and generation is observed (Fig. 3), suggesting that the Brafords are becoming a distinct breed.

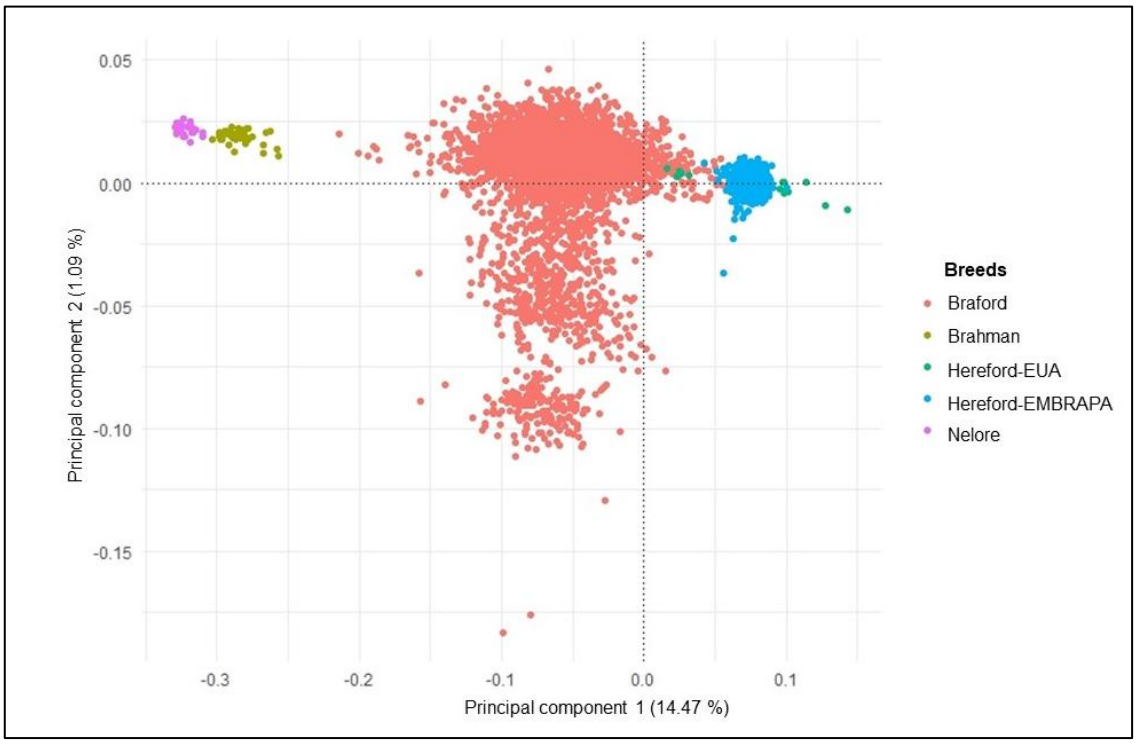

Figure 3. Plot of first and second principal components for of the founding breeds of Braford cattle.

After editing the PCA database (Fig. 4), the same distribution and genetic distance between the founding breeds and the Brafords individuals can be observed, now classified according to the expected composition in the crossing.

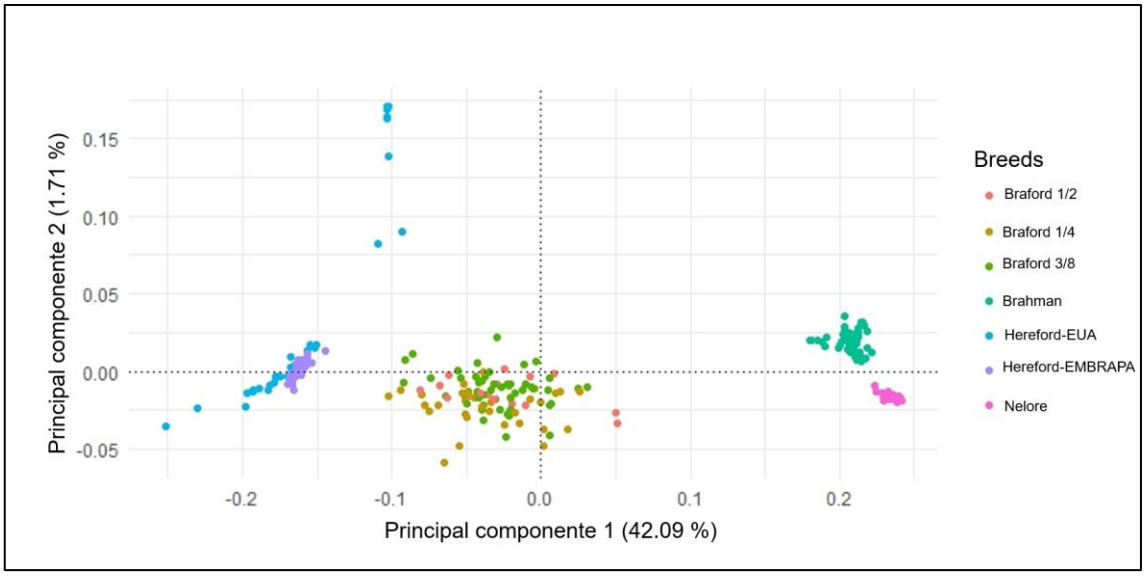

Figure 4. The plot of the first and second main components after editing the database, composed of the founding breeds and Braford animals identified by the composition of the percentage of zebu in the crosses.

3.2. Runs of homozygosity

It detected 210,948 homozygous segments in Braford, 330.146 in Taurus (Hereford- Embrapa and Hereford- Widde), and 5,841 in Zebu. The highest percentage is of short runs, as expected because they are abundant in the genome, and the lowest percentage of longer runs indicates recent inbred mattings, a similar pattern observed in Braford and founder breeds (Tab.2). The maximum size of segments located in Braford was 555.105 Mb, in Taurine 1491.61 and Zebu 626.88, indicating the presence of longer ROHs in Taurine, which also had more ROH segments, 177 maximum located in an individual, as in Braford it was 124 and in Zebu with 104 segments.

Table 2. Descriptive statistics of runs of homozygosity number (n ROH) and mean lengths (Standard deviation in brackets) for five ROH length in Braford, Taurus e Zebu cattle breeds.

Class	Braford			Taurus			Zebu		
	n ROH	(%)	Mean length	n ROH	(%)	Mean length	n ROH	(%)	Mean length
ROH $_{1\text{-}2\ Mb}$	118169	56.02	1.36 (0.28)	161207	48.83	1.38 (0.28)	4045	69.25	1.29 (0.25)
ROH $_{2\text{-}4\ Mb}$	55839	26.47	2.79 (0.56)	96760	29.31	2.81 (0.56)	838	14.35	2.73 (0.56)
ROH $_{4\text{-}8\ Mb}$	26576	12.60	5.46 (1.09)	51537	15.61	5.49 (1.10)	498	8.53	5.63 (1.13)
ROH $_{8\text{-}16\ Mb}$	8075	3.83	10.63 (2.09)	16289	4.93	10.66 (2.12)	301	5.15	11.08 (2.23)
ROH $_{>16\ Mb}$	2289	1.09	25.00 (10.48)	4353	1.32	24.68 (10.40)	159	2.72	27.09 (11.42)

The only region shared by more than 50% of individuals (3,634) was in *Bos taurus autosome* (BTA) 6 (15050230:117776264 bp) containing 11,751 SNPs totaling 10272604 Kb. This region is present in at least 1,532 Brafords, 2,092 Taurus and 10 Zebu. As it is an extensive region, many QTLs were located, we retain only those located in Hereford and Braford, which are related to traits of average daily gain (QTL:164129)(AKANNO *et al*., 2018), body weight (QTL:67424) (SNELLING *et al*., 2010), body weight gain (QTL:66348) (SNELLING *et al*., 2010), carcass weight (QTL:191294) (WANG *et al*., 2020), dry matter intake (QTL:181925) (WANG *et al*., 2020), lean meat yield (QTL:192911) (WANG *et al*., 2020), longissimus muscle area (QTL:191818) (WANG *et al*., 2020), mean corpuscular hemoglobin concentration (QTL:213451) (CHINCHILLA-VARGAS *et al*., 2020), mean corpuscular hemoglobin content (QTL:213438) (CHINCHILLA-VARGAS *et al*., 2020), metabolic body weight (QTL:186480) (WANG *et al*., 2020), residual feed intake (QTL:130954) (SEABURY *et al*., 2017), tick resistance (QTL:135794) (SOLLERO *et al*., 2017), infectious bovine keratoconjunctivitis susceptibility (QTL:238504) (COMIN *et al*., 2021). For all QTLs presented in cattle in this region, a word cloud was plotted which is a data visualization tool to represent words in an image, the larger the word size the greater the frequency with which it appeared.

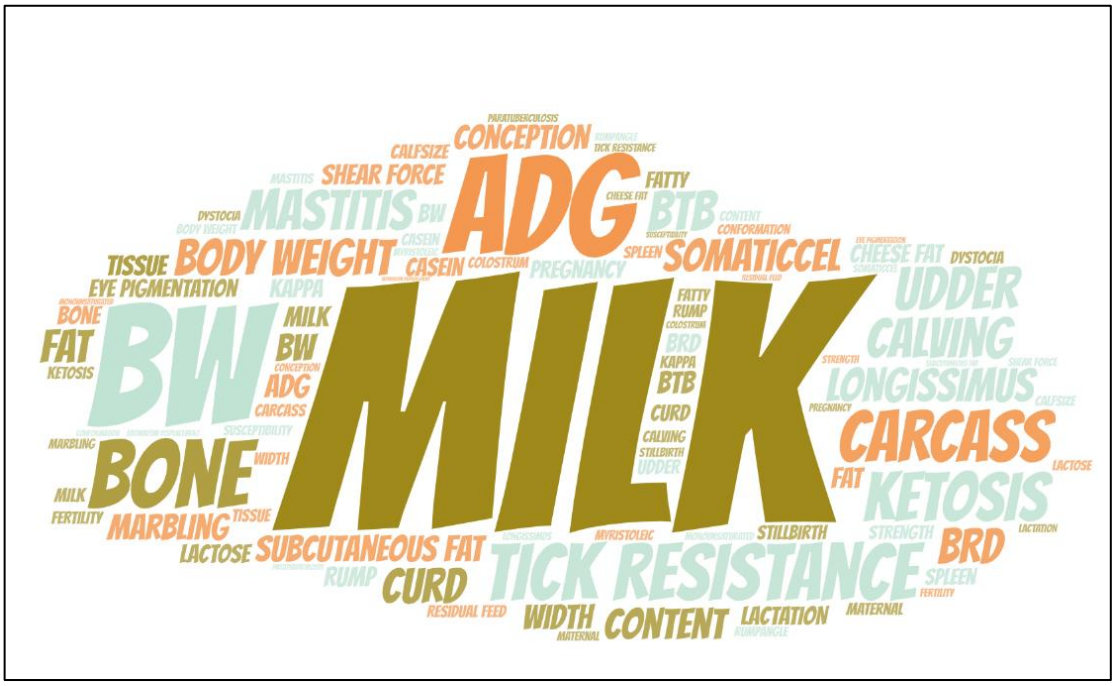

Figure 5. The most frequent QTls, present in the overlap region (BTA6:15050230:117776264 bp), where the size of each word represents the frequency with which it appeared in the results.

Genetic prospecting of this region revealed 14 biological processes, 4 cellular components, 8 molecular functions and 7 KEGG pathways (Supplementary material, Table 1). The complete list of QTLs and genes found in this region can be consulted in the complementary material (Tab.1).

3.3. Inbreeding coefficient calculated based on the ROH

Individuals of the Braford composed breed have a lower FROH on average, when compared to individuals of the founder breeds, they have the lowest value of FROH 8-16 Mb and FROH >16 Mb, which reflects recent inbreeding with the smallest standard deviation indicating low date variation. The Hereford$_{\text{-Widde}}$ (HFD) animals are the most inbreeding (Fig. 6), which was expected since these animals come from a closed population (Tab. 3).

Table 3. Inbreeding coefficients[1] based on runs of homozygosity (ROH), for different lengths of ROH, of the Braford composed ($BO_{1/2}$, $BO_{1/4}$, $BO_{3/8}$), Hereford$_{Embrapa}$ (HH), Hereford$_{Widde}$ (HFD), Nellore (NEL), and Brahman (BRM) breeds.

Coefficients[1]	FROH-total	FROH $_{1-2\ Mb}$	FROH $_{2-4\ Mb}$	FROH $_{4-8\ Mb}$	FROH $_{8-16\ Mb}$	FROH $_{>16\ Mb}$
$BO_{1/2}$	4.25 ±2.81	1.02 ±0.34	1.01 ±0.49	0.84 ±0.60	0.69 ±0.76	0.68 ±1.44
$BO_{3/8}$	4.32 ±1.26	1.12 ±0.24	1.06 ±0.36	0.96 ±0.46	0.62 ±0.42	0.54 ±0.88
$BO_{1/4}$	4.45 ±1.54	1.09 ±0.34	1.08 ±0.37	1.18 ±0.60	0.74 ±0.70	0.35 ±0.61
HH	9.11 ±1.32	2.00 ±0.25	2.42 ±0.42	2.42 ±0.66	1.43 ±0.69	0.69 ±0.83
HFD	14.73 ±7.2	1.81 ±0.31	2.71 ±0.77	3.44 ±1.34	3.41 ±2.51	3.35 ±4.39
NEL	7.30 ±2.39	2.15 ±0.24	0.97 ±0.32	1.01 ±0.42	1.31 ±0.69	1.86 ±1.68
BRM	5.98 ±3.10	1.73 ±0.28	0.74 ±0.27	1.02 ±0.68	1.14 ±1.01	1.32 ±2.06

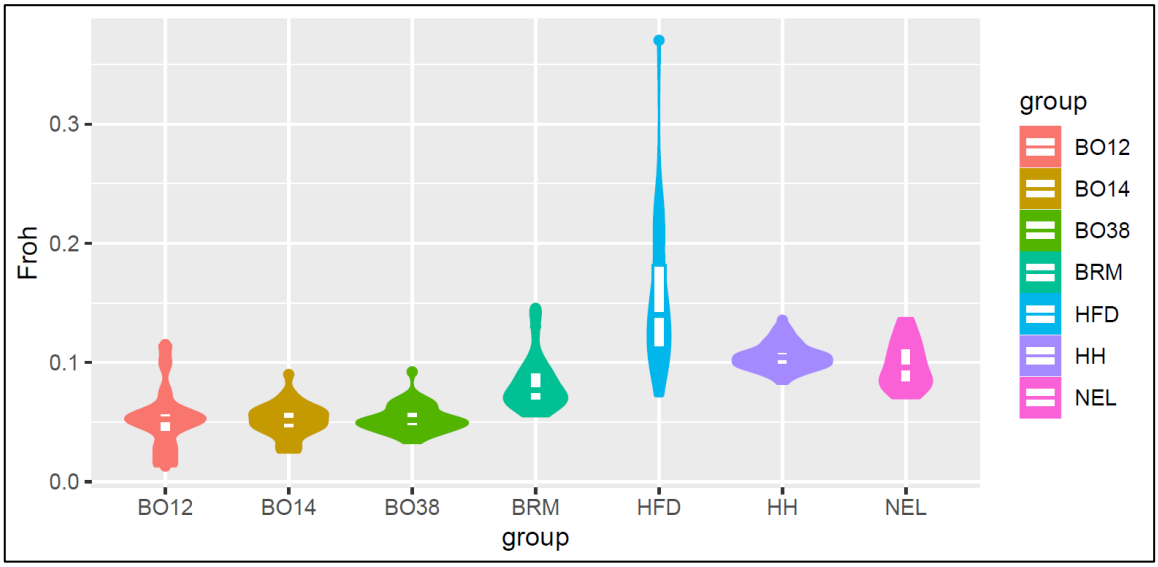

Figure 6. Inbreeding levels distribution plotted of the Braford composed ($BO_{1/2}$, $BO_{1/4}$, $BO_{3/8}$), Hereford-Embrapa (HH), Hereford-USA (HFD), Nellore (NEL), and Brahman (BRM) breeds.

3.4. Islands of runs homozygosity

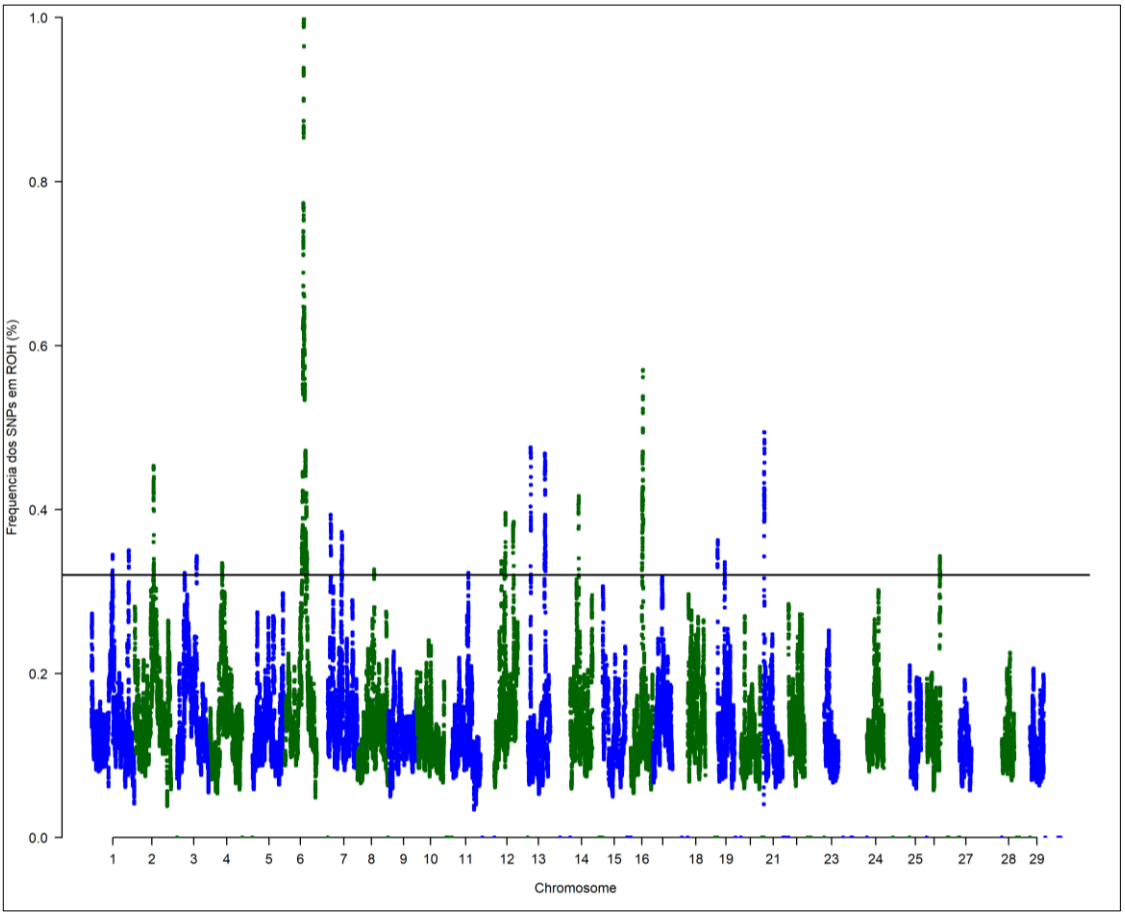

Figure 7. Frequency of each SNP in a run of homozygosity (ROH) in Braford population according to the chromosome and position. The horizontal line indicates the 1% threshold to classify the SNP to be in an ROH island.

Nineteen islands of homozygosity were identified in the Braford (Fig.7), the on chromosomes 1 (77565281:78498849 and 137760175:138388286 bp), 2 (70972542:72683773 bp), 3 (71933237:73140260 bp), 4 (46023834:46826291 bp), 6 (62689412;82152955 bp), 7 (10581357:11613756 and 50207376:53313843 bp), 8 (61264237:61735410 bp), 11 (61473501:61810984 bp), 12 (25795085:41733489 and 69673372:71343009 bp), 13 (10778845:65716252 bp), 14 (30638513:31626008 bp), 16 (41831878:5976821 bp), 19 (601148:1202469 bp), 21 (1104519:3372256 bp) and 26 (1104519:3372256 bp).

Annotation analysis using the Ensembl genome browser revealed 535 genes in the Braford ROH islands, after which functional enrichment analysis identified biological process, cellular component, molecular function and only one KEGG pathways (Tab.4), the genes present in these pathways are related to milk production, amount of fat and protein in milk, amount of somatic cells in milk, fertility traits, parturition and number of stillborn children, traits of body conformation and udder morphology, and pigmentation traits of the skin (Supplementary material Tab. 2).

Tabela 4. Ontology Genes (GO) annotation analysis of terms and pathways KEGG enriched for significant genes (p<0.01) by Fisher's test in Braford.

	Genes[1] (BTA[2])	*P-value*
Biological Process		
(GO:0007156)		0.000002
Homophilic cell adhesion via plasma membrane adhesion molecules	*CLSTN1* (16) *G3MYX2_BOIN (7)* *LOC104968820 (7)* *PCDHA13* (7) *PCDHA5* *PCDHA8 (7)* *PCDHB1* (7) *PCDHB4 (7)* *PCDHGC3* (7)	
Cell Component		
(GO:0005887)		0.00048
Integral component of the plasma membrane	*ADGRL3* (6) *ADGRE3 (7)* *ATP10D (6)* *G3MYX2_BOVIN* *GABRB1* (6) *KIT (6)* *LOC100337213 (7)* *LOC104968820 (7)* *LOC112447333 (7)* *MMP24* (13) *PCDHA13 (7)* *PCDHB1 (7)* *PCDHGA5* *PCDHGC3 (7)* *PDGFRA* (6) *TSPAN2 (3)*	
(GO:0005813)		0.0074
Centrosome	*SLAIN2 (6)* *TGIF2 (13)*	

	CEP135 (6) *CEP250 (13)* *CSPP1 (14)* *DYNLRB1 (13)* *NINL (13)* *PROCR (13)* *PRKACA (7)*	
Molecular Function		
(GO:0008013) beta-catenin binding	*CTNNA1 (7)* *CTNNBIP1 (16)* *LZIC (16)* *KDM6B (19)*	0.0097
(GO:0005509) Calcium ion binding	*ADGRE3* (7) *ADGRL*3 (6) *CLSTN1* (16) *G3MYX2_BOVIN* *LOC104968820 (7)* *MASP2* (16) *MYL9* (13) *NINL (13)* *PCDHA13* (7) *PCDHB1 (7)* *PCDHGA5 (7)* *PCDHGA8 (7)* *PCDHGB4 (7)* *PCDHGC3* (7)	0.00014
KEGG pathways		
Huntington disease	*NDUFB7 (7)* *RESTA (6)* *RESTB (6)* *POLR2A (19)* *POLR2B (19)* *DNAH2 (19)* *MTOR (16)*	0.0097

[1] BTA: *Bos taurus autosome*, [2]ARS-UCD1.2 *Bos taurus* genome assembly

3.5. Ancestry of the composite Braford

The ratio of Taurine and Zebuine in the Braford genome was performed with all SNPs present in the bank covering all autosomes.

The average percentage of zebu for the final Braford 3/8 compound was 0.329, close to the expected average in crosses (0.37 Zebu), where 4 animals in the sample were below 1/4, and 13 animals were above the expected. The

compound Braford ½ was the one that presented the greatest difference between the composition expected by the crosses and the genomic composition, where, on average, 0.34% of the genome is of Zebuine origin (expected 0.50), two animals are very close to the expected composition, four animals above 3/8 and 15 above 1/4. Of the 31 animals in the Braford 1/4 composition, 24 had a composition above 0.25 Zebu, that is, 77% of the sampled population (Fig. 8).

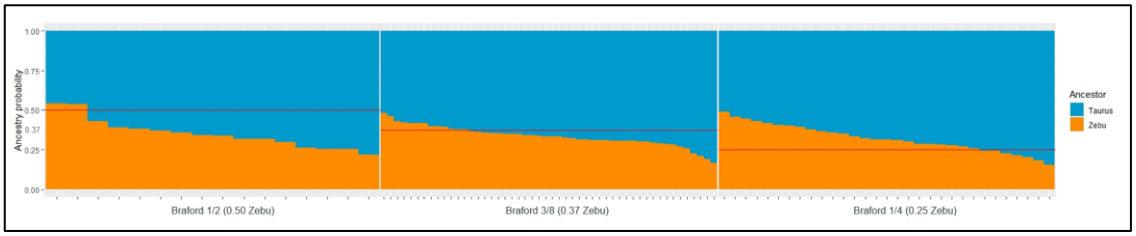

Figure 8. The average probability of ancestry in the genome of three Braford compositions. The red line represents the expected proportion of Zebu in the genome. Each vertical line of the graph corresponds to a sample animal.

4. Discussion

4.1. Principal component analysis

Initially, the presence of genetic groupings was verified through the PCA (Fig. 3) where the Braford presented a greater dispersion of eigenvectors when compared to the other breeds, an indication of the genetic variability of the composite breed. (BUZANSKAS *et al*., 2021), dispersion in the second PCA2 suggests that Braford is becoming a distinct grouping (BLACKBURN *et al*., 2014; PAIM *et al*., 2020b). With increasing variability among hybrid progeny, it is possible to develop populations capable of adapting more quickly to climate variability, which is an emerging issue (BECKER *et al*., 2013). Its proximity to Hereford confirms the greater contribution of the Taurine breed to its racial composition (BUZANSKAS *et al*., 2017). Figure 4 shows that the sampled Braford compounds are not grouped by the expected composition, which reflects that the calculated composition is not the one observed in the genome, which may be due

to the effect of Mendelian sampling during recombination in meiosis (KUEHN *et al*., 2011).

4.2. Runs of homozygosity

Runs of homozygosity can be used to identify selective footprints in the genome, as individuals that are selected will exhibit long periods of homozygosity around the target locus (FORUTAN *et al*., 2018; REBELATO; CAETANO, 2018). Our results are similar regarding the size of the ROH segments in the genome, and those obtained by other authors for different bovine breeds. The presence of short ROH (1-2 Mb and 2-4 Mb) was evident for all breeds, as described in taurine cattle (PURFIELD *et al*., 2012; ZHAO *et al*., 2021) Zebu (PERIPOLLI *et al*., 2018). The size of the segments indicates approximately how many generations inbreeding events occurred (HOWRIGAN; SIMONSON; KELLER, 2011), crossing between indicine and taurine animals increases genetic diversity and contributes to the disruption of long stretches of homozygous genotypes within individuals (PURFIELD *et al*., 2012) which explains the maximum size of the segments located in Braford being smaller than in Hereford.

The only region overlapping in more than 50% of the individuals in the population was in BTA6 (15050230:117776264 bp), contains a selection signature (Fig.7), was shared by 2092 Taurus and only 10 Zebu individuals of this population. Specific regions of the genome of composite races may have a specific composition different from that calculated based on Mendelian sampling (Paim *et al*., 2020a).

This overlap region of taurine origin is associated with QTLs in the Hereford and Braford breeds regarding traits of average daily gain (QTL: 164129) (Akanno *et al*., 2018), body weight (QTL: 67424) (Snelling *et al*., 2010), body weight gain (QTL: 66348) (SNELLING *et al*., 2010), tick resistance (QTL: 135794) (SOLLERO *et al*., 2017). These traits are also included in the Braford and Hereford selection index (ASSOCIAÇÃO BRASILEIRA DE HEREFORD E BRAFORD, 2018). Therefore, it is likely that favorable alleles in high-effect genes

for these traits have increased in allele frequency and become similar in both populations (PAIM *et al*., 2020b).

The gene ontology and KEGG pathways identified significant terms ($p<0.01$) in this region. At the biological process the inflammatory response (GO:0006954) e cell component extracellular space (GO:0005615) where the *KIT* gene present in these pathways is related to the skin pigmentation trait associated with the eye area trait and pigmentation (QTL: 21154; QTL: 21160;) (PAUSCH *et al*., 2012). This is a feature of adaptation to temperate climate regions, where animals are selected by assigning visual scores (ABHB, 2020). Lack of ocular pigmentation predisposes to diseases such as infectious bovine keratoconjunctivitis (IBC) and ocular carcinoma (FONTANESI *et al*., 2010), these two diseases correspond to high economic losses in beef cattle.

The genes known to influence the protein content and composition in milk are the casein genes, which are in BTA6, in the so-called casein gene cluster, which encompasses ~250 kb (Boettcher *et al*., 2004). The genes *CSN1S1*, *CSN1S2*, and *CSN3* are related to 87 QTLs of milk quality and production (BARTONOVA *et al*., 2012; FONTANESI *et al*., 2014; PEGOLO *et al*., 2016; POULSEN *et al*., 2013; PRINZENBERG *et al*., 2003; VIALE *et al*., 2017) (Supplementary Tab. 2). Due to the proximity of the four casein genes in the bovine genome, the casein genes are not independently inherited but are often transmitted from parent to offspring as a single haplotype (MEIER *et al*., 2019), which may be related to selection for maternal ability such as post-weaning weight gain applied in these populations. In the QTL survey in this region, carried out without a breed filter, traits related to milk production and quality were the most frequent (Fig.5).

One of the complementarities sought in Braford is the hardiness of tropical cattle. The genetic prospection of this region revealed the biological process inflammatory response (GO:0006954) significant and related to the genes *CXCL2*, *CXCL5*, and *CXCL8*. These genes were in other cattle breeds also related to immune responses in Ayrshire (RAJAWAT *et al*., 2022). The expression of these genes is related to the innate immune response (KOGUT; ROTHWELL; KAISER, 2003).

4.3. Inbreeding coefficient calculated based on the ROH

The average FROH value (0.44%) for the Braford breed is lower than that reported in Brahman cattle (average FROH 0.53%) and relatively higher tropical composite (average FROH 0.42%) using a 700k panel (REVERTER *et al*., 2017). When compared to pure breeds, the estimate of the $F_{ROH\text{-}mean}$ of the Braford is much lower, reinforcing the concept that the introduction of new animals in the population, to explore the complementarity between the breeds, allows different genetic combinations, leading to a decrease in inbreeding, in addition to breaking the long ROH segments (KELLEHER *et al*., 2017; PERIPOLLI *et al*., 2020; LOPA, 2015).

4.4. Genes in consensus selection signature regions

The chromosomes 4 and 26 presented overlapping islands in the study carried out by Peripolli *et al*., (2018b) in the Nelore lineages the region (4:45080000:47310000) of the Godhavar lineage overlaps that found in the Braford. The BTA4 region (46,023,834:46,826,291 bp) has 3 QTLs (QTL:66167, QTL:66168, QTL:66169), involved with Immunoglobulin G level (LEACH *et al*., 2010), milk production (QTL: 224504, QTL: 2730, QTL: 106523, QTL: 112042, QTL: 5056) (LINDERSSON *et al*., 1998; MICHENET *et al*., 2016; ZHANG *et al*., 1998). BTA26 (1,104,519:3,372,256 bp) harbors the QTLs (QTL: 56582, QTL: 56583, QTL: 56584, QTL: 56585, QTL: 56586, QTL: 56587, and QTL: 56588) milk production and milk quality (BOUWMAN *et al*., 2011), making this region enriched, selected, reinforcing this signature.

The signatures on chromosomes 1, 2, 3, 7(10581357:11613756 bp), 8, 11, 12(25795085:41733489 bp), and 16, include genes related to important QTLs, in BTA7 the island position is overlap on the *ADGRE3* gene associated with fertility trait (QTL: 212165, QTL: 212602) (GALLIOU *et al*., 2020). The island in BTA16 is superimposed on two genes *RICTOR and* associated with 7 QTLs of milk production and quality traits (JIANG *et al*., 2019), immune responses like bovine

respiratory disease susceptibility (NEUPANE; KISER; NEIBERGS, 2018). The *RPTOR* gene associated with 13 QTLs is associated with traits of myristic acid content, myristoleic acid content, oleic acid content, and palmitoleic acid content (SASAGO *et al*., 2017).

The island in is superimposed on the *RESTB* gene region (QTL: 212155, QTL: 212585), the gene *SLAIN2* (QTL: 212153, QTL: 212583) associate fertility trait (GALLIOU *et al*., 2020) e gene *KIT* (QTL: 21160, QTL: 21154) associates with the trait of eye area pigmentation (PAUSCH *et al*., 2012), and milk somatic cell quantity (QTL: 31634, QTL: 31635) (FONTANESI *et al*., 2010). The BTA14 *CSPP1* gene is linked to fertility traits (QTL: 57157, QTL: 57113, QTL: 127018, QTL: 127033) (COCHRAN *et al*., 2013; ORTEGA *et al*., 2017), these print regions in the Braford genome suggest the complementarity of selection seeking to select favorable alleles for the traits of interest, such as ocular pigmentation, breed pattern and fertility in Taurus, knowing that heifers influenced by Zebu cattle have difficulty reaching puberty must have caused a high selection pressure (PAIM *et al*., 2020a; SARTORI *et al*., 2010) in Braford for precocious puberty by fixing these alleles.

The signature on BTA7 (50,207,376:53,313,843 bp) has been reported on overlapping islands in Brahman, Gyr, and Nellore cattle (7:51,502,500:52,353,000 bp) (Sölkner *et al*., 2014) in Holstein (7:51,574,295:52,419,683 bp) and Simmental (7:51,157,314:53,101,552 bp) (SZMATOŁA *et al*., 2016) spanning the same chromosomal region around 51–53 Mb. This mapping is useful to identify genes that affect traits of interest (MARRAS *et al*., 2015), as this region was common in cattle breeds selected for different purposes, it is suggested that selection pressure may also be occurring in traits different from those specific for milk or beef (PERIPOLLI *et al*., 2018). This region houses the *CTNNA1* gene in beta-catenin binding (GO:0008013), this gene encodes a member of the catenin family of proteins that play an important role in the cell adhesion process by connecting cadherins located on the plasma membrane to the actin filaments inside the cell, in cattle has been associated with the level of myostatin expression in the skeletal muscle of Holstein-Friesian bulls

(SADKOWSKI *et al*., 2008), this protein plays a fundamental role in meat production characteristics (PERIPOLLI *et al*., 2018).

The only significant KEGG pathway ($p<0.01$) was Huntington's disease, associated with neuronal dysfunction and neurodegeneration, where the *RESTA* gene (RE1 silencing transcription factor A) plays a key role in the development of the disease (BUCKLEY *et al*., 2010).

4.5. Ancestry of the Braford compounds

The genetic makeup of a composite breed is dynamic and changes over generations (PAIM *et al*., 2020a) and individuals and their genetic makeup vary in proportion but maintain an average percentage expected for the breed. The selection and crosses carried out in the Braford transmitted and preserved some regions of the founding breeds, as the genetic contribution of the Hereford (Taurus) is greater, a greater similarity between the Braford and the Hereford is expected.

However, predicting race composition in advanced generations of crossbred populations is more difficult with limited markers because unique race alleles are not necessarily transmitted to advanced generations, as in the case of the Braford 1/4 and 3/8 compounds. Because of crossover events and chromosomal variety during gametogenesis in the F1 parents of the subsequent generation, variation in breed composition not captured by strict pedigree-based breed composition may have caused this genomic composition (KUEHN *et al*., 2011). Apparent discrepancies between pedigree-determined breed composition and predictions based on SNP markers are not just a function of errors in prediction; variation attributable to chromosomal sampling around the mean (pedigree) also contributes to this (KUEHN *et al*., 2011).

Since the result of 34% Zebu composition in the 1/2 product, was not expected, perhaps a likely explanation for this result would be an estimation bias in the SNP finding, which was based in part on sequence data from the draft of Hereford (KUEHN *et al*., 2011).

5. Final considerations

The QTLs related to selected productive traits in the founding breeds were identified in the regions of the ROH islands; as well as biological processes involved in the expression of phenotypes of interest. The detections of selection signatures with QTLs related to meat production demonstrate that the objective of producing a composite animal focused on beef production left marks in the genome of these populations.

Breed composition is useful for tracking the herd of origin, and its composition in composite breeds both in disease transmission and inbreeding control and pedigree checking. Estimates of racial composition were not comprehensive for the Braford 1/2 compounds analyzed.

Acknowledgment

The present work was carried out with the support of the Coordination for the Improvement of Higher Education Personnel - Brazil (CAPES) – Financing code 001. The authors thanks to the Empresa Brasileira de Pesquisa Agropecuária - Embrapa Pecuária Sul (Bagé/RS) and Delta G connection for providing the datasets

REFERENCIES

ABHB - ASSOCIAÇÃO BRASILEIRA DE HEREFORD E BRAFORD. **As raças Hereford e Braford**. Bagé: ABHB, 2020. Disponível em: https://www.abhb.com.br/. Acesso em: 14 nov. 2022.

ABHB - ASSOCIAÇÃO BRASILEIRA DE HEREFORD E BRAFORD. **Manual do criador:** setor de registro genealógico. Bagé: ABHB, 2018. Disponível em: https://abhb.com.br/wp-content/uploads/2014/06/Manual_do_Criador.pdf. Acesso em: 14 nov. 2022.

AKANNO, E. C. *et al*. Genome-wide association scan for heterotic quantitative trait loci in multi-breed and crossbred beef cattle. **Genetics Selection Evolution**, Paris, v. 50, n. 1, [art.] 48, 2018. Disponível em: https://doi.org/10.1186/s12711-018-0405-y. Acesso em: 10 nov. 2021.

ALEXANDER, D. H.; NOVEMBRE, J.; LANGE, K. Fast model-based estimation of ancestry in unrelated individuals. **Genome Research**, New York, v. 19, n. 9, p. 1655–1664, Sept. 2009.

BARTONOVA, P. *et al*. Association between CSN3 and BCO2 gene polymorphisms and milk performance traits in the Czech Fleckvieh cattle breed. **Genetics and Molecular Research**, Ribeirão Preto, v. 11, n. 2, p. 1058-1563, 2012.

BECKER, M. *et al*. Hybridization may facilitate in situ survival of endemic species through periods of climate change. **Nature Climate Change**, London, v. 3, n. 12, p. 1039–1043, 2013.

BIEGELMEYER, P. *et al*. Linkage disequilibrium, persistence of phase and effective population size estimates in Hereford and Braford cattle. **BMC Genetics**, London, v. 17, n. 1, [art.] 32, 2016.

BLACKBURN, T. M. *et al*. A unified classification of alien species based on the magnitude of their environmental impacts. **PLoS Biology**, San Francisco, v. 12, n. 5, [art.] e1001850, 2014.

BOETTCHER, P. J. *et al*. Effects of casein haplotypes on milk production traits in Italian holstein and Brown Swiss cattle. **Journal of Dairy Science**, Champaign, v. 87, n. 12, p. 4311-4317, 2004.

BOUWMAN, A. C. *et al*. Genome-wide association of milk fatty acids in Dutch dairy cattle. **BMC Genetics**, London, v. 12, [art.] 43, 2011.

BUCKLEY, N. J. *et al*. The role of REST in transcriptional and epigenetic dysregulation in Huntington's disease. **Neurobiology of Disease**, San Diego, v. 39, n. 1, p. 28-39, 2010.

BUZANSKAS, M. E. *et al.* Overlapping haplotype blocks indicate shared genomic regions between a composite beef cattle breed and its founder breeds. **Livestock Science**, Amsterdam, v. 254, [art.] 104747, 2021.

BUZANSKAS, M. E. *et al*. Study on the introgression of beef breeds in Canchim cattle using single nucleotide polymorphism markers. **PLoS ONE**, San Francisco, v. 12, n. 2, [art.] e0171660, 2017.

CHINCHILLA-VARGAS, J. *et al*. Genetic basis of blood-based traits and their relationship with performance and environment in beef cattle at weaning. **Frontiers in Genetics**, Lausanne, v. 11, [art.] 717, 2020.

COCHRAN, S. D. *et al*. Discovery of single nucleotide polymorphisms in candidate genes associated with fertility and production traits in Holstein cattle. **BMC Genetics**, London, v. 14, [art.] 49, 2013.

COMIN, H. B. *et al*. Genome-wide association study of resistance/susceptibility to infectious bovine keratoconjunctivitis in Brazilian Hereford cattle. **Animal Genetics**, Oxford, v. 52, n. 6, p. 881-886, 2021.

FAY, J. C.; WU, C. I. Hitchhiking under positive Darwinian selection. **Genetics**, Baltimore, v. 155, n. 3, p. 1405-1413, 2000.

FONTANESI, L. *et al*. A candidate gene association study for nine economically important traits in Italian Holstein cattle. **Animal Genetics**, Oxford, v. 45, n. 4, p. 576-580, 2014.

FONTANESI, L. *et al.* Genetic heterogeneity at the bovine KIT gene in cattle breeds carrying different putative alleles at the spotting locus. **Animal Genetics**, Oxford, v. 41, n. 3, p. 295-303, 2010.

FORUTAN, M. *et al.* Inbreeding and runs of homozygosity before and after genomic selection in North American Holstein cattle. **BMC Genomics**, London, v. 19, n. 1, [art.] 98, 2018.

GALLIOU, J. M. *et al*. Identification of loci and pathways associated with heifer conception rate in U.S. holsteins. **Genes**, Basel, v. 11, n. 7, [art.] 767, 2020.

GIBBS, R. A. *et al*. Genome-wide survey of SNP variation uncovers the genetic structure of cattle breeds. **Science**, Washington, DC, v. 324, n. 5926, p. 528-532, 2009.

GONZÁLEZ, A. R. M. *et al*. Process of introduction of australian braford cattle to south america: configuration of population structure and genetic diversity evolution. **Animals**, Basel, v. 12, n. 3, [art.] 275, 2022.

GRIGOLETTO, L. *et al.* Genome-wide associations and detection of candidate genes for direct and maternal genetic effects influencing growth traits in the Montana Tropical® Composite population. **Livestock Science**, Amsterdam, v. 229, p. 64-76, 2019.

HAASL, R. J.; PAYSEUR, B. A. Fifteen years of genomewide scans for selection: Trends, lessons and unaddressed genetic sources of complication. **Molecular Ecology**, Oxford, v. 25, n. 1, p. 5-23, 2016.

HOWRIGAN, D. P.; SIMONSON, M. A.; KELLER, M. C. Detecting autozygosity through runs of homozygosity: a comparison of three autozygosity detection algorithms. **BMC Genomics**, London, v. 12, [art.] 460, 2011.

JIANG, J. *et al*. A large-scale genome-wide association study in U.S. Holstein cattle. **Frontiers in Genetics**, Lausanne, v. 10, [art.] 412, May, 2019.

KELLEHER, M. M. *et al*. Inference of population structure of purebred dairy and beef cattle using high-density genotype data. **Animal**, Cambridge, v. 11, n. 1, p. 15–23, Jan. 2017.

KIM, H.-Y. Statistical notes for clinical researchers: chi-squared test and Fisher's exact test. **Restorative Dentistry & Endodontics**, Seoul, v. 42, n. 2, p. 152-155, 2017.

KOGUT, M. H.; ROTHWELL, L.; KAISER, P. Differential regulation of cytokine gene expression by avian heterophils during receptor-mediated phagocytosis of opsonized and nonopsonized Salmonella enteritidis. **Journal of Interferon and Cytokine Research**, Larchmont, v. 23, n. 6, p. 319-327, 2003.

KREITMAN, M. Methods to detect selection in populations with applications to the human. **Annual Review of Genomics and Human Genetics**, Palo Alto, v. 1, p. 539-559, 2000.

KUEHN, L. A. *et al*. Predicting breed composition using breed frequencies of 50,000 markers from the US Meat Animal Research Center 2,000 bull project. **Journal of Animal Science**, Champaign, v. 89, n. 6, p. 1742–1750, 2011.

LEACH, R. J. *et al*. Quantitative trait loci for variation in immune response to a Foot-and-Mouth Disease virus peptide. **BMC Genetics**, London, v. 11, [art.] 107, 2010.

LINDERSSON, M. *et al.* Mapping of serum amylase-1 and quantitative trait loci for milk production traits to cattle chromosome 4. **Journal of Dairy Science**, Champaign, v. 81, n. 5, p. 1454-1461, 1998.

LOPA, Thais Maria Bento Pires. **Estudo da estrutura populacional da raça Braford com base no pedigree**. 2015. 59 f. Dissertação (Mestrado em Ciência

Animal) - Universidade Federal do Pampa, Campus Uruguaiana, Uruguaiana, 2015.

MARRAS, G. *et al*. Analysis of runs of homozygosity and their relationship with inbreeding in five cattle breeds farmed in Italy. **Animal Genetics**, Oxford, v. 46, n. 2, p. 110–121, Apr. 2015.

MEIER, S. *et al*. DNA sequence variants and protein haplotypes of casein genes in german black pied cattle (DSN). **Frontiers in Genetics**, Lausanne, v. 10, [art.] 1129, 2019.

MICHENET, A. *et al*. Detection of quantitative trait loci for maternal traits using high-density genotypes of Blonde d'Aquitaine beef cattle. **BMC Genetics**, London, v. 17, n. 1, [art.] 88, 2016.

NEUPANE, M.; KISER, J. N.; NEIBERGS, H. L. Gene set enrichment analysis of SNP data in dairy and beef cattle with bovine respiratory disease. **Animal Genetics**, Oxford, v. 49, n. 6, p. 527-538, 2018.

ORTEGA, M. S. *et al*. Association of single nucleotide polymorphisms in candidate genes previously related to genetic variation in fertility with phenotypic measurements of reproductive function in Holstein cows. **Journal of Dairy Science**, Champaign, v. 100, n. 5, p. 3725-3734, 2017.

PAIM, T. P. *et al*. Dynamics of genomic architecture during composite breed development in cattle. **Animal Genetics**, Oxford, v. 51, n. 2, p. 224-234, 2020a.

PAIM, T. P. *et al*. genomic breed composition of selection signatures in brangus beef cattle. **Frontiers in Genetics**, Lausanne, v. 11, [art.] 710, 2020b.

PEACOCK, F. M. *et al*. Additive genetic and heterosis effects in crosses among cattle breeds of British, European and Zebu origin. **Journal of Animal Science**, Champaign, v. 52, n. 5, p. 1007-1013, 1981.

PEGOLO, S. *et al*. Effects of candidate gene polymorphisms on the detailed fatty acids profile determined by gas chromatography in bovine milk. **Journal of Dairy Science**, Champaign, v. 99, n. 6, p. 4558-4573, 2016.

PERIPOLLI, E. *et al*. Autozygosity islands and ROH patterns in Nellore lineages: Evidence of selection for functionally important traits. **BMC Genomics**, London, v. 19, [art.] 680, 2018.

PERIPOLLI, E. *et al*. Genome-wide scan for runs of homozygosity in the composite Montana Tropical® beef cattle. **Journal of Animal Breeding and Genetics**, Berlin, v. 137, n. 2, p. 155-165, 2020.

POULSEN, N. A. *et al*. The occurrence of noncoagulating milk and the association of bovine milk coagulation properties with genetic variants of the

caseins in 3 Scandinavian dairy breeds. **Journal of Dairy Science**, Champaign, v. 96, n. 8, p. 4830-4842, 2013.

PRINZENBERG, E. M. *et al.* Polymorphism of the bovine CSN1S1 promoter: Linkage mapping, intragenic haplotypes, and effects on milk production traits. **Journal of Dairy Science**, Champaign, v. 86, n. 8, p. 2696-2705, 2003.

PURCELL, S. *et al*. Plink: a tool set for whole-genome association and population-based linkage analyses. **American Journal of Human Genetics**, Baltimore, v. 81, n. 3, p. 559–575, 2007.

PURFIELD, D. C. *et al*. Runs of homozygosity and population history in cattle. **BMC Genetics**, London, v. 13, [art.] 70, 2012.

PURFIELD, D. C. *et al*. The distribution of runs of homozygosity and selection signatures in six commercial meat sheep breeds. **PLoS ONE**, San Francisco, v. 12, n. 5, [art.] 0176780, 2017.

RAJAWAT, D. *et al*. Identification of important genomic footprints using eight different selection signature statistics in domestic cattle breeds. **Gene**, Amsterdam, v. 816, [art.] 146165, Mar. 2022.

REBELATO, A. B.; CAETANO, A. R. Runs of homozygosity for autozygosity estimation and genomic analysis in production animals. **Pesquisa Agropecuária Brasileira**, Brasília, DF, v. 53, n. 9, p. 975-984, 2018.

REVERTER, A. *et al*. Genomic inbreeding depression for climatic adaptation of tropical beef cattle. **Journal of Animal Science**, Champaign, v. 95, n. 9, p. 3809-3821, 2017.

SADKOWSKI, T. *et al*. Gene expression profiling in skeletal muscle of Holstein-Friesian bulls with single-nucleotide polymorphism in the myostatin gene 5′-flanking region. **Journal of Applied Genetics**, Cheshire, v. 49, n. 3, p. 237-250, 2008.

SARTORI, R. *et al*. Physiological differences and implications to reproductive management of Bos taurus and Bos indicus cattle in a tropical environment. **Society of Reproduction and Fertility Supplement**, Packington, v. 67, p. 357-375, 2010.

SASAGO, N. *et al*. Genome-wide association study for carcass traits, fatty acid composition, chemical composition, sugar, and the effects of related candidate genes in Japanese Black cattle. **Animal Science Journal**, Richmond, v. 88, n. 1, p. 33-44, 2017.

SEABURY, C. M. *et al*. Genome-wide association study for feed efficiency and growth traits in U.S. beef cattle. **BMC Genomics**, London, v. 18, n. 1, [art.] 386, 2017.

SEMPÉRÉ, G. *et al*. WIDDE: a web-Interfaced next generation database for genetic diversity exploration, with a first application in cattle. **BMC Genomics**, London, v. 16, [art.] 940, 2015.

SNELLING, W. M. *et al*. Genome-wide association study of growth in crossbred beef cattle. **Journal of Animal Science**, Champaign, v. 88, n. 3, p. 837-848, 2010.

SOLLERO, B. P. *et al.* Tag SNP selection for prediction of tick resistance in Brazilian Braford and Hereford cattle breeds using Bayesian methods. **Genetics Selection Evolution**, Paris, v. 49, [art.] 49, 2017.

SZMATOŁA, T. *et al*. Characteristics of runs of homozygosity in selected cattle breeds maintained in Poland. **Livestock Science**, Amsterdam, v. 188, p. 72–80, June 2016.

VIALE, E. *et al*. Association of candidate gene polymorphisms with milk technological traits, yield, composition, and somatic cell score in Italian Holstein-Friesian sires. **Journal of Dairy Science**, Champaign, v. 100, n. 9, p. 7271-7281, 2017.

WANG, Y. *et al*. Genetic architecture of quantitative traits in beef cattle revealed by genome wide association studies of imputed whole genome sequence variants: II: carcass merit traits. **BMC Genomics**, London, v. 21, n. 1, [art.] 36. 2020.

WILLIAMS, J. L. *et al*. Inbreeding and purging at the genomic Level: The Chillingham cattle reveal extensive, non-random SNP heterozygosity. **Animal Genetics**, Oxford, v. 47, n. 1, p. 19-27, 2016.

WRIGHT, S. Genetical structure of populations. **Nature**, London, v. 166, n. 4215, p. 247–249, 1949.

YURCHENKO, A. A. *et al.* Scans for signatures of selection in Russian cattle breed genomes reveal new candidate genes for environmental adaptation and acclimation. **Scientific Reports**, London, v. 8, [art.] 12984, 2018.

ZHANG, Q. *et al*. Mapping quantitative trait loci for milk production and health of dairy cattle in a large, outbred pedigree. **Genetics**, Baltimore, v. 149, n. 4, p. 1959-1973, 1998.

ZHAO, G. *et al*. Runs of homozygosity analysis reveals consensus homozygous regions affecting production traits in Chinese Simmental beef cattle. **BMC Genomics**, London, v. 22, [art.] 678, 2021.

COMPLEMENTARY MATERIAL

Table1. The QTL search retrieved from the gene pool of the overlapping region.

BTA [1]	Gene Symbol	Gene[2]	QTL	Trait name	Vertebrate Trait Ontology	Authors
6	CPEB2	Cytoplasmic polyadenylation element binding protein 2	QTL:28119;	Stature	Body height	(WU *et al*., 2013)
6	CSN1S1	Casein alpha s1	QTL:25035; QTL:25039; QTL:25033;	Curd firming rate; Milk rennet coagulation time	n/a	(POULSEN *et al*., 2013)
6	CSN1S1	Casein alpha s1	QTL:31637;	Length of productive life	Life span trait	(FONTANESI *et al*., 2014)
6	CSN1S1	Casein alpha s1	QTL:20558;	Milk alpha-casein content	Milk alpha-casein amount	(FONTANESI *et al*., 2014)
6	CSN1S1	Casein alpha s1	QTL:20596;	Milk alpha-casein to beta-casein ratio	Milk casein amount	(HUANG *et al*., 2012)

6	CSN1S1	Casein alpha s1	QTL:136200; QTL:136201;	Milk casein percentage	Milk casein amount	(VIALE *et al*., 2017)
6	CSN1S1	Casein alpha s1	QTL:122294;	Milk docosanoic acid content	Milk fatty acid C22:0 amount	(PEGOLO *et al*., 2016)
6	CSN1S1	Casein alpha s1	QTL:140390; QTL:136198;	Milk fat percentage	Milk fat amount	(VIALE *et al*., 2017)
6	CSN1S1	Casein alpha s1	QTL:136197;	Milk fat yield	Milk total fat amount	(VIALE *et al*., 2017)
6	CSN1S1	Casein alpha s1	QTL:122284;	Milk margaric acid content	Milk fatty acid C17:0 amount	(PEGOLO *et al*., 2016)
6	CSN1S1	Casein alpha s1	QTL:124228; QTL:136199; QTL:3857; QTL:124227; QTL:140391;	Milk protein percentage	Milk protein amount	(VIALE *et al*., 2017)
6	CSN1S1	Casein alpha s1	QTL:3856;	Milk protein yield	Milk protein amount	(PRINZENBERG *et al*., 2003)
6	CSN1S1	Casein alpha s1	QTL:136295;	Milk protein-to-fat ratio	n/a	(VIALE *et al*., 2017)
6	CSN1S1	Casein alpha s1	QTL:3855;	Milk yield	Milk amount	(PRINZENBERG *et al*., 2003)
6	CSN1S1	Casein alpha s1	QTL:31636;	Somatic cell count	Milk somatic cell quantity	(FONTANESI *et al*., 2014)

6	CSN1S2	Casein alpha-S2	QTL:20562; QTL:20563; QTL:20561;	Milk beta-casein content	Milk beta-casein amount	(HUANG *et al*., 2012)
6	CSN1S2	Casein alpha-S2	QTL:20561; QTL:20562; QTL:20563;	Milk beta-casein content	Milk beta-casein amount	(HUANG *et al*., 2012)
6	CSN1S2	Casein alpha-S2	QTL:20590; QTL:20591; QTL:20589;	Milk protein content	Milk protein amount	(HUANG *et al*., 2012)
6	CSN1S2	Casein alpha-S2	QTL:20589; QTL:20590; QTL:20591;	Milk protein content	Milk protein amount	(HUANG *et al*., 2012)
6	CSN2	Casein beta	QTL:13560; QTL:36287;	Milk alpha-lactalbumin percentage	Milk alpha-lactalbumin amount	(VISKER *et al*., 2011)
6	CSN3	Casein kappa	QTL:21193;	Average daily milk yield	Milk amount	(BARTONOVA *et al*., 2012)
6	CSN3	Casein kappa	QTL:25036; QTL:25032; QTL:25040;	Curd firming rate	n/a	(POULSEN *et al*., 2013)
6	CSN3	Casein kappa	QTL:136224; QTL:136223; QTL:136229; QTL:25034; QTL:25029;	Curd firmness; Milk rennet coagulation time	n/a	(VIALE *et al*., 2017)

6	CSN3	Casein kappa	QTL:13571;	Milk alpha-lactalbumin percentage	Milk alpha-lactalbumin amount	(HECK *et al*., 2009)
6	CSN3	Casein kappa	QTL:13573;	Milk alpha-S1-casein percentage	Milk alpha-S1-casein amount	(HECK *et al*., 2009)
6	CSN3	Casein kappa	QTL:13574;	Milk alpha-S2-casein percentage	Milk alpha-S2-casein amount	(HECK *et al*., 2009)
6	CSN3	Casein kappa	QTL:13575;	Milk beta-casein percentage	Milk beta-casein amount	(HECK *et al*., 2009)
6	CSN3	Casein kappa	QTL:13572;	Milk beta-lactoglobulin percentage	Milk beta-lactoglobulin amount	(HECK *et al*., 2009)
6	CSN3	Casein kappa	QTL:136222; QTL:136217; QTL:136227; QTL:136225;	Milk casein content; Milk casein percentage	Milk casein amount	(VIALE *et al*., 2017)
6	CSN3	Casein kappa	QTL:13577;	Milk casein index	Milk casein amount	(HECK *et al*., 2009)
6	CSN3	Casein kappa	QTL:10467; QTL:136219; QTL :13569;	Milk fat yield	Milk total fat amount	(BOVENHUIS; WELLER, 1994)
6	CSN3	Casein kappa	QTL:20569; QTL:20572; QTL: 20575; QTL:20578; QTL:2057	Milk kappa-casein content	Milk kappa-casein amount	(HUANG *et al*., 2012)

			0; QTL:20573; QTL:20576; QTL:20579; QTL:20571; QTL:20574; QTL:20577;			
6	CSN3	Casein kappa	QTL:13576;	Milk kappa-casein percentage	Milk kappa-casein amount	(HECK *et al*., 2009)
6	CSN3	Casein kappa	QTL:20593; QTL:20594; QTL:20592;	Milk protein content	Milk protein amount	(HUANG *et al*., 2012)
6	CSN3	Casein kappa	QTL:136226; QTL:13570; QTL:10466; QTL:136221; QTL:13568; QTL:136216;	Milk protein percentage; Milk protein yield	Milk protein amount	(VIALE *et al*., 2017)
6	CSN3	Casein kappa	QTL:13567; QTL:136215; QTL:10465;	Milk yield	Milk amount	(VIALE *et al*., 2017)
6	CSN3	Casein kappa	QTL:21194;	Somatic cell count	Milk somatic cell quantity	(BARTONOVA *et al*., 2012)
6	CSN3	Casein kappa	QTL:136218; QTL:136228;	Somatic cell score	Milk somatic cell quantity	(VIALE *et al*., 2017)
6	CSN3	Casein kappa	QTL:13571;	Milk alpha-lactalbumin percentage	Milk alpha-lactalbumin amount	(HECK *et al*., 2009)

6	ELOVL6	ELOVL fatty acid elongase 6	QTL:161547; QTL:161550; QTL:161545; QTL:161546;	Average daily milk yield	Milk amount	(CHEN *et al*., 2018)
6	ELOVL6	ELOVL fatty acid elongase 6	QTL:161548;	Milk fat percentage	Milk fat amount	(CHEN *et al*., 2018)
6	ELOVL6	ELOVL fatty acid elongase 6	QTL:161549;	Somatic cell score	Milk somatic cell quantity	(CHEN *et al*., 2018)
6	KIT	V-kit Hardy-Zuckerman 4 feline sarcoma viral oncogene homolog	QTL:21154; QTL:21160;	Eye area pigmentation	Skin pigmentation trait	(PAUSCH *et al*., 2012)
6	KIT	V-kit Hardy-Zuckerman 4 feline sarcoma viral oncogene homolog	QTL:31634; QTL:31635;	Somatic cell count	Milk somatic cell quantity	(FONTANESI *et al*., 2014)
6	LETM1	Leucine zipper and EF-hand	QTL:42550; QTL:42560;	v	n/a	(COLE *et al*., 2011)

		containing transmembrane protein 1				
6	LETM1	Leucine zipper and EF-hand containing transmembrane protein 1	QTL:42551;	Calving ease (maternal)	Parturition trait	(COLE *et al*., 2011)
6	LETM1	Leucine zipper and EF-hand containing transmembrane protein 1	QTL:42552;	Dairy form	Back conformation trait	(COLE *et al*., 2011)
6	LETM1	Leucine zipper and EF-hand containing transmembrane protein 1	QTL:42555;	Feet and leg conformation	Limb conformation trait	(COLE *et al*., 2011)
6	LETM1	Leucine zipper and EF-hand containing	QTL:42554;	Foot angle	Hoof angle	(COLE *et al*., 2011)

		transmembrane protein 1				
6	LETM1	Leucine zipper and EF-hand containing transmembrane protein 1	QTL:42561;	Milk protein yield	Milk protein amount	(COLE *et al*., 2011)
6	LETM1	Leucine zipper and EF-hand containing transmembrane protein 1	QTL:42559;	Milk yield	Milk amount	(COLE *et al*., 2011)
6	LETM1	Leucine zipper and EF-hand containing transmembrane protein 1	QTL:42556;	PTA type	Body conformation trait	(COLE *et al*., 2011)
6	LETM1	Leucine zipper and EF-hand containing	QTL:42562;	Rear leg placement - rear view	Hindlimb conformation trait	(COLE *et al*., 2011)

		transmembrane protein 1				
6	LETM1	Leucine zipper and EF-hand containing transmembrane protein 1	QTL:42565;	Rump width	Rump width	(COLE *et al*., 2011)
6	LETM1	Leucine zipper and EF-hand containing transmembrane protein 1	QTL:42566;	Somatic cell score	Milk somatic cell quantity	(COLE *et al*., 2011)
6	LETM1	Leucine zipper and EF-hand containing transmembrane protein 1	QTL:42567;	Stature	Body height	(COLE *et al*., 2011)
6	LETM1	Leucine zipper and EF-hand containing	QTL:42553;	Stillbirth (maternal)	Stillborn offspring quantity	(COLE *et al*., 2011)

		transmembrane protein 1				
6	LETM1	Leucine zipper and EF-hand containing transmembrane protein 1	QTL:42568;	Strength	Chest width	(COLE *et al*., 2011)
6	LETM1	Leucine zipper and EF-hand containing transmembrane protein 1	QTL:42557; QTL:42563; QTL:42558; QTL:42564;	Teat placement - front; Teat placement - rear; Udder attachment; Udder height	Udder morphology trait	(COLE *et al*., 2011)
6	LETM1	Leucine zipper and EF-hand containing transmembrane protein 1	QTL:42569;	Udder cleft	Udder cleft morphology trait	(COLE *et al*., 2011)
6	LETM1	Leucine zipper and EF-hand containing	QTL:42570;	Udder depth	Udder height, floor to tarsal joint	(COLE *et al*., 2011)

		transmembrane protein 1				
6	LOC100140503	Alpha-fetoprotein-like	QTL:174118;	Milk fat yield	Milk total fat amount	(JIANG *et al*., 2019)
6	LOC100140503	Alpha-fetoprotein-like	QTL:174475;	Milk yield	Milk amount	(JIANG *et al*., 2019)
6	ODAM	Odontogenic, ameloblast associated	QTL:238618;	Milk calcium content	Milk calcium amount	(SANCHEZ *et al*., 2021)
6	ODAM	Odontogenic, ameloblast associated	QTL:238617;	Milk magnesium content	Milk magnesium amount	(SANCHEZ *et al*., 2021)
6	SLIT2	Slit homolog 2 (Drosophila)	QTL:62391;	Interval from first to last insemination	Female fertility trait	(HÖGLUND *et al*., 2015)
6	SLIT2	Slit homolog 2 (Drosophila)	QTL:238606;	Milk potassium content	Milk potassium amount	(SANCHEZ *et al*., 2021)

6	SLIT2	Slit homolog 2 (Drosophila)	QTL:174824; QTL:174823; QTL:175455;	Milk protein percentage; Milk protein yield	Milk protein amount	(JIANG *et al*., 2019)
6	SNCA	Synuclein alpha	QTL:160091; QTL:160089; QTL:160090;	Bovine respiratory disease susceptibility	n/a	(NEUPANE *et al*., 2018)
6	STAP1	Signal transducing adaptor family member 1	QTL:212159; QTL:212589;	First service conception; Inseminations per conception	Fertility trait	(GALLIOU *et al*., 2020)

[1] BTA: Bos taurus autosome, [2]ARS-UCD1.2 Bos taurus genome assembly

REFERENCIES TABLE 1.

BARTONOVA, P. *et al*. Association between CSN3 and BCO2 gene polymorphisms and milk performance traits in the Czech Fleckvieh cattle breed. **Genetics and Molecular Research**, Ribeirão Preto, v. 11, n. 2, p. 1058-1563, 2012.

BOVENHUIS, H.; WELLER, J. I. Mapping and analysis of dairy cattle quantitative trait loci by maximum likelihood methodology using milk protein genes as genetic markers. **Genetics**, Baltimore, v. 137, n. 1, p. 267-280, 1994.

CHEN, S. *et al*. Genetic variants of fatty acid elongase 6 in Chinese Holstein cow. **Gene**, Amsterdam, v. 670, p. 123-170, 2018.

COLE, J. B. *et al*. Genome-wide association analysis of thirty one production, health, reproduction and body conformation traits in contemporary U.S. Holstein cows. **BMC Genomics**, London, v. 12, [art.] 408, 2011.

FONTANESI, L. *et al*. A candidate gene association study for nine economically important traits in Italian Holstein cattle. **Animal Genetics**, Oxford, v. 45, n. 4, p. 576-580, 2014.

GALLIOU, J. M. *et al*. Identification of loci and pathways associated with heifer conception rate in U.S. holsteins. **Genes**, Basel, v. 11, n. 7, [art.] 767, 2020.

HECK, J. M. L. *et al*. Effects of milk protein variants on the protein composition of bovine milk. **Journal of Dairy Science**, Champaign, v. 92, n. 3, p. 1192-1202, 2009. Disponível em: https://doi.org/10.3168/jds.2008-1208. Acesso em:16 nov. 2021.

HÖGLUND, J. K. *et al.* Genome-wide association study for female fertility in Nordic Red cattle. **BMC Genetics**, London, v. 16, [art.] 110, 2015. Disponível em: https://doi.org/10.1186/s12863-015-0269-x. Acesso em:15 out. 2021.

HUANG, W. *et al*. Association between milk protein gene variants and protein composition traits in dairy cattle. **Journal of Dairy Science**, Champaign, v. 95, n. 1, p. 440-449, 2012. Disponível em: https://doi.org/10.3168/jds.2011-4757. Acesso em: 15 jan. 2021.

JIANG, J. *et al*. A large-scale genome-wide association study in U.S. Holstein cattle. **Frontiers in Genetics**, Lausanne, v. 10, [art.] 412, May, 2019.

NEUPANE, M.; KISER, J. N.; NEIBERGS, H. L. Gene set enrichment analysis of SNP data in dairy and beef cattle with bovine respiratory disease. **Animal Genetics**, Oxford, v. 49, n. 6, p. 527-538, 2018.

PAUSCH, H. *et al*. Identification of QTL for UV-protective eye area pigmentation in cattle by progeny phenotyping and genome-wide association analysis. **PLoS ONE**, San Francisco, v. 7, n. 5, [art.]. e36346, 2012.

PEGOLO, S. *et al*. Effects of candidate gene polymorphisms on the detailed fatty acids profile determined by gas chromatography in bovine milk. **Journal of Dairy Science**, Champaign, v. 99, n. 6, p. 4558-4573, 2016.

POULSEN, N. A. *et al*. The occurrence of noncoagulating milk and the association of bovine milk coagulation properties with genetic variants of the caseins in 3 Scandinavian dairy breeds. **Journal of Dairy Science**, Champaign, v. 96, n. 8, p. 4830-4842, 2013.

PRINZENBERG, E. M. *et al.* Polymorphism of the bovine CSN1S1 promoter: Linkage mapping, intragenic haplotypes, and effects on milk production traits. **Journal of Dairy Science**, Champaign, v. 86, n. 8, p. 2696-2705, 2003.

SANCHEZ, M. P. *et al*. Sequence-based GWAS and post-GWAS analyses reveal a key role of SLC37A1, ANKH, and regulatory regions on bovine milk mineral content. **Scientific Reports**, London, v. 11, [art.] 7537, 2021.

VIALE, E. *et al*. Association of candidate gene polymorphisms with milk technological traits, yield, composition, and somatic cell score in Italian Holstein-Friesian sires. **Journal of Dairy Science**, Champaign, v. 100, n. 9, p. 7271-7281, 2017.

VISKER, M. H. P. W. *et al*. Association of bovine β-casein protein variant I with milk production and milk protein composition. **Animal Genetics**, Oxford, v. 42, n. 2, p. 212-218, 2011.

WU, X. *et al*. Genome wide association studies for body conformation traits in the Chinese Holstein cattle population. **BMC Genomics**, London, v. 14, [art.] 897, 2013.

Table 2. The QTL search for islands of homozygosity

BTA[1]	Gene Symbol[2]	QTL[3]	Trait name	Vertebrate Trait Ontology	Authors
3	*ADGRE3*	QTL:212165, QTL:212602	First service conception; Inseminations per conception	Fertility trait	(GALLIOU *et al*., 2020)
6	*RESTB*	QTL:212155, QTL:212585	First service conception	Fertility trait	(GALLIOU *et al*., 2020)
	SLAIN2	QTL:212153, QTL:212583	First service conception; Inseminations per conception	Fertility trait	(GALLIOU *et al*., 2020)
	KIT	QTL:21160, QTL:21154	Eye area pigmentation	Skin pigmentation trait	(PAUSCH *et al*., 2012)
		QTL:31634, QTL:31635	Somatic cell count	Milk somatic cell quantity	(FONTANESI *et al*., 2010)
5	*KITLG*	QTL:21151	Eye area pigmentation	Skin pigmentation trait	(PAUSCH *et al*., 2012)
7	*PRKACA*	QTL:160102	Bovine respiratory disease susceptibility	n/a	(NEUPANE *et al*., 2018)
	PCDHA13	QTL:43041, QTL:43049	Body depth; Net merit	n/a; n/a	(COLE *et al*., 2011)
		QTL:43042, QTL:43052	Calving ease (maternal); Calving ease	Parturition trait	(COLE *et al*., 2011)
		QTL:43043	Foot angle	Hoof angle	(COLE *et al*., 2011)
		QTL:43044	Milk fat percentage	Milk fat amount	(COLE *et al*., 2011)
		QTL:43047	Milk fat yield	Milk total fat amount	(COLE *et al*., 2011)
		QTL:43050, QTL:176289	Milk protein yield	Milk protein amount	(JIANG *et al*., 2019)
		QTL:43048	Milk yield	Milk amount	(COLE *et al*., 2011)
		QTL:43045	PTA type	Body conformation trait	(COLE *et al*., 2011)
		QTL:43051	Rear leg placement - rear view	Hindlimb conformation trait	(COLE *et al*., 2011)
		QTL:43054	Stature	Body height	(COLE *et al*., 2011)
		QTL:43053	Stillbirth	Stillborn offspring quantity	(COLE *et al*., 2011)
		QTL:43055	Strength	Chest width	(COLE *et al*., 2011)

		QTL:43046	Udder attachment	Udder morphology trait	(COLE *et al*., 2011)
14	*CSPP1*	QTL:127050	Calving to conception interval	Female fertility trait	(ORTEGA *et al*., 2017)
		QTL:57157, QTL:57113	Conception rate; Daughter pregnancy rate	Fertility trait	(COCHRAN *et al*., 2013)
		QTL:127018, QTL:127033	First service conception; Inseminations per conception	Fertility trait	(ORTEGA *et al*., 2017)
		QTL:57184	Length of productive life	Life span trait	(COCHRAN *et al*., 2013)
16	*RICTOR*	QTL:157117	Longissimus muscle area	Longissimus thoracis muscle area	(LI *et al*., 2017)
		QTL:160207	Bovine respiratory disease susceptibility	n/a	(NEUPANE *et al*., 2018)
		QTL:173918	Milk fat percentage	Milk fat amount	(JIANG *et al*., 2019)
		QTL:176127, QTL:161878, QTL:175284	Milk protein percentage	Milk protein amount	(JIANG *et al*., 2019)
		QTL:174758	Milk yield	Milk amount	(JIANG *et al*., 2019)
	RPTOR	QTL:22551, QTL:107675, QTL:107676, QTL:107757, QTL:107674, QTL:22558, QTL:107693, QTL:107787, QTL:107725, QTL:107830, QTL:107829, QTL:107811, QTL:107812	Myristic acid content; Myristoleic acid content; Oleic acid content; Palmitoleic acid content	n/a	(SASAGO *et al*., 2017)

1 BTA: Bos taurus autosome, 2ARS-UCD1.2 Bos taurus genome assembly, [3]QTL Quantitative trait loci

REFERENCES TABLE 2.

FONTANESI, L. *et al.* Genetic heterogeneity at the bovine KIT gene in cattle breeds carrying different putative alleles at the spotting locus. **Animal Genetics**, Oxford, v. 41, n. 3, p. 295-303, 2010.

GALLIOU, J. M. *et al*. Identification of loci and pathways associated with heifer conception rate in U.S. holsteins. **Genes**, Basel, v. 11, n. 7, [art.] 767, 2020.

JIANG, J. *et al*. A large-scale genome-wide association study in U.S. Holstein cattle. **Frontiers in Genetics**, Lausanne, v. 10, [art.] 412, May, 2019.

LI, Y. *et al*. A whole genome association study to detect additive and dominant single nucleotide polymorphisms for growth and carcass traits in Korean native cattle, Hanwoo. **Asian-Australasian Journal of Animal Sciences**, Seoul, v. 30, n. 1, p. 8-19, 2017. Disponível em: Disponível em: https://doi.org/10.5713/ajas.16.0170. Acesso em: 19 mai. 2020.

NEUPANE, M.; KISER, J. N.; NEIBERGS, H. L. Gene set enrichment analysis of SNP data in dairy and beef cattle with bovine respiratory disease. **Animal Genetics**, Oxford, v. 49, n. 6, p. 527-538, 2018.

ORTEGA, M. S. *et al*. Association of single nucleotide polymorphisms in candidate genes previously related to genetic variation in fertility with phenotypic measurements of reproductive function in Holstein cows. **Journal of Dairy Science**, Champaign, v. 100, n. 5, p. 3725-3734, 2017.

PAUSCH, H. *et al*. Identification of QTL for UV-protective eye area pigmentation in cattle by progeny phenotyping and genome-wide association analysis. **PLoS ONE**, San Francisco, v. 7, n. 5, [art.]. e36346, 2012.

SASAGO, N. *et al*. Genome-wide association study for carcass traits, fatty acid composition, chemical composition, sugar, and the effects of related candidate genes in Japanese Black cattle. **Animal Science Journal**, Richmond, v. 88, n. 1, p. 33-44, 2017.

Table3. Gene ontology (GO) terms and Kyoto Encyclopedia of Genes and Genomes (KEGG) enriched by Fisher's test (p<0.01) of islands of homozygosity

Biological Process		P-value	Genes[2] (BTA[1])
GO:0006069	Ethanol oxidation	3,7E-7	*ADH4, ADH5, ADH6, ADH7*
GO:0070098	Chemokine-mediated signaling pathway	2,3E-4	*CXCL13, CXCL8, GRO1, CXCL2, CXCL5, PPBP*
GO:0070175	Positive regulation of enamel mineralization	4,8E-4	*AMTN, ENAM, ODAPH*
GO:0061844	Antimicrobial humoral immune response mediated by antimicrobial peptide	6,1E-4	*CXCL13, CXXL8, GRO1, CXCL2, CXCL5, PPBP*
GO:0030593	Neutrophil chemotaxis	9,1E-4	*CXCL13, CXCL8, GRO1, CXCL2, CXCL5, PPBP*
GO:0071222	Cellular response to lipopolysaccharide	1,1E-3	CXCL13, CXCL8, GRO1, CXCL2, CXCL5, PPBP, STAP1
GO:0032355	Response to estradiol	1,4E-3	*AREG, CSN1S1, CSN1S2, CSN3*
GO:1903496	Response to 11-deoxycorticosterone	1,6E-3	*CSB1S1, CSN1S2, CSN3*
GO:1903494	Response to dehydroepiandrosterone	1,6E-3	*CSB1S1, CSN1S2, CSN4*
GO:0042475	Odontogenesis of dentin-containing tooth	2,0E-3	*AMBN, AMTN, LEF1, ODAM, PDGFRA*
GO:0042573	Retinoic acid metabolic process	4,3E-3	*ADH6, ADH6, ADH7*
GO:0042572	Retinol metabolic process	5,3E-3	*ADH4, ADH6, ADH6, ADH7*
GO:0045741	Positive regulation of epidermal growth factor-activated receptor activity	8,2E-3	*AREG, EREG, EPGN*
GO:0006954	Inflammatory response	8,9E-3	*CXCL13, CXCL8, KIT, GRO1, CXCL2, CXCL5, LIAS, ODAM, PPBP*
Cell Component			
GO:0005796	Golgi lumen	3,0E-3	*CSN1S1, CSN1S2, CSN3*
GO:0070652	HAUS complex	3,9E-3	*HAUS3, A0A3Q1MNS4 BOVIN, A0A3Q1N3P3 BOVIN*
GO:0005615	Extracellular space	4,9E-3	*CXCL13, CXCL8, KIT, AFM, ALB, AFP, LOC1001405303, AREG, BMP3, CPZ, CSN1S1, CSN1S2, CSN3, GRO1, CXCL2, CXCL3, CXCL5, DKK2, EREG, EPGN, FGF5, ODAM, PPBP, SLIT2, SOD3, SNCA*

GO:0005783	Endoplasmic reticulum	6,8E-3	*ATP10D, DNAJB14, ELOVL6, LRPAP1, USO1, ALB, CWH43, KLB, SRP72, SLC30A9, STBD1, SRD5A3, STIM2, STX18, TMEM129, TMEM33*
Molecular Function		P-Value	
GO:005236	CXCR chemokine receptor binding	8,5E-8	*CXCL13, CXCL8, GRO1, CXCL2, CXCL5, PPBP*
GO:0004024	Alcohol dehydrogenase activity, zinc-dependent	1,7E-7	*ADH4, ADH5, ADH6, ADH6, ADH7*
GO:0008009	Chemokine activity	6,7E-6	*CXCL13, CXCL8, GRO1, CXCL2, CXCL3, CXCL5, PPBP*
GO:0005504	Fatty acid binding	1,9E-5	*AFM, ALB, ADH5, AFP, LOC100140503*
GO:0004745	Retinol dehydrogenase activity	4,6E-4	*ADH4, ADH6, ADH6, ADH7*
GO:0008083	Growth factor activity	5,5E-4	*AMBN, AREGM BMO3, GRO1, CXCL2, EREG, EPGN, FGF5*
GO:0043022	Ribosome binding	3,1E-3	*GUF1, A0A3Q1MDZ8 BOVIN, CPEB2, LETM1, SRP72*
GO:0004559	Alpha-mannosidase activity	5,5E-3	*LOC523503, LOC528518, LOC532207*
KEGG pathways			
	Alcoholic liver disease	8,4E-5	*CXCL8, ADH1C, ADH4, ADH5, ADH6, ADH7, GRO1, CXCL2, CXCL3, LEF1*
	Drug metabolism - cytochrome P450	8,1E-4	*ADH1C, ADH4, ADH5, ADH6, ADH7, APGDS*
	Viral protein interaction with cytokine and cytokine receptor	9,0E-4	*CXCL13, CXCL8, GRO1, CXCL2, CXCL3, CXCL5, PPBP*
	Glycolysis / gluconeogenesis	9,4E-4	*ADH1C, ADH4, ADH5, ADH6, ADH7, PGM2*
	Tyrosine metabolism	1,1E-3	*ADH1C, ADH4, ADH5, ADH6, ADH7*
	Metabolism of xenobiotics by cytochrome P450	1,2E-3	*ADH1C, ADH4, ADH5, ADH6, ADH7, APGDS*
	Fatty acid degradation	1,8E-3	*ADH1C, ADH4, ADH5, ADH6, ADH7*
	Pyruvate metabolism	1,8E-3	*ADH1C, ADH4, ADH5, ADH6, ADH8*
	Other glycan degradation	2,4E-3	*LOC523503, LOC528518, LOC532207, MANBA*

[1] BTA: Bos taurus autosome, [2]ARS-UCD1.2 Bos taurus genome assembly

Supplementary material

Left view of the proportion of times each SNP falls within a race, along chromosome position. Straighten all ROH executions experienced in an individual with respect to position along chromosomes, across different races. Highlighted in yellow, draws attention to the contracted selection signature on the chromosomes.

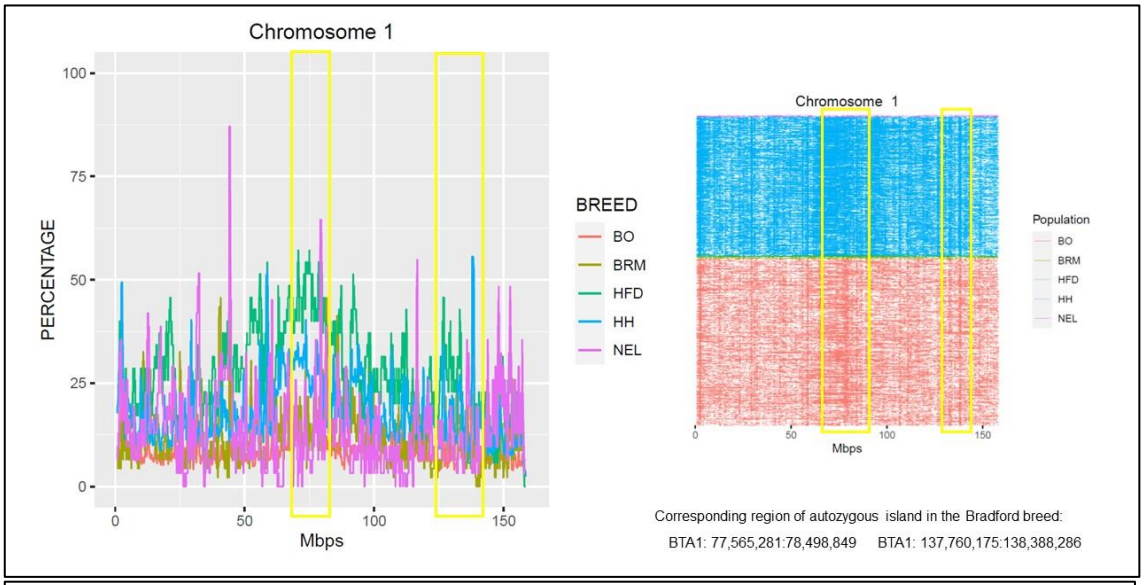

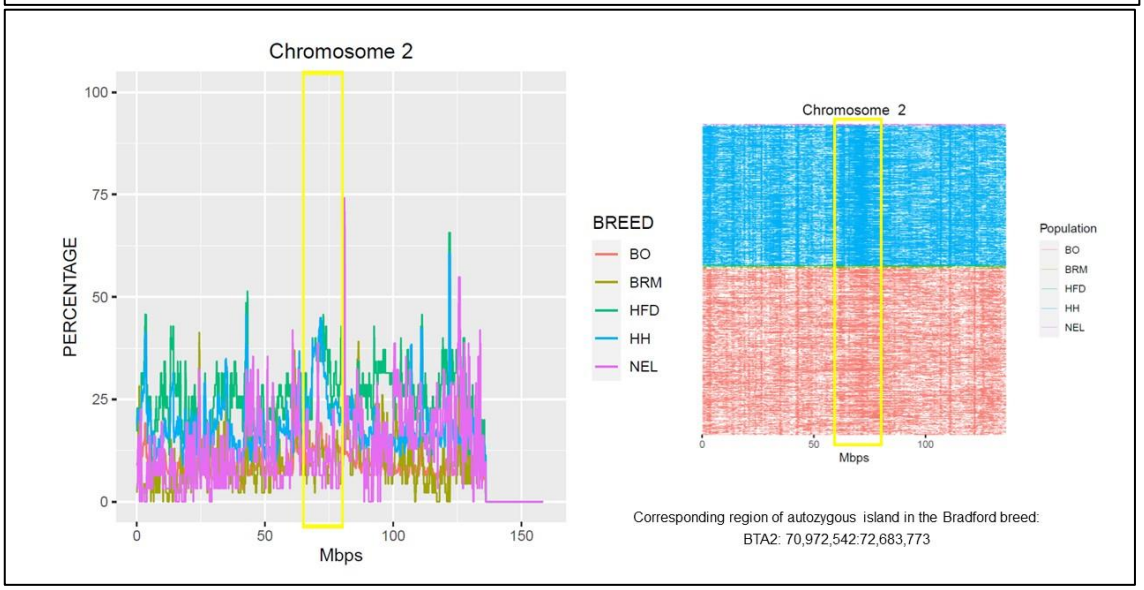

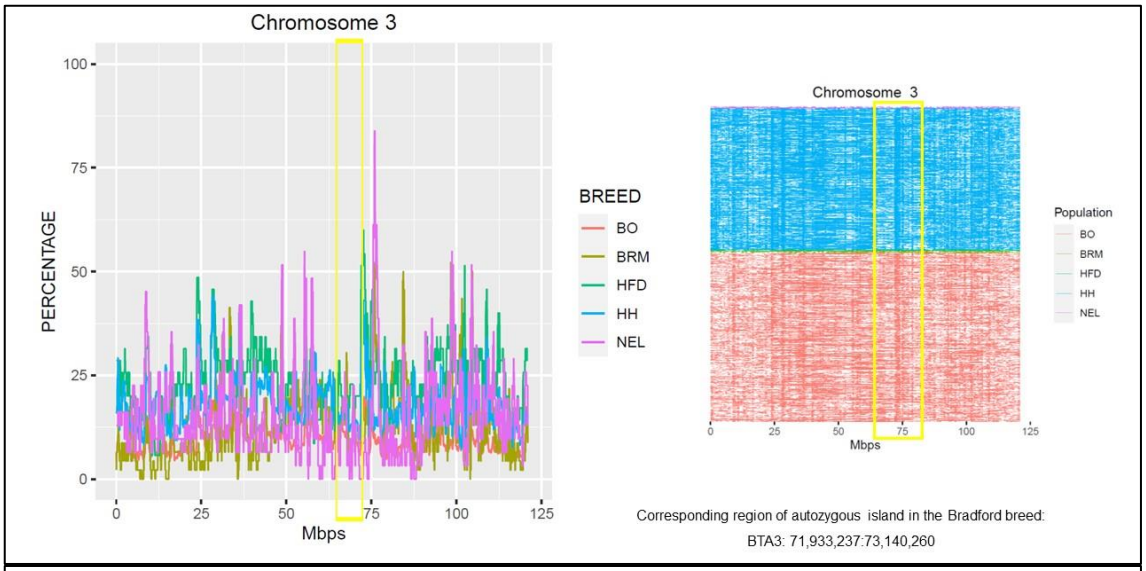

Corresponding region of autozygous island in the Bradford breed:

BTA3: 71,933,237:73,140,260

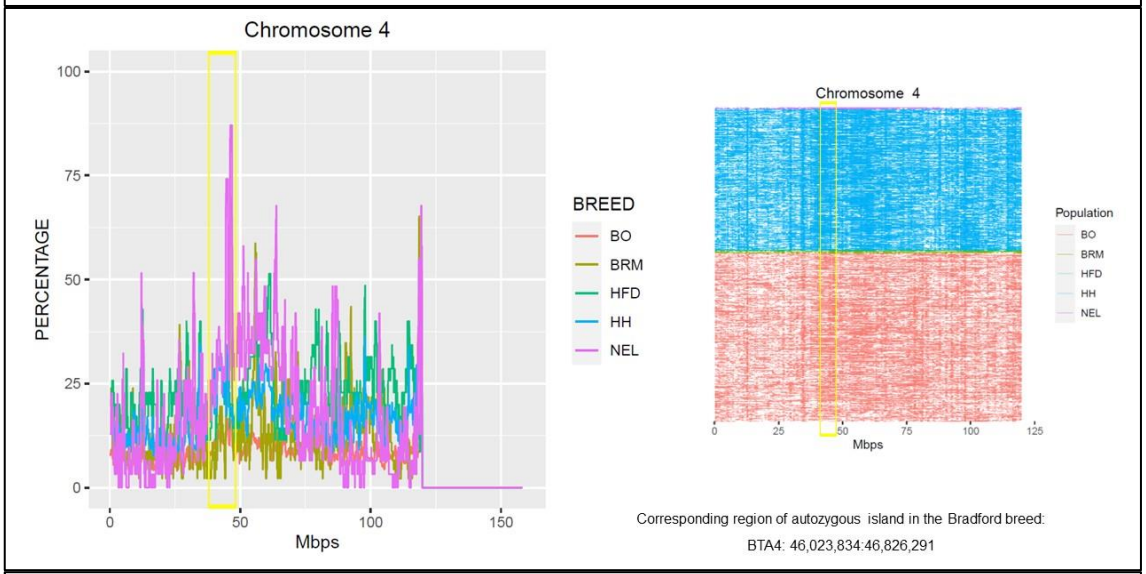

Corresponding region of autozygous island in the Bradford breed:

BTA4: 46,023,834:46,826,291

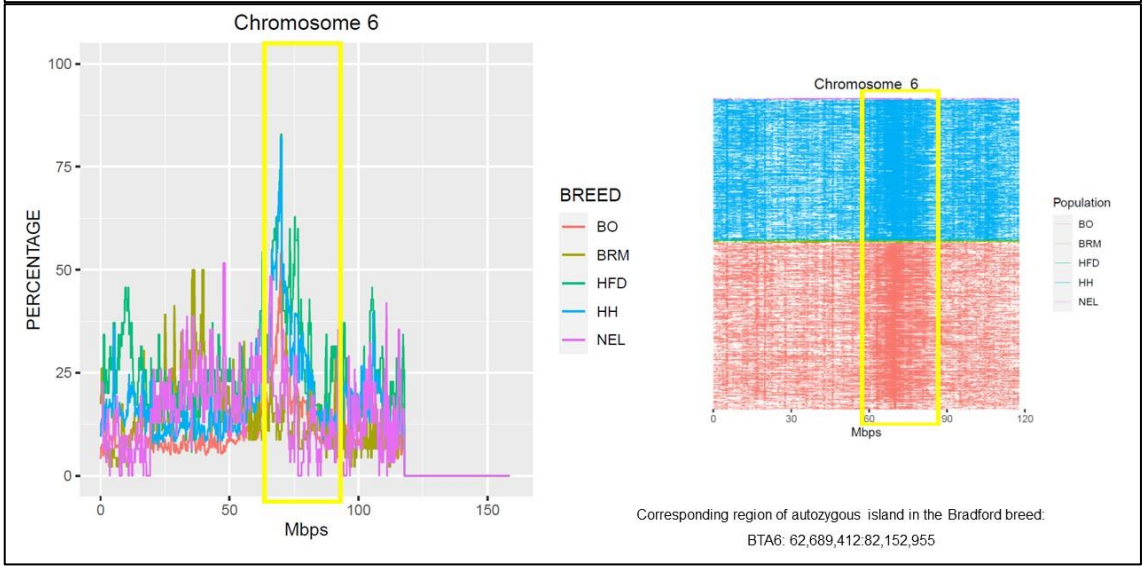

Corresponding region of autozygous island in the Bradford breed:

BTA6: 62,689,412:82,152,955

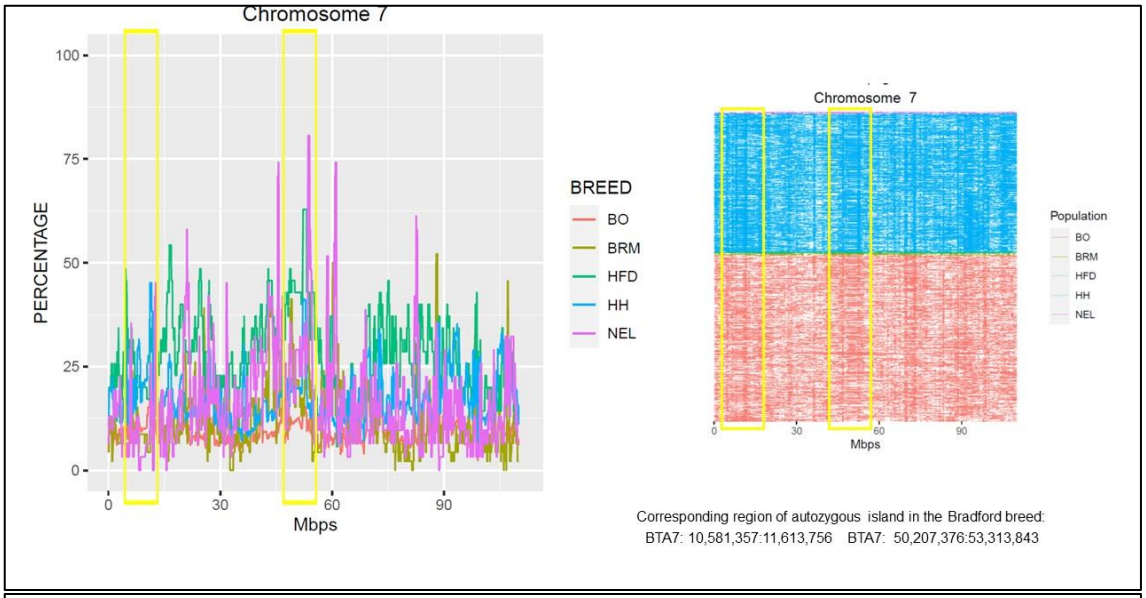

Corresponding region of autozygous island in the Bradford breed:
BTA7: 10,581,357:11,613,756 BTA7: 50,207,376:53,313,843

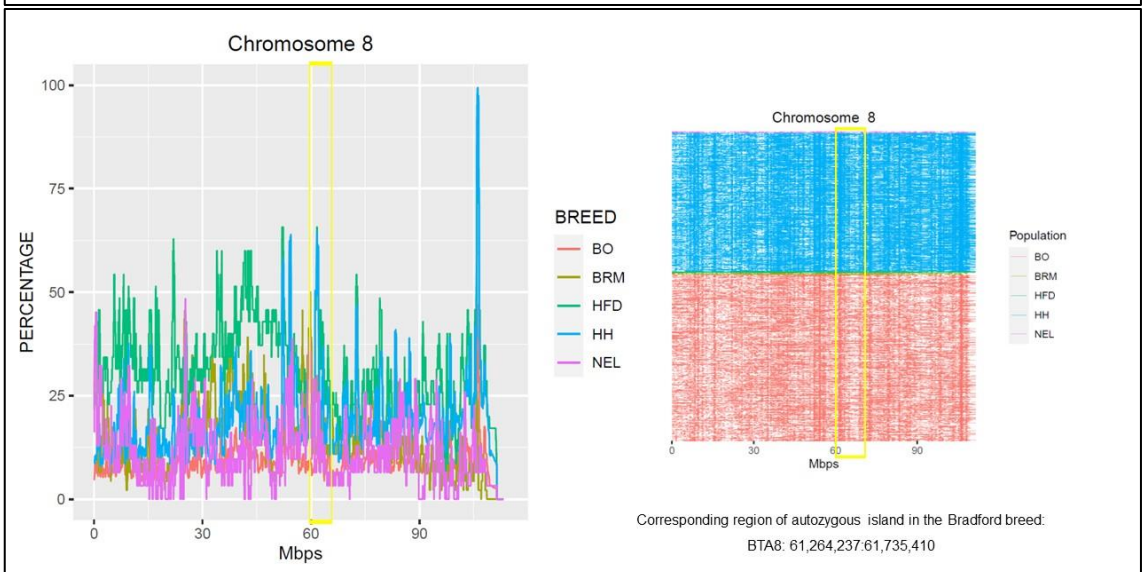

Corresponding region of autozygous island in the Bradford breed:
BTA8: 61,264,237:61,735,410

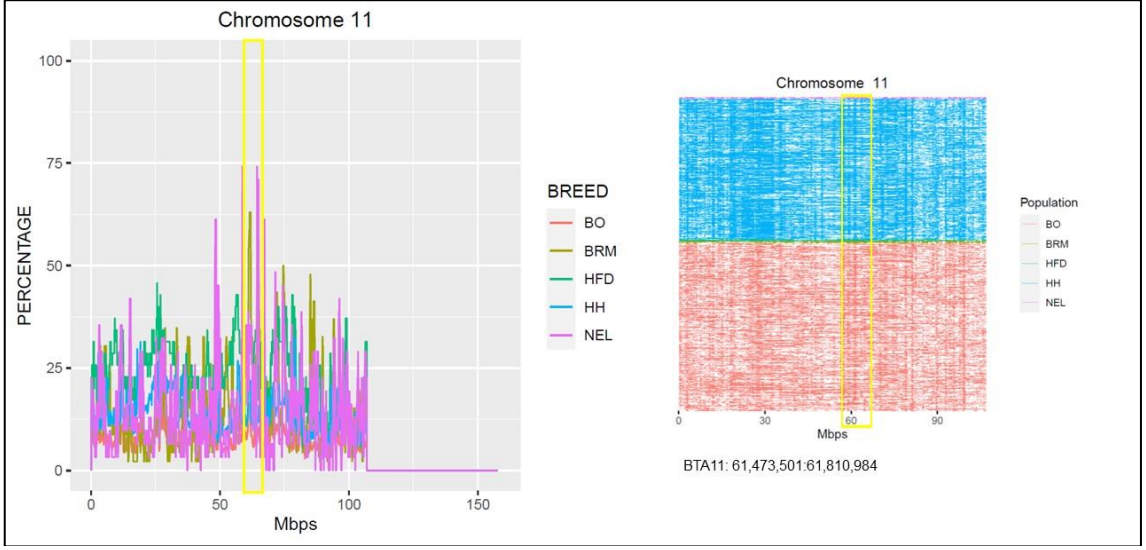

BTA11: 61,473,501:61,810,984

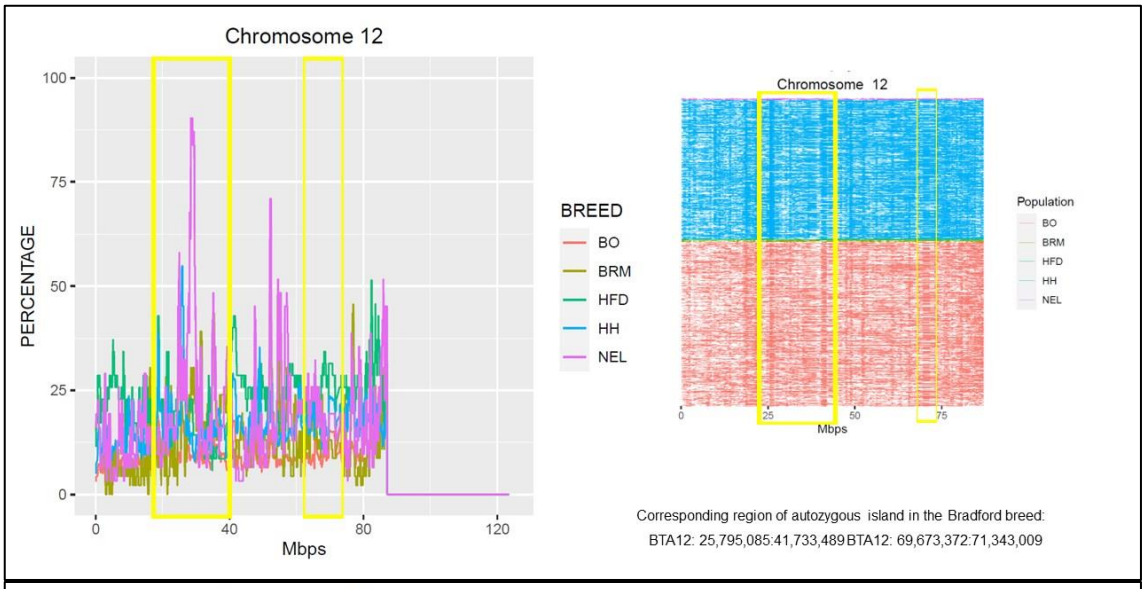

Corresponding region of autozygous island in the Bradford breed:
BTA12: 25,795,085:41,733,489 BTA12: 69,673,372:71,343,009

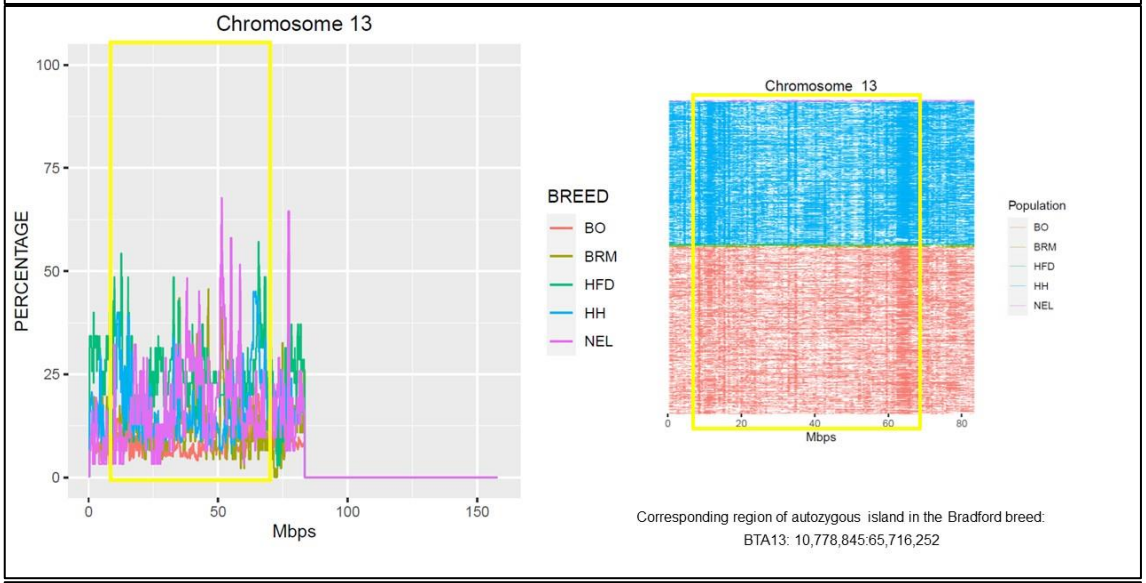

Corresponding region of autozygous island in the Bradford breed:
BTA13: 10,778,845:65,716,252

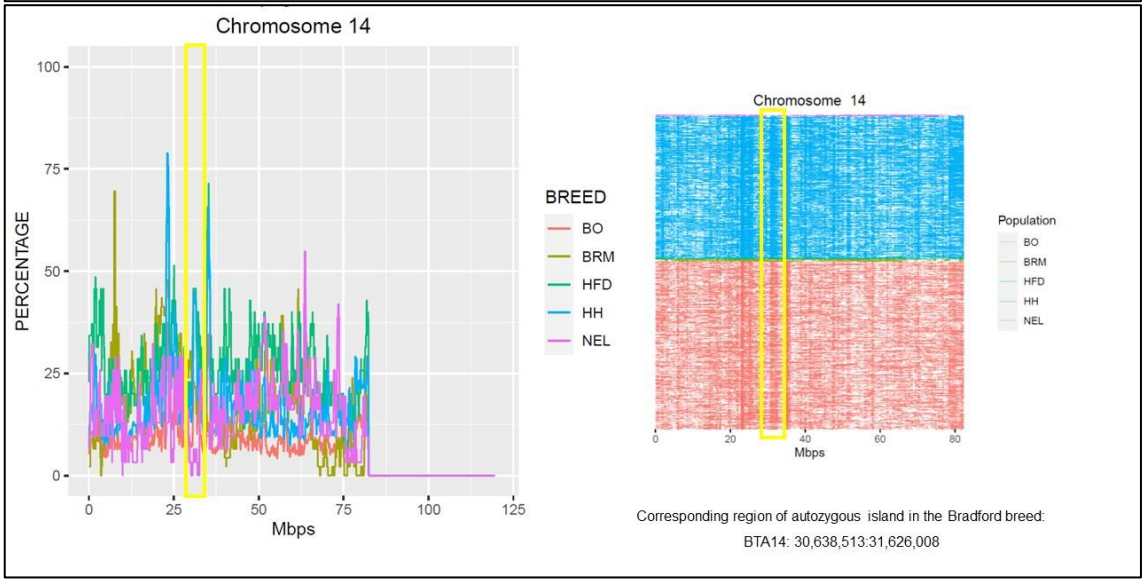

Corresponding region of autozygous island in the Bradford breed:
BTA14: 30,638,513:31,626,008

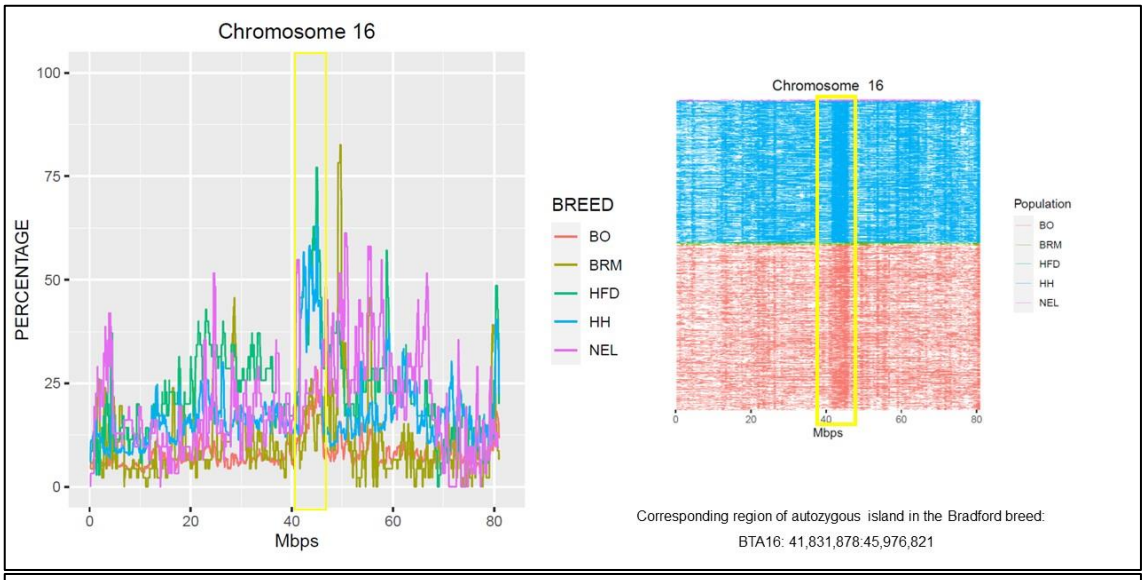

Corresponding region of autozygous island in the Bradford breed:

BTA16: 41,831,878:45,976,821

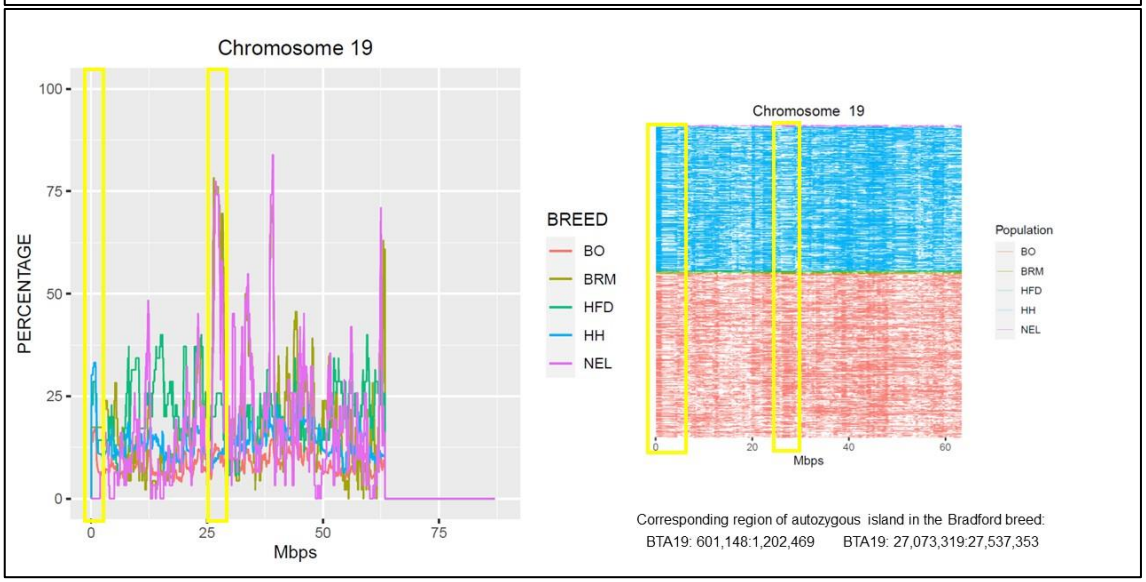

Corresponding region of autozygous island in the Bradford breed:

BTA19: 601,148:1,202,469 BTA19: 27,073,319:27,537,353

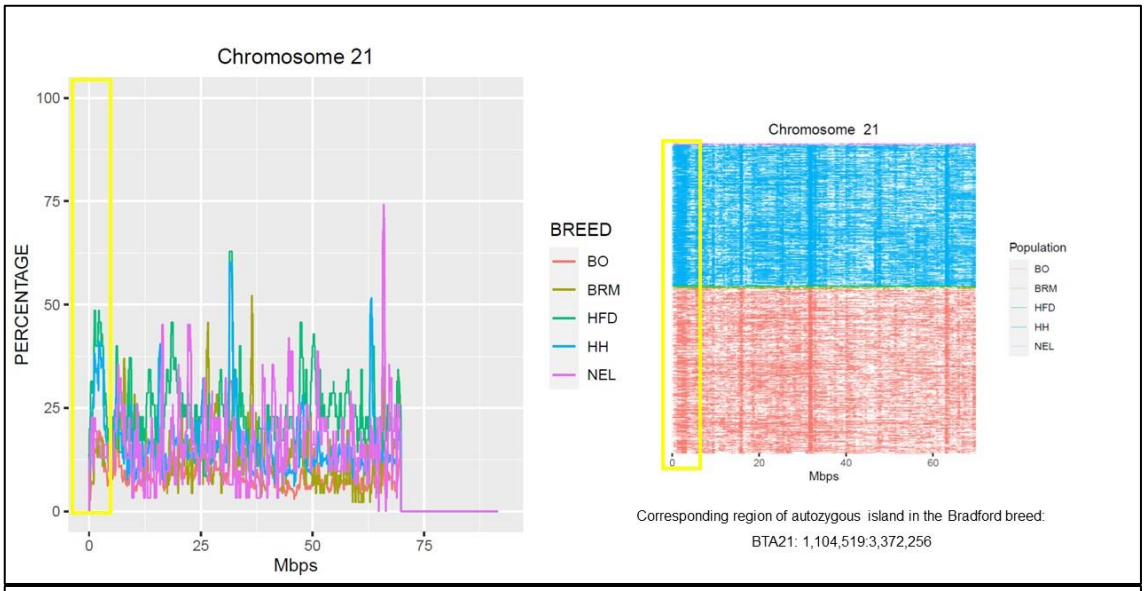

Corresponding region of autozygous island in the Bradford breed:
BTA21: 1,104,519:3,372,256

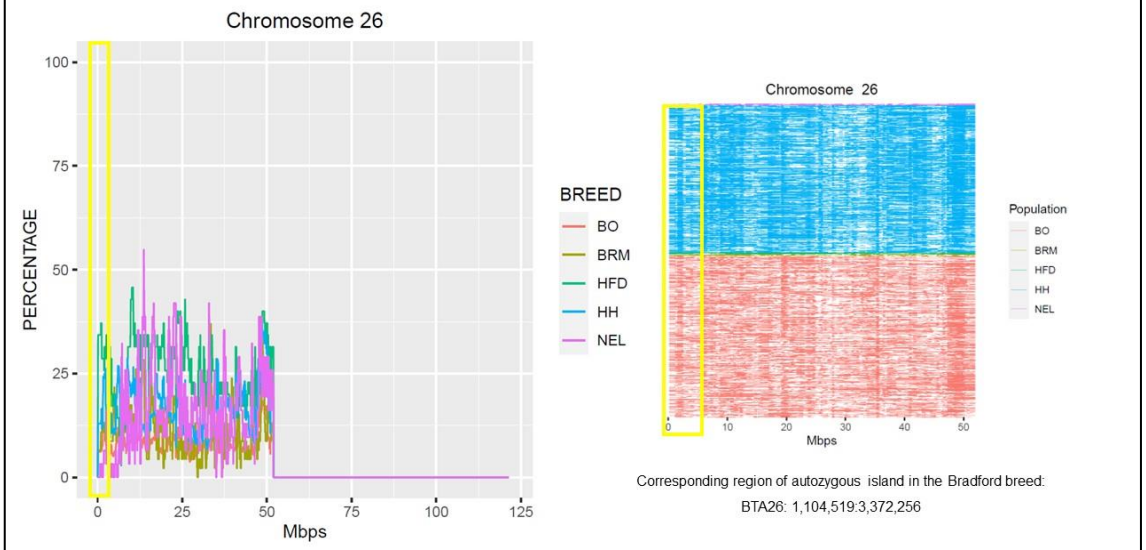

Corresponding region of autozygous island in the Bradford breed:
BTA26: 1,104,519:3,372,256

5. Considerações finais

O uso de abordagens genômicas trouxe avanços, contribuindo com estimativas mais próximas da similaridade genética dos indivíduos da população. Os animais Hereford apresentaram mais e maiores segmentos de ROH quando comparados aos animais Braford, por serem uma raça pura e estarem mais sujeitos à endogamia.

Coeficientes de endogamia estimados através de segmentos homozigotos no genoma (F_{ROH}) podem ser usados como estimadores mais acurados dos níveis de endogamia individual nos programas de melhoramento das raças visando o melhor direcionamento dos acasalamentos e cálculo de acurácia. Neste estudo vale ressaltar que a maior correlação obtida foi entre o F_{ROH} longo com o coeficiente calculado com base no pedigree, evidenciando a capacidade do F_{ROH} em capturar níveis mais profundos de autozigosidade. Estudos futuros para identificar quanto a endogamia antiga e recente afetam as características produtivas são necessários.

As ilhas de ROH e regiões altamente compartilhadas entre os indivíduos, englobam um número relevante de genes e QTLs relacionados a características produtivas, como a qualidade de carne, peso corporal, produção de leite e fertilidade, bem como genes que expressam o padrão racial dessas raças. Essas descobertas fornecem evidências de que os padrões de ROH podem ser usados para rastrear regiões de pontos críticos genômicos que abrigam assinaturas de seleção.

Por meio do padrão de homozigose no genoma de Braford, foi possível identificar dezenove assinaturas, por meio de marcadores moleculares comuns às raças fundadoras. Essas pegadas se destacam nos BTAs: 12, 14, 19, 21 4, 7 26 e 6. Os QTLs relacionados à produção de leite foram os mais frequentes nessas ilhas.

A identificação da composição em raças compostas é útil tanto na rastreabilidade de transmissão de doenças quanto no controle de endogamia e verificação de pedigree. As estimativas da composição racial não foram abrangentes para os compostos Braford 1/2 analisados.

REFERÊNCIAS

ALLARD, R. W. **Princípios do melhoramento genético das plantas**. São Paulo: Edgard Blucher, 1971.

ALMEIDA, O. A. C. *et al*. Identification of selection signatures involved in performance traits in a paternal broiler line. **BMC Genomics**, London, v. 20, n. 1, [art.] 449, 2019.

BAES, C. F. *et al.* Symposium review: the genomic architecture of inbreeding: How homozygosity affects health and performance. **Journal of Dairy Science**, Champaign, v. 102, n. 3, p. 2807–2817, 2019.

BARTONOVA, P. *et al*. Association between CSN3 and BCO2 gene polymorphisms and milk performance traits in the Czech Fleckvieh cattle breed. **Genetics and Molecular Research**, Ribeirão Preto, v. 11, n. 2, p. 1058-1563, 2012.

BISCARINI, F. *et al*. Insights into genetic diversity, runs of homozygosity and heterozygosity-rich regions in maremmana semi-feral cattle using pedigree and genomic data. **Animals**, Basel, v. 10, n. 12, [art.] 2285, 2020.

BOSSE, M. *et al*. Regions of homozygosity in the porcine genome: consequence of demography and the recombination landscape. **PLoS Genetics**, San Francisco, v. 8, n. 11, [art.] e1003100, 2012.

BOURDON, R. M. **Understanding animal breeding**. Harlow: Pearson Education, 1997.

BOVENHUIS, H.; WELLER, J. I. Mapping and analysis of dairy cattle quantitative trait loci by maximum likelihood methodology using milk protein genes as genetic markers. **Genetics**, Baltimore, v. 137, n. 1, p. 267-280, 1994.

BROMAN, K. W.; WEBER, J. L. Long homozygous chromosomal segments in reference families from the centre d'Etude du polymorphisme humain. **American Journal of Human Genetics**, Baltimore, v. 65, n. 6, p. 1493–500, 1999.

BROWNING, S. R.; BROWNING, B. L. High-resolution detection of identity by descent in unrelated individuals. **American Journal of Human Genetics**, Cambridge, v. 86, n. 4, p. 526–539, 2010.

BUCKLEY, N. J. *et al*. The role of REST in transcriptional and epigenetic dysregulation in Huntington's disease. **Neurobiology of Disease**, San Diego, v. 39, n. 1, p. 28-39, 2010.

CAIVIO-NASNER, S. *et al*. Diversity analysis, runs of homozygosity and genomic inbreeding reveal recent selection in Blanco Orejinegro cattle. **Journal of Animal Breeding and Genetics**, Berlin, v. 138, n. 5, p. 613-627, 2021.

CHEN, S. *et al*. Genetic variants of fatty acid elongase 6 in Chinese Holstein cow. **Gene**, Amsterdam, v. 670, p. 123-170, 2018.

COCHRAN, S. D. *et al*. Discovery of single nucleotide polymorphisms in candidate genes associated with fertility and production traits in Holstein cattle. **BMC Genetics**, London, v. 14, [art.] 49, 2013.

COLE, J. B. *et al*. Genome-wide association analysis of thirty one production, health, reproduction and body conformation traits in contemporary U.S. Holstein cows. **BMC Genomics**, London, v. 12, [art.] 408, 2011.

CURIK, I.; FERENČAKOVIĆ, M.; SÖLKNER, J. Inbreeding and runs of homozygosity: a possible solution to an old problem. **Livestock Science**, Amsterdam, v. 166, n. 1, p. 26–34, 2014.

DIXIT, S. P. *et al.* Genome-wide runs of homozygosity revealed selection signatures in *Bos indicus*. **Frontiers in Genetics**, Lausanne, v. 11, [art.] 92, 2020.

FERENČAKOVIĆ, M.; SÖLKNER, J.; CURIK, I. Estimating autozygosity from high-throughput information: effects of SNP density and genotyping errors. **Genetics Selection Evolution**, Paris, v. 45, [art.] 42, 2013.

FONTANESI, L. *et al*. A candidate gene association study for nine economically important traits in Italian Holstein cattle. **Animal Genetics**, Oxford, v. 45, n. 4, p. 576-580, 2014.

FONTANESI, L. *et al.* Genetic heterogeneity at the bovine KIT gene in cattle breeds carrying different putative alleles at the spotting locus. **Animal Genetics**, Oxford, v. 41, n. 3, p. 295-303, 2010.

FORUTAN, M. *et al.* Inbreeding and runs of homozygosity before and after genomic selection in North American Holstein cattle. **BMC Genomics**, London, v. 19, n. 1, [art.] 98, 2018.

GALLIOU, J. M. *et al*. Identification of loci and pathways associated with heifer conception rate in U.S. holsteins. **Genes**, Basel, v. 11, n. 7, [art.] 767, 2020.

GIBSON, J.; MORTON, N. E.; COLLINS, A. Extended tracts of homozygosity in outbred human populations. **Human Molecular Genetics**, Oxford, v. 15, n. 5, p. 789–795, 25 Jan. 2006.

GOMEZ-RAYA, L. *et al*. Genomic inbreeding coefficients based on the distribution of the length of runs of homozygosity in a closed line of Iberian pigs. **Genetics Selection Evolution**, Paris, v. 47, [art.] 41, 2015.

GUSEV, A. *et al*. Whole population, genome-wide mapping of hidden relatedness. **Genome Research**, New York, v. 19, n. 2, p. 318–326, 2009.

HECK, J. M. L. *et al*. Effects of milk protein variants on the protein composition of bovine milk. **Journal of Dairy Science**, Champaign, v. 92, n. 3, p. 1192-1202, 2009. Disponível em: https://doi.org/10.3168/jds.2008-1208. Acesso em: 16 nov. 2021.

HÖGLUND, J. K. *et al.* Genome-wide association study for female fertility in Nordic Red cattle. **BMC Genetics**, London, v. 16, [art.] 110, 2015. Disponível em: https://doi.org/10.1186/s12863-015-0269-x. Acesso em: 15 out. 2021.

HOWRIGAN, D. P.; SIMONSON, M. A.; KELLER, M. C. Detecting autozygosity through runs of homozygosity: a comparison of three autozygosity detection algorithms. **BMC Genomics**, London, v. 12, [art.] 460, 2011.

HUANG, W. *et al*. Association between milk protein gene variants and protein composition traits in dairy cattle. **Journal of Dairy Science**, Champaign, v. 95, n. 1, p. 440-449, 2012. Disponível em: https://doi.org/10.3168/jds.2011-4757. Acesso em: 15 jan. 2021.

JIANG, J. *et al*. A large-scale genome-wide association study in U.S. Holstein cattle. **Frontiers in Genetics**, Lausanne, v. 10, [art.] 412, May 2019.

KARIMI, Z. **Runs of homozygosity patterns in Taurine and Indicine cattle breeds**. 2013. Thesis (Master) - University of Natural Resources and Life Sciences, Vienna, 2013.

KIM, E. S. *et al*. Effect of artificial selection on runs of homozygosity in U.S. Holstein cattle. **PLoS ONE**, San Francisco, v. 8, n. 11, [art.] e80813, [p. 1–14], 2013.

KU, C. S. *et al*. Regions of homozygosity and their impact on complex diseases and traits. **Human Genetics**, Berlin, v. 129, n. 1, p. 1–15, 2011.

LAWSON, D. J. *et al*. Inference of population structure using dense haplotype data. **PLoS Genetics**, San Francisco, v. 8, n. 1, [art.] e1002453, [p. 11–17], 2012.

LENCZ, T. *et al*. Runs of homozygosity reveal highly penetrant recessive loci in schizophrenia. **Proceedings of the National Academy of Sciences of the United States of America**, Washington, DC, v. 104, n. 50, p. 19942-19947, 2007.

LEPPÄLÄ, K.; NIELSEN, S. V.; MAILUND, T. Admixturegraph: an R package for admixture graph manipulation and fitting. **Bioinformatics**, v. 33, n. 11, p. 1738-1740, 2017.

LI, Y. *et al*. A whole genome association study to detect additive and dominant single nucleotide polymorphisms for growth and carcass traits in Korean native cattle, Hanwoo. **Asian-Australasian Journal of Animal Sciences**, Seoul, v. 30, n. 1, p. 8-19, 2017. Disponível em: Disponível em: https://doi.org/10.5713/ajas.16.0170. Acesso em: 19 mai. 2020.

LI, Y.; KIM, J. J. Multiple linkage disequilibrium mapping methods to validate additive quantitative trait loci in Korean native cattle (Hanwoo). **Asian-Australasian Journal of Animal Sciences**, Seoul, v. 28, n. 7, p. 926-935, 2015.

LOFTUS, R. T. *et al*. Evidence for two independent domestications of cattle. **Proceedings of the National Academy of Sciences of the United States of America**, Washington, DC, v. 91, n. 7, p. 2757–2761, 1994.

MARRAS, G. *et al*. Analysis of runs of homozygosity and their relationship with inbreeding in five cattle breeds farmed in Italy. **Animal Genetics**, Oxford, v. 46, n. 2, p. 110–121, Apr. 2015.

MARTIKAINEN, K.; KOIVULA, M.; UIMARI, P. Identification of runs of homozygosity affecting female fertility and milk production traits in Finnish Ayrshire cattle. **Scientific Reports**, London, v. 10, n. 1, [art.] 3804, 2020.

MCQUILLAN, R. *et al*. Runs of homozygosity in european populations. **American Journal of Human Genetics**, Cambridge, v. 83, n. 3, p. 359–372, 2008.

METZGER, J. *et al*. Runs of homozygosity reveal signatures of positive selection for reproduction traits in breed and non-breed horses. **BMC Genomics**, London, v. 16, [art.] 764, 2015.

MEYERMANS, R. *et al*. How to study runs of homozygosity using PLINK? A guide for analyzing medium density SNP data in livestock and pet species. **BMC Genomics**, London, v. 21, n. 1, [art.] 94, 2020.

MIRKENA, T. *et al*. Genetics of adaptation in domestic farm animals: a review. **Livestock Science**, Amsterdam, v. 132, n. 1/3, p. 1-12, 2010.

NEUPANE, M.; KISER, J. N.; NEIBERGS, H. L. Gene set enrichment analysis of SNP data in dairy and beef cattle with bovine respiratory disease. **Animal Genetics**, Oxford, v. 49, n. 6, p. 527-538, 2018.

OLEKSYK, T. K.; SMITH, M. W.; O'BRIEN, S. J. Genome-wide scans for footprints of natural selection. **Philosophical Transactions of the Royal Society B: Biological Sciences**, London, v. 365, n. 1537, p. 185-205, 2010.

ORTEGA, M. S. *et al*. Association of single nucleotide polymorphisms in candidate genes previously related to genetic variation in fertility with phenotypic measurements of reproductive function in Holstein cows. **Journal of Dairy Science**, Champaign, v. 100, n. 5, p. 3725-3734, 2017.

PAIM, T. P. *et al*. Genomic breed composition of selection signatures in brangus beef cattle. **Frontiers in Genetics**, Lausanne, v. 11, [art.] 710, 2020.

PAUSCH, H. *et al*. Identification of QTL for UV-protective eye area pigmentation in cattle by progeny phenotyping and genome-wide association analysis. **PLoS ONE**, San Francisco, v. 7, n. 5, [art.]. e PERIPOLLI 36346, 2012.

PEGOLO, S. *et al*. Effects of candidate gene polymorphisms on the detailed fatty acids profile determined by gas chromatography in bovine milk. **Journal of Dairy Science**, Champaign, v. 99, n. 6, p. 4558-4573, 2016.

PERIPOLLI, E. *et al.* "Autozygosity islands and ROH patterns in Nellore lineages: evidence of selection for functionally important traits." ***BMC genomics*** 19, pp.1-14 2018a.

PERIPOLLI, E. *et al*. Assessment of runs of homozygosity islands and estimates of genomic inbreeding in Gyr (*Bos indicus*) dairy cattle. **BMC Genomics**, London, v. 19, [art.] 34, [p. 1–13], 2018b.

PERIPOLLI, E. *et al*. Genome-wide scan for runs of homozygosity in the composite Montana Tropical® beef cattle. **Journal of Animal Breeding and Genetics**, Berlin, v. 137, n. 2, p. 155-165, 2020.

PERIPOLLI, E. *et al*. Runs of homozygosity: current knowledge and applications in livestock. **Animal Genetics**, Oxford, v. 48, n. 3, p. 255–271, June 2017.

PICKRELL, J. K.; PRITCHARD, J. K. Inference of population splits and mixtures from genome-wide allele frequency data. **PLoS Genetics**, San Francisco, v. 8, n. 11, [art.] e1002967, 2012.

PILON, B. *et al*. Inbreeding calculated with runs of homozygosity suggests chromosome-specific inbreeding depression regions in line 1 Hereford. **Animals**, Basel, v. 11, n. 11, [art.] 3105, Oct. 2021.

POULSEN, N. A. *et al*. The occurrence of noncoagulating milk and the association of bovine milk coagulation properties with genetic variants of the caseins in 3 Scandinavian dairy breeds. **Journal of Dairy Science**, Champaign, v. 96, n. 8, p. 4830-4842, 2013.

PRINZENBERG, E. M. *et al.* Polymorphism of the bovine CSN1S1 promoter: Linkage mapping, intragenic haplotypes, and effects on milk production traits. **Journal of Dairy Science**, Champaign, v. 86, n. 8, p. 2696-2705, 2003.

PURCELL, S. *et al*. Plink: a tool set for whole-genome association and population-based linkage analyses. **American Journal of Human Genetics**, Baltimore, v. 81, n. 3, p. 559–575, 2007.

PURFIELD, D. C. *et al*. Runs of homozygosity and population history in cattle. **BMC Genetics**, London, v. 13, [art.] 70, 2012.

REBELATO, A. B.; CAETANO, A. R. Runs of homozygosity for autozygosity estimation and genomic analysis in production animals. **Pesquisa Agropecuária Brasileira**, Brasília, DF, v. 53, n. 9, p. 975-984, 2018.

SABETI, P. C. *et al*. Detecting recent positive selection in the human genome from haplotype structure. **Nature**, London, v. 419, n. 6909, p. 832-837, 2002.

SADKOWSKI, T. *et al*. Gene expression profiling in skeletal muscle of Holstein-Friesian bulls with single-nucleotide polymorphism in the myostatin gene 5′-flanking region. **Journal of Applied Genetics**, Cheshire, v. 49, n. 3, p. 237-250, 2008.

SANCHEZ, M. P. *et al*. Sequence-based GWAS and post-GWAS analyses reveal a key role of SLC37A1, ANKH, and regulatory regions on bovine milk mineral content. **Scientific Reports**, London, v. 11, [art.] 7537, 2021.

SARAVANAN, K. A. *et al*. Selection signatures in livestock genome: A review of concepts, approaches and applications. **Livestock Science**, Amsterdam, v. 241, [art.] 104257, Nov. 2020.

SARTORI, R. *et al*. Physiological differences and implications to reproductive management of Bos taurus and Bos indicus cattle in a tropical environment. **Society of Reproduction and Fertility Supplement**, Packington, v. 67, p. 357-375, 2010.

SASAGO, N. *et al*. Genome-wide association study for carcass traits, fatty acid composition, chemical composition, sugar, and the effects of related candidate genes in Japanese Black cattle. **Animal Science Journal**, Richmond, v. 88, n. 1, p. 33-44, 2017.

SÖLKNER, J. *et al*. Genomic metrics of individual autozygosity, applied to a cattle population. *In*: ANNUAL MEETING OF THE EUROPEAN ASSOCIATION OF ANIMAL PRODUCTION, 61., 2010, Wageningen. **Book of abstracts**. Wageningen: Wageningen Academic, 2010. p. 306-307.

SORBOLINI, S. *et al*. Detection of selection signatures in Piemontese and Marchigiana cattle, two breeds with similar production aptitudes but different selection histories. **Genetics Selection Evolution**, Paris, v. 47, n. 1, [art.] 52, 2015.

SUMREDDEE, P. *et al*. Runs of homozygosity and analysis of inbreeding depression. **Journal of Animal Science**, Champaign, v. 98, n. 12, [art.] skaa361, 2020.

TORO OSPINA, A. M. *et al*. Genome-wide identification of runs of homozygosity islands in the Gyr breed (*Bos indicus*). **Reproduction in Domestic Animals**, Berlin, v. 55, n. 3, p. 333-342, 2020.

URBINATI, I. *et al*. Selection signatures in Canchim beef cattle. **Journal of Animal Science and Biotechnology**, London, v. 7, [art.] 29, mai 2016.

VANRADEN, P. M. Efficient methods to compute genomic predictions. **Journal of Dairy Science**, Champaign, v. 91, n. 11, p. 4414-4423, 2008. Disponível em: https://doi.org/10.3168/jds.2007-0980. Acesso em: 11 mar. 2021.

VIALE, E. *et al*. Association of candidate gene polymorphisms with milk technological traits, yield, composition, and somatic cell score in Italian Holstein-Friesian sires. **Journal of Dairy Science**, Champaign, v. 100, n. 9, p. 7271-7281, 2017.

VISKER, M. H. P. W. *et al*. Association of bovine β-casein protein variant I with milk production and milk protein composition. **Animal Genetics**, Oxford, v. 42, n. 2, p. 212-218, 2011.

WILLIAMS, J. L. *et al*. Inbreeding and purging at the genomic Level: The Chillingham cattle reveal extensive, non-random SNP heterozygosity. **Animal Genetics**, Oxford, v. 47, n. 1, p. 19-27, 2016.

WRIGHT, S. Genetical structure of populations. **Nature**, London, v. 166, n. 4215, p. 247–249, 1949.

WRIGHT, S. Genetical structure of populations. **Nature**, London, v. 166, n. 4215, p. 247–249, 1949.

WU, X. *et al*. Genome wide association studies for body conformation traits in the Chinese Holstein cattle population. **BMC Genomics**, London, v. 14, [art.] 897, 2013.

ZAVAREZ, L. B. *et al.* Assessment of autozygosity in Nellore cows (*Bos indicus*) through high-density SNP genotypes. **Frontiers in Genetics**, Lausanne, v. 6, [art.] 5, Jan. 2015.

ZHANG, L. *et al*. cgaTOH: Extended approach for identifying tracts of homozygosity. **PLoS ONE**, San Francisco, v. 8, n. 3, [art.] e57772, 2013.

ZHAO, G. *et al*. Genome-wide assessment of runs of homozygosity in chinese wagyu beef cattle. **Animals**, Basel, v. 10, n. 8, [art.] 1425, 2020.

ZHAO, G. *et al*. Runs of homozygosity analysis reveals consensus homozygous regions affecting production traits in Chinese Simmental beef cattle. **BMC Genomics**, London, v. 22, [art.] 678, 2021.

Vita

Darilene Ursula Tyska nasceu em 08 de fevereiro de 1987 no município de Porto Alegre, no estado do Rio Grande do Sul. Filha de Flávio Luiz Tyska e Eliana Tyska.

Ingressou no segundo semestre de 2010, no Curso de Zootecnia da Universidade Federal de Pelotas- UFPel, localizado no município de Pelotas. No mês de dezembro de 2014, graduou-se Zootecnista com mérito acadêmico do Conselho Federal de Medicina Veterinária.

Ingressou no primeiro semestre de 2015, no Programa de Pós-Graduação em Zootecnia da Universidade Federal de Pelotas, na Faculdade de Agronomia Eliseu Maciel, mestrado, sob orientação do Professor Dr. Nelson José Laurindo Dionello, e em fevereiro de 2017 defendeu a dissertação intitulada Avaliação das características produtivas de codornas de corte e qualidade de ovos por meio de análises multivariadas, obtendo o título de Mestre em Ciências, na área de concentração: Produção de Aves.

Ingressou no primeiro semestre de 2017, no Programa de Pós-Graduação em Zootecnia da Universidade Federal do Rio Grande do Sul, na Faculdade de Agronomia, doutorado, sob orientação do Professor Dr. José Braccini Neto, desenvolvendo pesquisa na área de Melhoramento genético animal – com dados genômicos em raças de bovinos de corte.